Agricultural Engineering Institute, Department of Agricultural) for milling quality test equipments. Thanks also are due to graduate students of mechanical engineering program (Mahanakorn University of Technology): Karn Karnjanabat, Siam Buntaowong, Arnut Suksa-add, Niwat Yimyoo, Arrun Maneenun, Arkom Siamol, Vacharapong Rukthongloh, Ubol Somjai, Apisit Prasertvit, Pakpoom Srilian, Itipon Yatoonkroh, and Nipol Chaitui for their assistance in experiments.

REFERENCES

1. Pallai, E.; Szentmarjay, T.; Mujumdar, A.S. Spouted bed drying. In *Handbook of Industrial Drying, Vol. 1*; 2nd Ed.; Mujumdar, A.S., Ed.; Marcel Dekker, Inc.; New York, 1995; 753–773.
2. Passos, M.L.; Mujumdar, A.S.; Raghavan, G.S.V. Spouted bed drying. In *Principles and Design Consideration in Drying, Vol. 4*; Mujumdar, A.S., Ed.; Hemisphere: New York, 1987; 359–398.
3. Mujumdar, A.S. *Spouted Bed Technology: A Brief Review, Drying'84*; Hemisphere: Washington, 1984; 151–157.
4. Kalwar, M.I.; Kudra T.; Raghavan, G.S.V.; Mujumdar A.S. Drying of grains in a drafted two dimensional spouted bed. Journal of Food Process Engineering **1991**, *13*, 321–332.
5. Kalwar, M.I.; Raghavan, G.S.V. Batch drying of shelled corn in two-dimensional spouted beds with draft plates. Drying Technology—An International Journal **1993**, *11* (2), 339–354.
6. Kalwar, M.I.; Raghavan, G.S.V. Circulation of particles in two-dimensional spouted beds with draft plates. Powder Technology **1993**, *77*, 233–242.
7. Wetchacama, S.; Soponronnarit, S.; Swasdisevi, T.; Panich-ing-orn, J.; Suthicharoenpanich, S. *Drying of high moisture paddy by two-dimensional spouted bed technique*. In Proceedings of the First Asian-Australian Drying Conference (ADC '99), Bali: Indonesia, October 24–27, 1999, 300–307.
8. Nguyen, L.H. *Evaluation of a Modified Spouted Bed Dryer for High Moisture Grain Drying*. Ph.D. Thesis, University of New South Wales: Australia, 2000.
9. Nguyen, L.H.; Driscoll, R.H.; Srzednicki, G. Drying of high moisture content paddy in a pilot scale triangular spouted bed dryer. Drying Technology—An International Journal **2001**, *19* (2), 375–387.
10. Wiriyaumpaiwong, S.; Soponronnarit, S.; Prachayawarakorn, S. Soybean drying by two-dimensional spouted bed. Drying Technology—An International Journal **2003**, *21* (9), 1735–1757.
11. Madhiyanon, T.; Soponronnarit, S.; Tia, W. A two-region mathematical model for batch drying of grains in a two-dimensional spouted bed. Drying Technology—An International Journal **2001**, *19* (5), 1045–1064.
12. Tulasidas, T.N.; Kudra, T.; Raghavan, G.S.V. Effect of bed height on simultaneous heat and mass transfer in a two-dimensional spouted bed dryer. Heat Mass Transfer **1993**, *20*, 79–88.
13. Becker, H.A.; Sallans, H.R. Drying wheat in a spouted bed. Chemical Engineering Science **1960**, *13*, 97–112.

14. Zuritz, C.A.; Singh, R.P. In *Simulation of Rough Rice Drying in a Spouted Bed, Drying'82*; Mujumdar, A.S., Ed.; McGraw-Hill Hemisphere: New York, 1982; 239–247.
15. Zahed, A.H.; Epstein, N. Batch and continuous spouted bed drying of cereal grains: The thermal equilibrium model. Canadian Journal of Chemical Engineering **1992**, *70*, 945–953.
16. Zahed, A.H.; Epstein, N. On the diffusion mechanism during spouted bed drying of cereal grains. Drying Technology—An International Journal **1993**, *11* (2), 339–354.
17. Jumah, R.Y.; Mujumdar, A.S.; Raghavan, G.S.V. A mathematical model for constant and intermittent batch drying of grains in a novel rotating jet spouted bed. Drying Technology—An International Journal **1996**, *14* (3–4), 765–802.
18. Jumah, R.Y.; Mujumdar, A.S.; Raghavan, G.S.V. A mathematical model for constant and intermittent batch drying of grains in a novel rotating jet spouted bed. In *Mathematical Modeling and Numerical Techniques in Drying Technology;* Mujumdar, A.S., Turner, I., Eds.; Marcel Dekker, Inc.: New York, 1997; 339–380.
19. Madhiyanon, T.; Soponronnarit, S.; Tia, W. Industrial-scale prototype of continuous spouted bed paddy dryer. Drying Technology—An International Journal **2001**, *19* (1), 207–216.
20. Madhiyanon, T.; Soponronnarit, S.; Tia, W. A mathematical model for continuous drying of grains in a spouted bed dryer. Drying Technology—An International Journal **2002**, *20* (3), 587–614.
21. Tirawanichakul, S.; Prachayawarakorn, S.; Tungtrakul, P.; Warunyanond, W.; Soponronnarit, S. *Effect of drying temperature on physical property of high and low amylose content paddy*. In Proceedings of the International Conference on Innovation in Food Processing Technology and Engineering, AIT, Bangkok, Thailand, December 11–13, 2002; Jindal et al., Eds.; Asian Institute of Technology: Bangkok, Thailand, 2002, 467–480.
22. Poomsa-ad, N.; Soponronnarit, S.; Prachayawarakorn, S.; Terdyothin, A. *Head rice yield after drying by fluidization technique and tempering*. In Proceedings of 2nd Asian-Oceania Drying Conference (ADC), Batu Feringhi, Pulau Pinang, Malaysia, August 20–22, 2001; Daud et al., Eds.; The Institute of Chemical Engineers: Malaysia, 2001, 717–726.
23. Prachayawarakorn, S.; Soponronnarit, S. Mathematical model of fluidised bed paddy drying. Engineering Journal: Research and Development **1993**, *4*, 101–109 (in Thai).
24. Tumambing, J.A.; Driscoll, R.H. *Modelling the performance of a continuous fluidised bed dryer for rapid pre-drying of paddy*. In Proceedings of the 14th ASEAN Seminar on Grain Post-Harvest Technology; Naewbanij, J.O.; Manilay, A.A., Eds.; Manila, Philippines. AGGP, Bangkok, Thailand, 1991, 193–213.
25. Soponronnarit, S.; Prachayawarakorn, S.; Wangji, M. *Commercial fluidised bed paddy dryer*. In Proceedings of the 10th International Drying Symposium, Krakow, Poland, 1996; Strumillo, C.; Pakowski, Z., Eds.; Poland. Lodz Technical University: Poland, 1996, Vol. A, 638–644.

Available online at www.sciencedirect.com
SCIENCE DIRECT®
Applied Energy 81 (2005) 198–208
APPLIED ENERGY
www.elsevier.com/locate/apenergy

Closed-ended oscillating heat-pipe (CEOHP) air-preheater for energy thrift in a dryer

S. Rittidech *, W. Dangeton, S. Soponronnarit

Faculty of Engineering, Mahasarakham University, Thailand

Accepted 2 June 2004
Available online 5 January 2005

Abstract

The CEOHP air-preheater consisted of two main parts, i.e. the rectangular house casing and the CEOHP. The house casing was designed to be suitable for the CEOHP. The inside house casing divided the CEOHP into three parts, i.e. the evaporator, the adiabatic section and condenser section. The CEOHP air-preheater design employed copper tubes: thirty-two sets of capillary tubes with an inner diameter of 0.002 m, an evaporator and a condenser length of 0.19 m, and each of which has eight meandering turns. The evaporator section was heated by hot-gas, while the condenser section was cooled by fresh air. In the experiment, the hot-gas temperature was 60, 70 or 80 °C with the hot-gas velocity of 3.3 m/s. The fresh-air temperature was 30 °C. Water and R123 was used as the working fluid with a filling ratio of 50%. It was found that, as the hot-gas temperature increases from 60 to 80 °C, the thermal effectiveness slightly increases. If the working fluid changes from water to R123, the thermal effectiveness slightly increases. The designed CEOHP air-preheater achieves energy thrift.

Keywords: Closed-ended oscillating heat-pipe air-preheater; Energy thrift dryer

* Corresponding author. Tel.: +66-43-754316; fax: +66-43-754316.
E-mail address: s_rittidej@hotmail.com (S. Rittidech).

0306-2619/$ - see front matter © 2004 Elsevier Ltd. All rights reserved.
doi:10.1016/j.apenergy.2004.06.003

Nomenclature

A	area (m^2)
C_p	specific heat at constant pressure (J/kg K)
D	diameter (m)
g	gravitational acceleration (m/s^2)
h_{fg}	latent heat of vaporization (kJ/kg)
Ku	Kutateladze number $\left(\frac{q}{h_{fg}\rho_v\left(\sigma g(\rho_l-\rho_v)/\rho_v^2\right)^{1/4}}\right)$ (–)
k	thermal conductivity (W/mK)
L	length (m)
n	number of the capillary tube (–)
Pr_v	Prandtl number of vapor $\left(\frac{C_{pv}\mu_v}{k_v}\right)$ (–)
Q	heat-transfer rate (W)
q	heat flux (W/m^2)
T	temperature (°C)
V	velocity (m/s)

Greek symbols

μ	viscosity (Pa s)
ρ	density (kg/m^3)
σ	surface tension (N/m)

Subscripts

c	cold
e	evaporator
i	inside, inlet
l	liquid
o	outet
t	total
v	vapor

1. Introduction

1.1. Target

The effort to reduce energy consumption is a main goal for the dryer. Traditionally the dryer is unable to use its waste heat. Compared with other conventional heat-exchangers, the closed-ended oscillating heat-pipe (CEOHP) heat-exchanger has many advantages, e.g. large quantities of heat are transported through a small cross-section area. The CEOHP is a very effective heat-transfer device [1]: it has a simple structure and a fast thermal-response. The CEOHP consists of a long capil-

lary tube bent into many turns and the evaporator, adiabatic section and condenser section are located at these turns. However, there is no wick structure to return the condensate liquid from the condenser to the evaporator section. Heat is transported from the evaporator section to the condenser section by the pulsation of the working fluid moving in an axial direction in the tube. The inner diameter of the pipe is important. It must be small enough so that, under operational conditions, liquid slugs and vapor plugs can be formed. If the diameter is too large, the liquid and vapor inside the tube will become stratified and operation cannot be established. Rittidech et al. [3] investigated the effect of inclination angles, evaporator lengths and working-fluid properties on the heat-transfer characteristics of the CEOHP under normal operating condition. Rittidech et al. [4] devised a correlation to predict the heat-transfer characteristics of a CEOHP. Yang et al. [5] studied a water heat-pipe heat-exchanger using automotive-exhaust gas. The experimental results indicate it is worthwhile using a heat-pipe heat-exchanger employing the exhaust gas.

The application of CEOHPs, in order to save energy, is considered. The CEOHP can have many applications such as, economizers or air preheaters, electronic-cooling devices and solar collectors to name just a few. The new type of heat-pipe or CEOHP, shown in Fig. 1, can help in energy saving, specifically for air preheating in a dryer. The objective of the present study is to design, construct and test the CEOHP air-preheater for a dryer that can recover the waste heat from the drying process.

1.2. Conventional-drying process (see Fig. 2)

First, the air is heated by fuel combustion. Then the hot air moves through the layers of the product. The heat is transferred to the product and evaporation occurs.

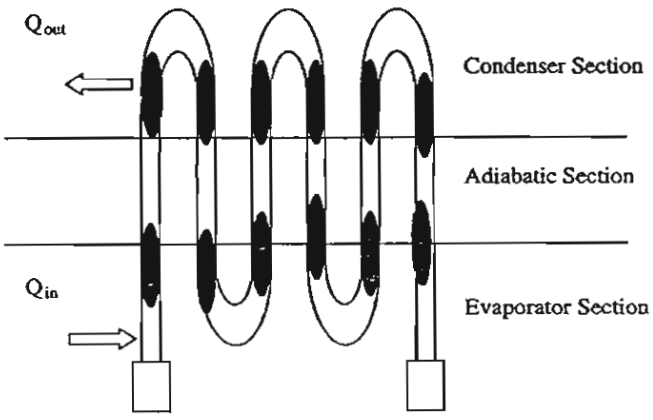

Fig. 1. Closed-end oscillating heat-pipe (CEOHP).

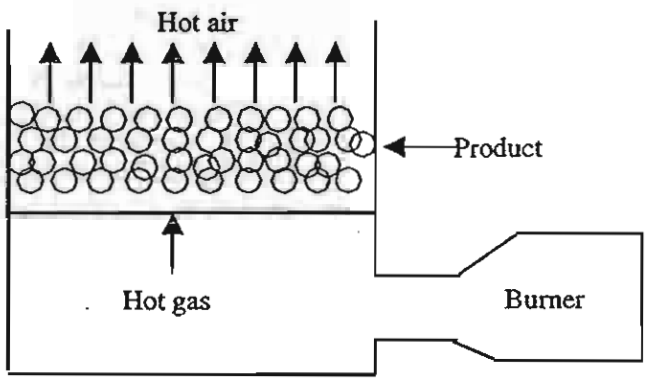

Fig. 2. Conventional drying-process.

2. CEOHP air-preheater system – design concept and calculation

Some fundamental design parameters e.g. the maximum heat-transfer rate of the drying system (Q_{max}, W) and the installation site depending on the available space have to be considered. Hence for the counterflow air-preheater heat-exchanger, the following set of equations applies [6]:

$$Q_{max} = C_{min}(T_{hi} - T_{ci}),$$
$$C_{min} = \rho V A C_p. \tag{1}$$

2.1. CEOHP air-preheater design

When considering the design of the CEOHP air-preheater, the size and position of the air-preheater are taken into consideration, as well as the maintenance and budget costs. In addition, insulating the ducts and air-preheater also decreases the heat loss. The CEOHP air-preheater heat-transfer design was solved in six steps as follows:

- The hot-gas temperature of initial and fresh air temperature from drying process is obtained.
- The working temperature is calculated and the tube material is selected.
- The type of working fluid that is appropriate to the operational temperature.
- The inner diameter of the CEOHP is calculated from Maezawa et al. [2].

$$D_{max} \leqslant \sqrt{\frac{\sigma}{\rho_l g}}. \tag{2}$$

- L_e, L_a, L_c, L_t, and n are defined corresponding to the duct size of the dryer and the installation area.

- Pr_v, ρ_v, ρ_l, h_{fg} and the oscillation phenomena of the working fluid at working temperature are described and the heat flux of CEOHP air-preheater is solved by the correlation from [4]. The standard deviation of this equation is ±30%.

$$Ku_{90} = 0.0067\left[\left(\frac{D_i^{3.1}L_t^{0.1}}{L_c^{3.2}}\right)n^{0.9}Pr_v^{-12}\left(\frac{\rho_v}{\rho_l}\right)^{-0.1}\left(\frac{\omega\mu_v^3}{\sigma^2\rho_v}\right)^{0.01}\right]^{0.175}. \quad (3)$$

It was necessary to change from the heat flux (q) from to the heat-transfer (Q)

$$Q_{90} = (Aq_{90}). \quad (4)$$

From this correlation, the meaning of each parameter can be discussed as follows:

Ku_{90} indicates the ratio of heat flux to critical heat flux for the vertical orientation.

$D_i^{3.1}L_t^{0.1}/L_c^{3.2}$ defines the size of the CEOHP. For example, if the value of $D_i^{3.1}L_t^{0.1}/L_c^{3.2}$ was very high, then the tube would be large and the evaporator section would be short. Because of the boiling phenomenon, the value of Ku_{90} or heat flux would be high. If the value of $D_i^{3.1}L_t^{0.1}/L_c^{3.2}$ was very low, then the tube would be small and the evaporator section would be long. Because the boiling phenomenon within this type of tube will be akin to the boiling phenomenon in a confined channel, the values of Ku_{90} or heat flux will be low.

The number n indicates that of the capillary tubes which connect the evaporator and the condenser section of a CEOHP or represents the number of turns of a CEOHP; Pr_v indicates the ratio of momentum diffusivity to the thermal diffusivity of vapor slug. If the value is very low, the vapor slug will be able to transfer the thermal energy to the condenser section relatively efficient. Therefore, the vaule of Ku_{90} or heat flux will be high.

The ratio ρ_v/ρ_l indicates the vapor phase density to liquid phase density of the working fluid that represents the working pressure the working fluid within the CEOHP.

The oscillation phenomena within the CEOHP, can be described by $\omega\mu_v^3/\sigma^2\rho_v$, i.e.

$$\frac{\omega\mu_v^3}{\sigma^2\rho_v} = \left(\frac{g\mu_v^4/\rho_v\sigma^3}{\rho_v L_v\sigma/\mu_v^2}\right)^{0.5}\left(\frac{\rho_l}{\rho_v}\right)^{0.5},$$

where the capillary buoyancy number is $(g\mu_v^4/\rho_v\sigma^3)$ and the Suratman number $(\rho_v L_v\sigma/\mu_v^2)$.

The capillary bouyancy and Suratman numbers are the ratios of surface tension force and the viscous force. The frequency ω of the oscillating motion of the vapor slug in a tube is defined as the frequency of simple harmonic motion, i.e. $\omega = \sqrt{\rho_l g/\rho_v L_v}$.

Values of some of these parameters are shown in Table 1.

The effectiveness of CEOHP air-preheater, ε, is defined as the ratio of the actual heat-transfer rate for an air-preheater heat-exchanger to the maximum possible heat-transfer rate, i.e.,

Table 1
The parameters used in the correlation for predicting the heat-transfer rate

Characteristic and parameter	Description
Material of tube	Copper
Internal diameter of tube from criterion (2) (m)	0.002
Length of CEOHP	
Total length (m)	6
Evaporator length (m)	0.19
Condenser length (m)	0.19
Number of turns	8
Working fluid	Water
T_{hi}, T_{Ci} (°C)	80,30
Working temperature (°C)	55

Table 2
The results of calculation

Heat-transfer from correlation [3] (W)	111
Number of CEOHP (set)	32
Total heat-transfer from correlation [3] (W)	3552

$$\varepsilon = \frac{Q_{\text{Actual}}}{Q_{\text{Max}}}, \tag{5}$$

where

$$Q_{\text{Actual}} = \rho V A C_p (T_{co} - T_{ci}). \tag{6}$$

The results of the calculation are shown in Table 2.

3. Experimental set-up

3.1. Prototype

The CEOHP air-preheater for the drying process, see Fig. 3, was divided into two parts, i.e. the evaporator and condenser section with the length of 0.19 m. The tube arrangement was aligned in the direction of the hot-gas flow. The condenser section was connected to the fresh-air section and the evaporator section was in contact with the heat source from the gas burner. The dryer-bath type was selected to be appropriate to the CEOHP air-preheater. The prototype has a duct size area of 200 mm × 200 mm including the fibre insulation.

3.2. Test rig

This prototype was installed in a test rig, as shown in Fig. 4. The hot-gas coming from the gas burner flows through the CEOHP air-preheater. The initial and final temperatures are measured with thermocouples. Twelve thermocouples type K were

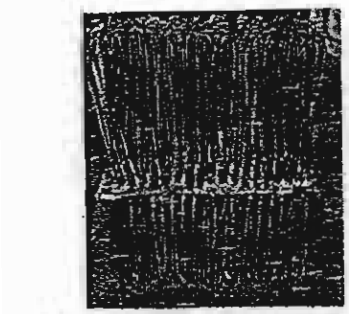

(a) CEOHP air-preheater

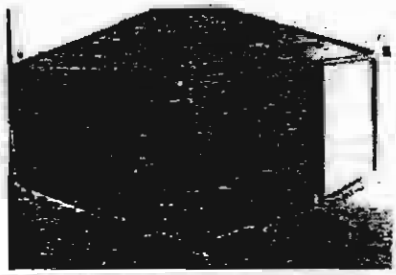

(b) Batch-type dryer

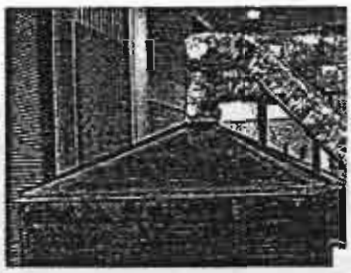

(c) Dryer with CEOHP air-preheater

Fig. 3. The prototype: (a) CEOHP air-preheater; (b) batch-type dryer; (c) dryer with CEOHP air-preheater.

installed on the evaporator section and twelve more on the condenser. These thermocouples were connected to a Yokogawa-MX100 acquisition data-system. When a steady state was achieved, the temperatures at the inlet and outlet of the evaporator and the condenser section were recorded. The heat-transfer rate and effectiveness were determined and compared with the predicted values.

The controlled parameter was the hot-gas velocity of 3.3 m/s

The variable parameters were:

- working-fluid water or R123,
- hot-gas temperature of 60, 70 or 80 °C.

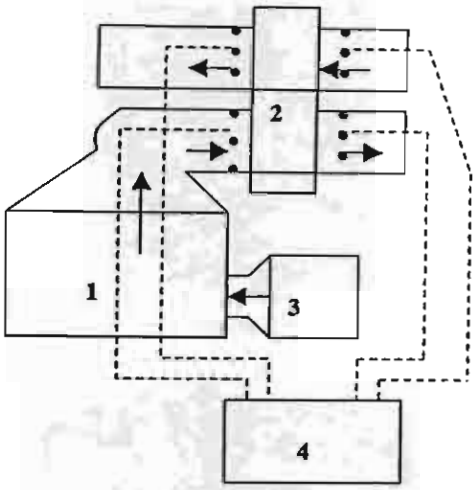

Fig. 4. Test rig: 1, dryer; 2, CEOHP air-preheater; 3, gas burner; 4, data logger; •, thermojunction.

4. Results and discussion

Table 3 shows the results of the experiment.

4.1. Effect of hot-gas temperature on heat-transfer rate

In this experiment, the CEOHP air-preheater had eight turns, 32 columns, and a hot-gas velocity of 3.3 m/s. The experimental results present the effect of the hot-gas temperature on the heat-transfer rate – see Fig. 5. This figure compares the experimental results with the predictions from the correlation [3]. It can be seen that, when the hot-gas inlet temperature increases, the heat-transfer rate also rises. This is because when the hot-gas inlet-temperature increases, the fresh-air outlet-temperature also increases. Thus, the temperature difference between the inlet and outlet air temperature also increases and the actual heat-transfer rate will be high. The heat-transfer rate as measured was lower than that predicted via the correlation [3]. However,

Table 3
The results of experiment

W	T_{hi}	T_{ci}	T_{co}	Q_{ac}	Q_{pred}	Q_{max}	ε
Water	80	30	48	2628	3552	373	0.41
	70	30	44	2044	3265	5356	0.38
	60	30	40	1460	2970	4288	0.34
R123	80	30	54	3504	3554	6373	0.54
	70	30	47	2482	3390	5356	0.46
	60	30	43	1898	3129	4288	0.44

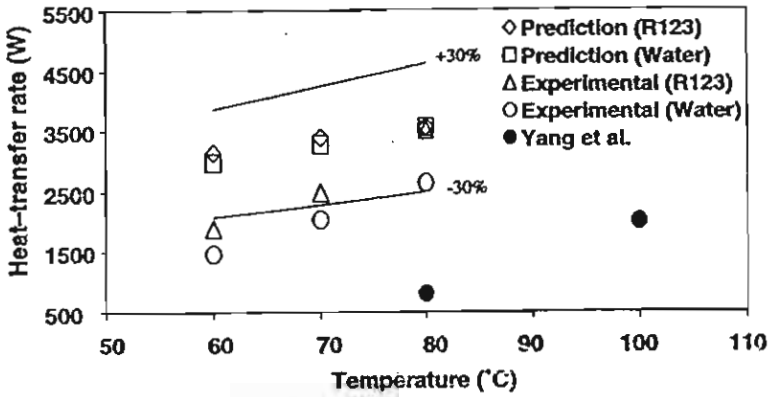

Fig. 5. Effect of temperature and working fluid on heat-transfer rate.

the predictions compare well with experimental data for the 80 °C run. In addition, when the hot-gas temperature increased from 70 to 80 °C the experimental data were within the standard deviation of ±30% from the correlation predictions. It can be concluded that, if the hot-gas temperature increases, the heat-transfer rate increases.

4.2. Effect of working fluid on heat-transfer rate (see Fig. 5)

In this experiment, the effect was measured for the CEOHP air-preheater with eight turns and 32 columns, and a hot-gas velocity of 3.3 m/s. Fig. 5 compares the heat-transfer rate experimental data to the heat-transfer rate predicted from the correlation [3] and the data [5]. If the working fluid changes from water to R123, the heat-transfer rate also increases, because the R123 has a lower latent heat of vaporization. It can be concluded that, if the working fluid is changed from water to R123, the heat-transfer rate increases.

4.3. Effect of hot-gas temperature on thermal effectiveness (see Fig. 6)

In this experiment, the CEOHP air-preheater has eight turns and 32 columns, and a hot-gas velocity of 3.3 m/s. Fig. 6 shows the effect of the hot-gas inlet-temperature on the effectiveness of the CEOHP air-preheater. It can be seen that, when the hot-gas inlet-temperature increases, the effectiveness also rises because the fresh-air outlet temperature also increases. Thus, the temperature difference between the inlet and outlet air also increases and the actual heat-transfer rate will be high. It can be concluded that, if the hot-gas inlet temperature increases, the effectiveness increases.

4.4. Effect of working fluid on thermal effectiveness (see Fig. 6)

In this experiment, the CEOHP air-preheater has eight turns and 32 columns, and a hot-gas velocity of 3.3 m/s. It can be seen in Fig. 6 that, if the working fluid changes

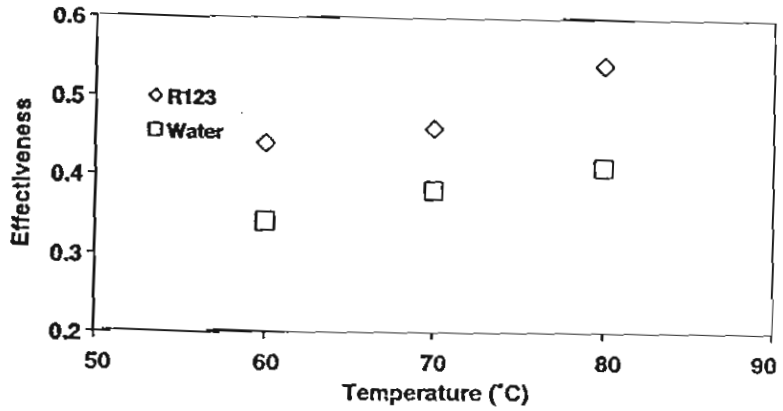

Fig. 6. Effect of temperature and working fluid on effectiveness.

from water to R123, the effectiveness also increases because the R123 has a lower latent heat of vaporization.

5. Conclusion

In this study, we designed and built an experimental prototype to investigate the applicability of a CEOHP air-preheater as a waste-heat recovery device for a drying process. It can be concluded that:

- As the hot-gas temperature increases from 60 to 80 °C, the heat-transfer rate slightly rises.
- If the working fluid changes from water to R123, the heat-transfer rate slightly increases.
- The designed CEOHP air-preheater can achieve energy thrift.

Acknowledgements

The research has been supported generously by the Thailand Research Fund (Under Contract No. MRG4680023). The authors express their sincere appreciation for all of the support provided.

References

[1] Akachi H, Polasek F, Stulc P. Pulsating heat-pipe. In: Proceedings of the fifth international heat-pipe symposium. Melbourne, Australia; 1996. p. 208–17.

[2] Maezawa S, Gi KY, Minimisawa A, Akachi H. Thermal performance of capillary-tube thermosyphon. In: Proceedings of the ninth international heat-pipe conference, vol. 2, Albuquerque, USA; 1996. p. 791–5.
[3] Rittidech S, Terdtoon P, Murakami M, Kamonpet P, Jompakdee W. Effect of inclination angles, evaporator-section lengths and working-fluid properties on the heat-transfer characteristics of a closed-ended osciilating heat-pipe, In: Proceedings of the sixth international heat-pipe symposium, Chiang Mai, Thailand; 2000. p. 413–21.
[4] Rittidech S, Terdtoon P, Murakami M, Kamonpet P, Jompakdee W. Correlation to predict the heat-transfer characteristics of a closed-ended oscillating heat-pipe under normal operating conditions. Appl Therm Eng 2003;23:497–510.
[5] Yang F, Yuan X, Lin G. Waste-heat recovery using a heat-pipe heat-exchanger for heating an automobile using its exhaust gas. Appl Therm Eng 2003;23:367–72.
[6] Incropera Frank P, Dewitt David P. Fundamentals of heat and mass transfer. 4th ed. New York: Wiley; 1976.

Available online at www.sciencedirect.com
SCIENCE DIRECT®
Journal of Stored Products Research 41 (2005) 479–497
Journal of STORED PRODUCTS RESEARCH
www.elsevier.com/locate/jspr

Comparison of performances of pulsed and conventional fluidised-bed dryers

Somkiat Prachayawarakorn[a,*], Warunee Tia[b], Korakot Poopaiboon[b], Somchart Soponronnarit[b]

[a]*Faculty of Engineering, King Mongkut's University of Technology Thonburi, Suksawat 48 Road, Tongkru, Bangkok 10140, Thailand*

[b]*School of Energy and Materials, King Mongkut's University of Technology Thonburi, Suksawat 48 Road, Tongkru, Bangkok 10140, Thailand*

Accepted 7 June 2004

Abstract

Consumption of energy, outlet moisture content and quality of the dried commodity are important parameters of paddy-dryer performance. The fluidised-bed paddy-dryer has been commercialised for several years and in this paper, paddy drying by pulsed and conventional fluidised-bed dryers are compared. Experimental results have shown that the variation of moisture content at the exits of both dryer types in test runs was very small. Heat utilisation was more effective when such dryers were used to dry paddy at moisture contents above 24% dry basis and up to 50% of the thermal energy was saved by recycling 70–80% of the air. Paddy qualities i.e. head-rice yield and colour of the dried white rice were similar with both dryers and almost the same as the original undried values, or slightly higher in the case of head-rice yield, depending upon the drying conditions. Below 28% dry basis, it is recommended that inlet-air temperature should be lower than 145 °C in order to maintain white colour. The cooked rice obtained from paddy dried at a temperature of 145 °C was harder than naturally dried control samples. A mathematical model based on energy and mass balance predicted values in good agreement with experimental results for both the pulsed and conventional fluidised-bed dryers. Calculated thermal and electrical energy consumptions indicated that the pulsed flow dryer was more economical than the conventional dryer.

Keywords: Modelling; Paddy drying; Quality; Pulsed fluidised beds

*Corresponding author. Tel.: +662-4270-9221; fax: +662-428-3534.
E-mail address: somkiat.pra@kmutt.ac.th (S. Prachayawarakorn).

0022-474X/$ - see front matter © 2004 Elsevier Ltd. All rights reserved.
doi:10.1016/j.jspr.2004.06.003

Nomenclature

C_a	specific heat of dry air, kJ/kg °C
C_v	specific heat of water vapour, kJ/kg °C
C_{pw}	specific heat of moist paddy, kJ/kg °C
h_{fg}	latent heat of water, kJ/kg
$M(t)$	moisture content of paddy at time t, decimal dry basis
M_{eq}	equilibrium moisture content of paddy, decimal dry basis
M_{in}	initial moisture content of paddy, decimal dry basis
M_f	outlet moisture content, decimal dry basis
$M_{i,n}$	moisture content of paddy at the inlet of the nth element, dry basis decimal
$M_{f,n}$	moisture content of paddy at the outlet of the nth element, dry basis decimal
$\dot{M}_p$	grain mass flow rate, kg/s
$\dot{m}_{inlet}$	total mass of dry air at drying chamber inlet, kg/s
m_s	total mass of paddy at drying chamber, kg
P	pressure drop, Pa
Q	specific thermal energy, kJ/kg water evaporated
R	ratio of mass of dry paddy to mass of dry air, kg dry paddy/kg dry air
SEC	specific electrical energy, kJ/kg water evaporated
T_i	temperature of ambient air, °C
$T_{f,avg}$	exhaust air temperature, °C
$T_{f,n}$	outlet-air temperature at the nth element, °C
T_{inlet}	inlet-air temperature at drying chamber, °C
T	drying time, s
$W_{f,avg}$	humidity ratio of air at the dryer outlet, kg H_2O/kg dry air
$W_{f,n}$	outlet-humidity ratio of air at the nth element, kg H_2O/kg dry air
W_{inlet}	inlet-humidity ratio of air, kg H_2O/kg dry air
θ_{in}	grain temperature, °C
η	combustion efficiency, decimal
η_{fan}	fan efficiency, decimal
ρ_{air}	air density, kg/m^3

1. Introduction

Fluidisation is a technique in which a bed of solid particles is transformed to a liquid-like condition by passing a stream of fluid through the solid bed, at a sufficiently high velocity that frictional forces between the particles and flowing fluid counterbalance the weight of particles. Above this velocity, the pressure drop across the bed is always constant even though fluid velocity increases. This velocity is referred to as the minimum fluidisation velocity. In the operation of a conventional fluidised bed, the air velocity used is at least 1.5 times the minimum fluidisation velocity, in order to obtain good gas–solid contact performance and sustain stable solid particle movement.

Whenever the fluidised-bed technique is applied to solid particles that have strong cohesive forces, fluidisation may not behave as well. Paddy kernels at high moisture content are easily agglomerated and their agglomerations result in poor heat and mass transfer rates. Use of high velocities to prevent agglomeration may not be appropriate for drying grains in which moisture transport inside grains is dominated by internal diffusion, resulting in wastage of energy. To solve this problem, different approaches are employed. Application of mechanical vibrations or pulsations to improve the fluidisation quality is an interesting technique (Gawrzynski and Glaser, 1996; Nie and Liu, 1998; Soponronnarit et al., 2001). Work on drying using the pulsation technique has shown that the pulsed gas stream can improve the drying rate, especially for solids that have a high moisture content.

Pulsed fluidised beds seem to be more fashionable than conventional fluidised beds requiring high velocity, because of lower power requirements in the air unit (Gawrzynski et al., 1996). Furthermore, pulsing the air influences the dynamics of the bubbles, which improves gas–solid contact performance. A bubble can break up into two small bubbles (Moussa and Fowle, 1985).

The objective of this work was to study the performance of industrial-scale pulsed and non-pulsed fluidised-bed paddy dryers, and to propose a mathematical model to predict the paddy moisture change and the energy consumption for both dryer types. The physical quality of the paddy, in terms of head-rice yield and whiteness, was also determined. In the pulsed fluidised bed, the airflow was relocated by rotating two metal sheets. Air was supplied to the dryer at the required flow rate and the metal sheet distributed the air to the respective sections of the plenum without stopping the flow. This redistribution did not affect the external design of the rigid-frame dryer because pulsation forces were directly conveyed to bed particles.

2. Material and methods

A pulsed fluidised-bed dryer (PFBD), of 20 tonnes/h capacity (Fig. 1), was operated in a continuous mode in which paddy was moved in cross-flow to the pulsed air. Air was transported through the main duct, containing two metal sheets rotating continuously at a particular angular velocity, as presented in Fig. 1b. The pulsed airflow was then passed through a particular section of the paddy bed (along the left or right of the drying chamber), thereby fluidising the paddy kernels. Paddy in the remaining part of the bed behaved as a packed bed. Operation of the conventional fluidised bed was similar to that of the pulsed fluidised bed, except that airflow in the conventional type was uniform throughout the bed.

The total exhaust air was cleaned by a cyclone separator before escaping to atmosphere. In the present work, a backward-curved blade centrifugal fan, with a 37 kW motor, was used to generate the required airflow, and a rice-husk furnace was used to heat the air to the specified temperature. The desired fan power was relatively lower in the pulsed fluidised bed than in the conventional fluidised-bed dryer (FBD), at least 25% less for the same capacity. Frequency of rotation for the plates was fixed at 25 cycles/min and grain residence time was 1.5 min.

Experiments were carried out at private rice mills, located in the northeast of Thailand. Initial moisture contents from harvest varied between 28% and 30% dry basis. Foreign materials present in the paddy bulk were removed before the paddy kernels were passed through the drying section. Superficial velocity in the drying chamber, measured by a static pitot tube, was 1.85 m/s. The

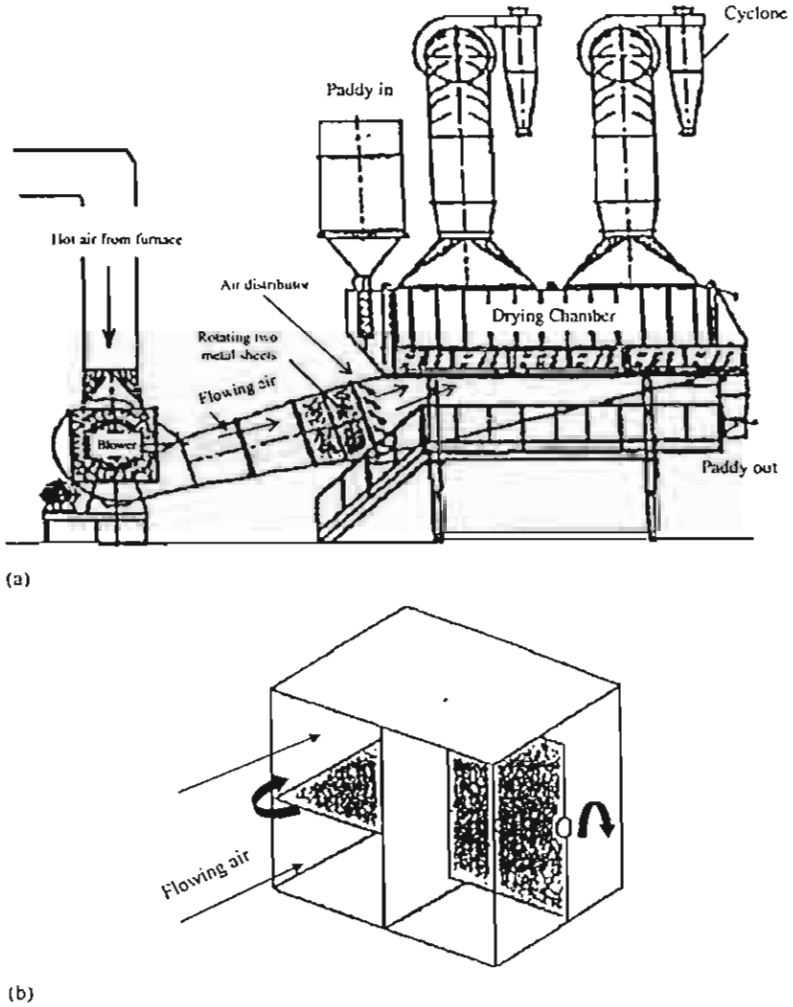

Fig. 1. Schematic diagram of pulsed fluidised bed with relocated air. (a) Pulsed fluidised-bed dryer. (b) Direction of rotating two metal sheets.

drying temperature used was dependent on initial moisture content; a high temperature was preferred at high moisture contents. For the present study, drying temperature was in the range of 144–154 °C. When conditions, i.e. drying air temperature and feed rate, reached steady state, outlet moisture content, temperature and paddy quality were examined. Inlet- and outlet-air temperatures were monitored by a data logger, with an accuracy of ±1 °C. Power consumed by the fan was measured by a clamp-on power meter, with an accuracy of ±3%.

Samples taken from the dryer outlet at various operating times were used to determine the moisture content, head-rice yield and rice whiteness. Moisture content was determined in a fan-forced oven at a temperature of 103 °C for 72 h. White rice colour was measured with a SATAKE whiteness meter. For head-rice yield, a 125 g paddy sample was dehusked with a two-rubber roller machine and the bran was removed with a SATAKE milling machine. Head-rice was separated

from brokens by a sieving screen. Head-rice yield was defined in this study as the ratio of head-rice mass to original paddy mass.

Hardness of cooked rice was measured with an Instron Universal Testing Machine (model TA-XT2i). A 30 g sample was placed in an aluminium cylindrical cup and the sample rinsed and strained to remove excess water. Distilled water was added at a ratio of 1:1.5 of rice to water by weight and the samples presoaked at room temperature for 10 min and then cooked in an automatic rice cooker. After completion of the cooking cycle, samples were held for a further 10–15 min in the cooker and then cooled to room temperature. A sample of 50 g of the cooked rice was taken from the middle cup. The test speed for compressing the sample was 0.5 mm/s and the post-test speed was 10 mm/s. The hardness of cooked rice was defined as the minimum force required to compress it to 90% of its initial height.

3. Mathematical model

In the pulsed fluidised bed, transport of kernels and air is at right angles with grains moving from one side of the dryer to the other while air flows upward. Under such movement, there exists a simultaneous heat and mass transfer and the product moisture content is reduced along the direction of grain movement. To describe the change in moisture content mathematically, the dryer is divided into N small elements as shown in Fig. 2. The mass balance equation for a single element is written as

$$W_{f,n} = R(M_{i,n} - M_{f,n}) + W_{inlet}, \tag{1}$$

where $W_{f,n}$ is outlet-humidity ratio of air at the nth element (kg H_2O/kg dry air), W_{inlet} is inlet-humidity ratio of the air, R is ratio of mass of dry paddy to mass of dry air (kg dry paddy/kg dry air), $M_{i,n}$ is paddy moisture content at the inlet of the nth element (dry basis decimal) and $M_{f,n}$ is paddy moisture content of paddy at the outlet of the nth element. From the heat balance equation for a single element, the outlet-air temperature, $T_{f,n}$, at the nth element is

$$T_{f,n} = (C_a T_{inlet} + W_{inlet}(h_{fg} + C_v T_{inlet}) - W_{inlet} h_{fg} + RC_{pw}\theta_{in})/(C_a + W_{f,n}C_v + RC_{pw}), \tag{2}$$

where C_a is specific heat of dry air (kJ/kg °C), C_v is specific heat of water vapour, C_{pw} is specific heat of moist paddy, h_{fg} is latent heat of water (kJ/kg), T_{inlet} is air temperature at drying chamber inlet and θ_{in} is grain temperature.

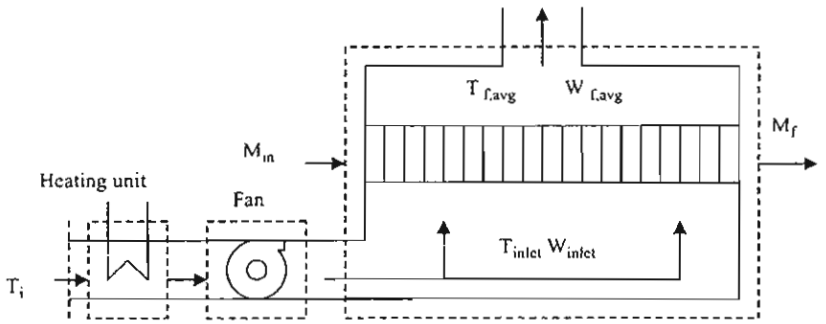

Fig. 2. Control volumes of fluidised bed.

Eqs. (1) and (2) describe the change in humidity and temperature in the gas phase. In writing Eq. (2), we make several simplifying assumptions. First, grain temperature is in thermal equilibrium with outlet-air temperature, implying a high transfer rate of heat between air and the grain bed. It will also be assumed that grain movement and pulsing air may be described by a plug flow model although grain dispersion may occur while the bed of particles is fluidised. This effect is small, however, based on observations during experiments. The proposed model is similar to the previous work reported by Soponronnarit et al. (1996a).

Average temperature and absolute humidity at the dryer outlet are calculated by the arithmetic means

$$T_{f,avg} = \frac{\sum_{i=1}^{n} \rho_{air} C_a T_{f,n}}{\sum_{i=1}^{n} \rho_{air} C_a} \tag{3}$$

and

$$W_{f,avg} = \frac{\sum_{i=1}^{n} W_{f,n}}{n}, \tag{4}$$

where $T_{f,avg}$ is exhaust air temperature, $W_{f,avg}$ is humidity ratio of air at the dryer outlet, ρ_{air} is air density (kg/m^3) and n is number of elements.

Change in moisture content of paddy during drying is modelled by the following empirical form:

$$\frac{M(t) - M_{eq}}{M_{in} - M_{eq}} = \exp(-xt^y), \tag{5}$$

where

$$\begin{aligned} x = {} & 0.00163100 T_{inlet} - 1.16202(\dot{m}_{inlet}/m_s) \\ & + 0.00415300(\dot{m}_{inlet}/m_s) T_{inlet} \\ & + 0.147383 \ln(\dot{m}_{inlet}/m_s) + 0.474743, \end{aligned}$$

$$\begin{aligned} y = {} & -0.00322000 T_{mix} - 0.835960(\dot{m}_{inlet}/m_s) \\ & + 0.0203190(\dot{m}_{inlet}/m_s) T_{inlet} \\ & - 0.143150 \ln(\dot{m}_{inlet}/m_s) + 0.548493, \end{aligned}$$

where M_{in} and M_{eq} are, respectively, moisture content of paddy at the beginning and at equilibrium, t is drying time (s), $\dot{m}_{inlet}$ is total mass flow rate at the drying chamber inlet (kg/s) and m_s is total mass of paddy in the drying chamber (kg).

Eq. (5) was developed by Sripawatakul (1994) and was valid for temperatures ranging from 90 to 150 °C and specific airflow rates of 0.03–0.16 kg/s/kg dry matter of paddy. Eq. (5) showed that faster drying rates were achieved with both higher temperatures and specific air flow rates, the first being the more significant effect. For calculating moisture content at any time t, Eq. (5) is differentiated with respect to t and the finite difference technique is then applied. Moisture content

of paddy in the next layer can be determined by substituting the known values of both moisture content in the previous layer and time step into the differentiated equation (5). By repeating the calculation procedure, outlet moisture content is eventually estimated.

Specific thermal energy used for evaporating water is calculated using

$$Q = \frac{\dot{m}_{inlet}(C_a + C_v W_i(T_i - T_{f,avg})}{\eta \dot{M}_P(M_{in} - M_f)}, \tag{6}$$

where Q is specific thermal consumption (kJ/kg water evaporated), $\dot{M}_p$ is grain mass flow rate (kg/s), M_f is moisture content at the dryer outlet and η is the combustion efficiency (decimal).

Electrical energy consumption can be determined using

$$SEC = P\left(\frac{\dot{m}_{inlet}/\rho_{air}\eta_{fan}}{\dot{M}_p(M_{in} - M_f) \times 1000}\right), \tag{7}$$

where SEC is electrical energy consumption (kJ/kg water evaporated), P is the pressure drop of the system (Pa) and η_{fan} is fan efficiency. The fan efficiency is about 0.8.

4. Results and discussion

4.1. Moisture content and grain temperature

Paddy quality, in particular head-rice yield, rice whiteness and cooking quality is usually affected by drying conditions: temperature and grain exposure time or moisture content from the dryer outlet. Poor head-rice yield is normally observed with non-uniform grain moisture at the outlet. In evaluation of dryer performance, it is thus necessary to consider all relevant parameters. Fig. 3 shows the variation in outlet moisture content (Fig. 3a) and outlet grain temperature (Fig. 3b) in the fluidised bed with no pulsation. The inlet moisture content was $33.0 \pm 0.3\%$ dry basis and when passed through the conventional dryer, the outlet moisture content was 25.3% dry basis with a standard deviation of 0.7% dry basis, indicating a small variation in outlet moisture content. This result also implied only limited dispersion of grains in the dryer. The outlet grain temperature was $77 \pm 1\,^{\circ}C$. Effect of pulsation on variation in grain temperature and moisture content, as shown in Fig. 4 (corresponding to Experiment 1 in Table 1), was not remarkable, as indicated by the standard deviation in outlet moisture content and grain temperature being 0.7% dry basis and $2\,^{\circ}C$, respectively. Such variations are still small and similar to those found in the conventional FBD. The other tests presented in Table 1 showed similar standard deviations of temperature and moisture content at the outlet.

As shown in Table 1, the moisture content at the dryer outlet was still relatively higher than the level appropriate for storage and the grain needed to be further dried. Reducing moisture content from 22.2% to 16% dry basis is a very difficult step since the remaining water, which exists in the interior of the grain, moves slowly through the diversity of components and chaotic void space to reach the exterior surface and eventually evaporates into the air stream. Hence, drying rate is low, although heat transfer and contact between solid particles and air are good. Application of fluidised-bed technology at this drying stage is not effective, since the energy is largely wasted, as

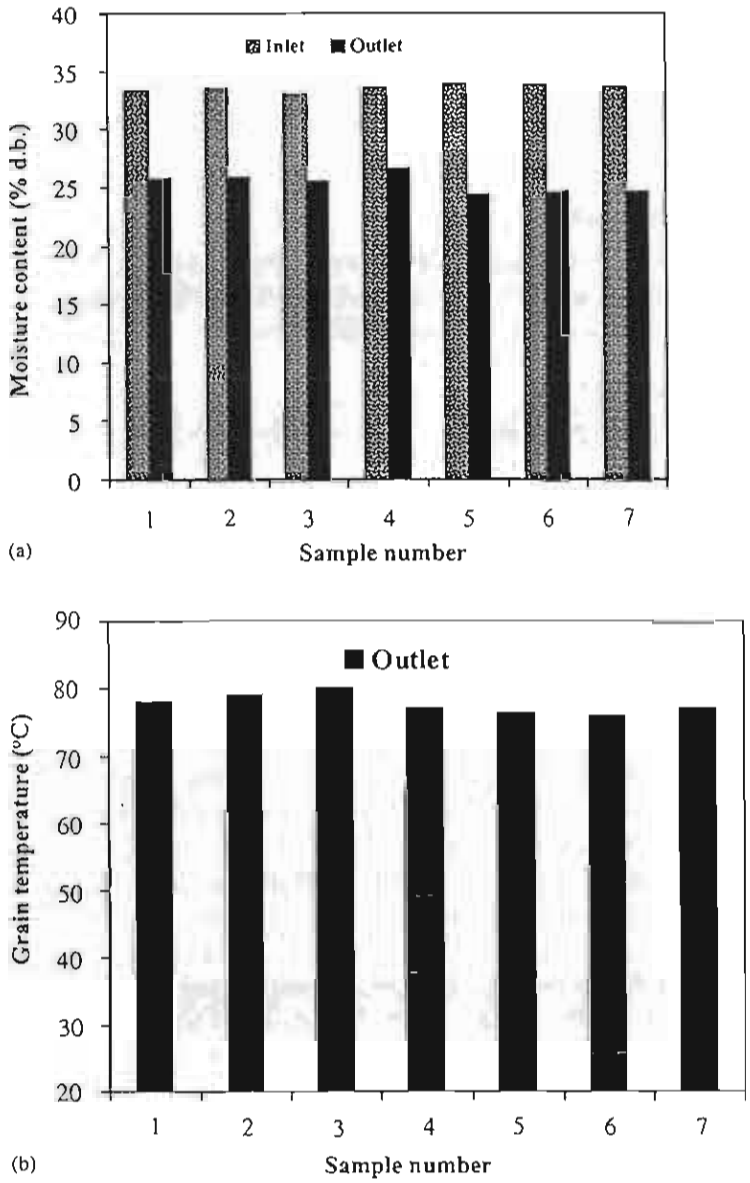

Fig. 3. Changes in moisture content and grain temperature in a conventional fluidised bed (feed rate of 3.8 tonnes/h, inlet-air temperature of 145 °C, superficial velocity of 2.8 m/s and residence time of 1.4 min, Soponronnarit et al., 1998). (a) Moisture content of paddy taken from dryer inlet and outlet. (b) Grain temperature taken from dryer outlet.

discussed in the following section, and the percentages of broken kernels are enormous. As is common practice at the rice mills, a fixed-bed or mixed-flow dryer should be applied for the slow-drying stage (Srzednicki and Driscoll, 1995; Soponronnarit et al., 1997; Giner et al., 1998).

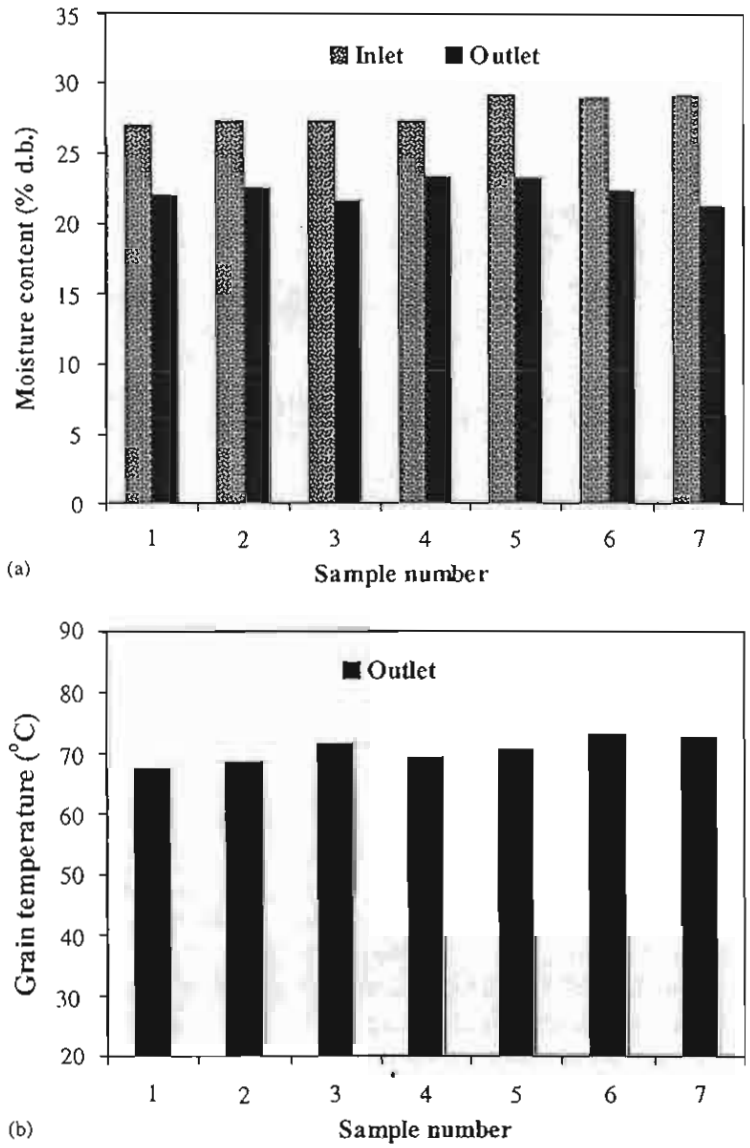

Fig. 4. Changes in moisture content and grain temperature in a pulsed fluidised bed (feed rate of 16.13 tonnes/h, inlet-air temperature of 145 °C and rotation speed of 25 cycles/min). (a) Moisture content of paddy taken from dryer inlet and outlet. (b) Grain temperature taken from dryer outlet.

4.2. *Energy consumption*

The thermal energy used for drying paddy in the rice industry is produced from two main energy sources, rice husk combustion in a cyclonic furnace and diesel oil in a burner. Gases resulting from combustion are used directly to dry paddy. When diesel oil is used as raw material for heating, a certain portion of the exhaust air is reused by mixing it with fresh air and the

Table 1
Experimental results: pulsed fluidised-bed paddy drying (no air recycling)

Experiment No.	1	2	3
Feed rate (tonnes/h)	16.13	15.87	15.18
Inlet-air temperature (°C)	145	144	154
Rotation speed of two metal sheets (cycle/min)	25	25	25
Grain temperature (°C)			
Inlet	40 ± 1[a]	40 ± 0.7	38 ± 0.5
Outlet	70 ± 2	71 ± 2	73 ± 1.8
Moisture content (% d.b.)			
Inlet	27.9 ± 0.9	28.4 ± 0.34	30.2 ± 0.9
Outlet	22.2 ± 0.7	23.1 ± 0.8	23.8 ± 0.4
Thermal energy (MJ/kg water evap.)	6.3	6.5	7.8
Hardness (kg)			
Before drying	29.4	29.4	NA
After drying	31.9	30.1	NA

[a]Mean ± standard deviation ($n = 7$ replicates).

remainder released to environment. By contrast, for a rice husk-type energy source, all exhaust air is vented to atmosphere. Specific data on conventional fluidised beds with/without air recirculation, presented in Fig. 5, were obtained from various workers (Soponronnarit et al., 1995, 1998; Meeso et al., 2000; Sungareeyakul et al., 2002). The amount of thermal energy consumed was calculated from Eq. (5), assuming a combustion efficiency of 70% for the rice husk (Swasdisevi et al., 1997) and complete combustion of diesel oil.

As shown in Fig. 5, for the FBD with no air recirculation, the energy consumption curve has an exponential decay characteristic when plotted against initial moisture content, showing the rapid reduction in energy consumption when the initial moisture content increases from low levels to 24% dry basis. The corresponding energy consumption drops from 14 MJ/kg water evaporated to approximately 7.2 MJ/kg water evaporated. At moisture contents higher than 24% dry basis, energy consumption changes only slightly with the initial moisture content. This result emphasises the powerful potential of a fluidised bed to remove water in the high moisture range, since the drying medium surrounds individual particles and comes into direct contact with water concentrated near the particle surface, thus allowing the water to evaporate easily without the interference of the physical structure of the paddy kernel. This performance, however, is not observed when a FBD is applied at relatively low moisture contents, where the particle surfaces are rather dry, although the convective heat transfer coefficient is high and has almost the same magnitude as for high moisture contents under similar drying conditions. Hence, high consumption is a consequence of reduced availability of surface moisture.

As observed from Fig. 4, the reduction in moisture transfer rate in the PFBD, calculated by ΔM% dry basis divided by the residence time, was 4.1% dry basis/min, slightly lower than in the

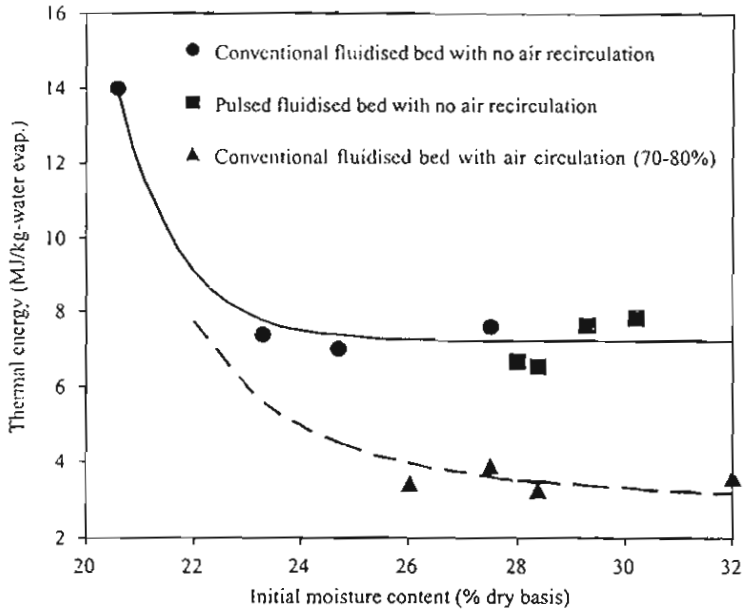

Fig. 5. Thermal energy consumption at different initial moisture contents (inlet-air temperature of 140–150 °C and final moisture content of 18–22% dry basis).

conventional dryer at 5.1% dry basis/min as shown in Fig. 3. The reduced drying rate for the PFBD does not imply poor performance, since in this case the amount of thermal energy consumption was also reduced with drying rate. Therefore, when energy consumption is plotted in terms of amount of consumed energy per kilogram water evaporated as shown in Fig. 5, the PFBD at a frequency of 25 cycles/min did not show much difference from the conventional dryer. According to these results, it would be difficult to indicate which technique is more efficient, and thus more investigation into the theory is needed as shown in a later section.

Fig. 5 also shows that thermal energy efficiency can be improved remarkably by recirculating exhaust air. Energy saved may be up to 50% at an air recycling ratio between 70% and 80%, at which the amount of consumed energy lies between 3 and 4 MJ/kg evaporated water if the initial moisture content is higher than 25% dry basis.

Table 2 presents electrical energy consumption for PFBD and conventional FBD systems. Data were recorded from a system having similar main components, such as a rice-husk cyclonic furnace and non-recirculating air. As illustrated in the conventional FBD, the larger amounts of electrical energy consumed were closely related to the lower initial moisture content, with values being 0.27, 0.33 and 0.65 MJ/kg evaporated water at initial moisture contents of 27.5%, 23.3% and 20.6% dry basis, respectively.

The beneficial effect of pulsation flow over a conventional FBD is in the reduced electrical energy consumption; the amount of electrical energy consumed under similar drying conditions is 0.19 MJ/kg evaporated water for the PFBD at 25 cycles/min, and 0.27 MJ/kg evaporated water for the FBD (Experiment No. 2).

Table 2
Electrical energy consumption for fluidised-bed dryer with no air recirculation

	Pulsed fluidised-bed dryer	Conventional fluidised-bed dryer		
		1	2	3
Feed rate (tonnes/h)	16.13	11.8	9.3	10.5
Inlet-air temperature (°C)	145	140	145	149
Moisture content (% d.b.)				
Inlet	28.0	27.5	23.3	20.6
Outlet	22.2	22.5	18.5	18.4
Evaporation rate (kg water evap/h)	731	461	362	192
Electrical energy consumption (MJ/kg water evap.)	0.19	0.27	0.33	0.65

4.3. Head-rice yield

Since the head-rice yield of freshly harvested paddy was different in each test depending upon harvest history and season, relative head-rice yield, defined as the value of head-rice yield of paddy dried by the hot-air drying divided by that dried by natural air, was presented in Fig. 6. Throughout the experiments, the initial moisture content of samples covering the range between 24% and 30% dry basis was reduced to 21–24% dry basis, depending upon the inlet-air temperature. The influence of inlet-air temperature and drying technique on the head-rice yield of paddy is shown in Fig. 6, indicating that head-rice yield was not related to airflow characteristics (whether uniform or pulsating), but was related negatively or positively with temperature. Drying at temperatures below 145 °C reflected a small reduction in head-rice yield, values varying between 95% and 98%. Breaking of kernels in milling is caused by the high moisture gradient of paddy during drying, enabling development of internal stresses causing fissures as a consequence (Kunze and Choudhury, 1972; Kobayashi et al., 1972). Head-rice yield for paddy dried at temperatures beyond 150 °C was improved and higher than that of the paddy dried naturally, relative head-rice yield at high-temperature drying being between 103% and 110%. The improved head-rice yield indicates that drying at this temperature directly affects the conformational structure of starch granules improving their ability to withstand milling forces. Swelling of starch granules along with subsequent leaching of amylose from the granules to outer space generates stronger intermolecular binding forces between granules, implying the gelatinisation of starch granules. Inprasit and Noomhorm (2001) reported that starch gelatinisation was occurring partially in this moisture range for paddy and some starch granules fused themselves to form composite clusters with a smooth interior.

4.4. Hardness

In testing the performance of a PFBD, paddy samples were taken from different seasons, the dry season in Experiments 1 and 2 as shown in Table 1. The hardness of cooked rice without heat treatment was 29.4 kg for Experiments 1 and 2. The hardness of cooked-rice samples for these

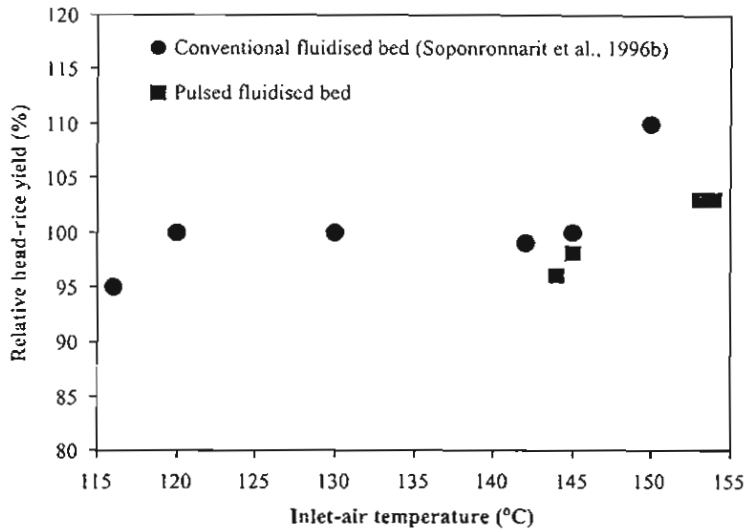

Fig. 6. Relative head-rice yield obtained from the pulsed and conventional fluidised-bed dryers (Soponronnarit et al., 1996b) operated at various temperatures (initial moisture content of 26–30% dry basis and final moisture content of 21–24% dry basis).

experiments tended to increase by 5.7–8.5% relative to the gently dried sample. Increased hardness is probably due to partial gelatinisation of the starch. Such an increase in hardness of cooked rice, after the paddy was thermally treated at high temperature, has also been reported by Gujral and Kumar (2003) and Inprasit and Noomhorm (2001).

It should be noted that the stronger inter-molecular binding forces resulting from the formation of partial gelatinisation may not always improve head-rice quality. This can be noticed easily in the case of paddy dried at 145 °C, as presented earlier in Fig. 6. This might be because the degree of gelatinisation produced is so small that binding forces between granules are weaker, compared with forces generated by moisture stresses, thereby reducing the proportion of whole kernels after milling.

4.5. Whiteness

As for head-rice yield, colour of milled rice was defined as relative whiteness. Colour of the paddy dried by conventional and pulsed FBD at different inlet-air temperatures is shown in Fig. 7. At an inlet temperature below 145 °C, colour of milled rice samples, with an initial moisture range of 24% to 30% dry basis, was slightly degraded by heat, as indicated by most data indicating the value of relative whiteness between 98% and 100%. Similarly, colour of milled rice from the paddy at the higher moisture content of 29% dry basis dried at a temperature higher than 150 °C was also slightly inferior. At a moisture content of 27% dry basis, however, it appeared to darken and yellow when a higher temperature of 150 °C was used. Consequently, colour of the white rice showed a relatively large drop to a value of 91% (see Fig. 7). Such a

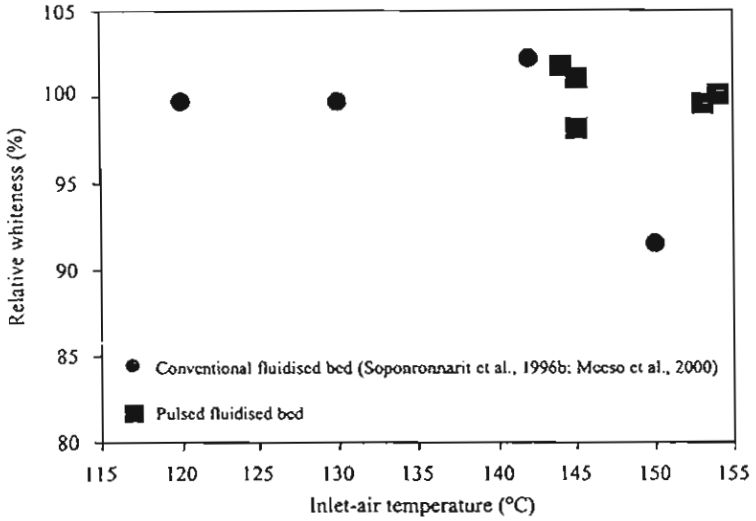

Fig. 7. Relative whiteness obtained from the pulsed and conventional fluidised-bed dryers (Soponronnarit et al., 1996b) operated at various temperatures (initial moisture content of 26–30% dry basis and final moisture content of 21–24% dry basis).

negative change in colour is induced by the more rapid increase in grain temperature for samples at lower moisture content, leading towards faster non-enzymatic browning.

To maintain colour at its original value, paddy at a lower moisture content of 27–28% dry basis should be in contact with drying air at a lower temperature, 145 °C being the maximum allowable temperature. Under these drying conditions, however, head-rice recovery falls slightly due to moisture stresses.

The experimental results previously presented on energy consumption and paddy quality, showed the PFBD as a possible alternative method for drying paddy. Paddy quality, in terms of head-rice yield and colour obtained from the pulsed and conventional FBD, was comparable. Drying at a temperature of 150 °C or slightly above should be applied only to a higher initial moisture content of 29% dry basis. High quality dried paddy can be achieved, particularly with head-rice yield being slightly higher than that of the original sample.

4.6. Validation of a mathematical model

To predict outlet moisture content, average absolute humidity of air leaving the dryer was calculated and a finite difference approach used to solve the resulting set of equations. Knowing T_{inlet} enabled determination of the moisture content of paddy leaving the first control volume, using Eq. (5). From Eqs. (1) and (2), humidity and temperature at the outlet of the first control volume were readily calculated. The same calculation procedure was repeated with successive control volumes until the dryer exit. Average outlet temperature and humidity were eventually determined by Eqs. (3) and (4). In addition, the thermal and electrical energy consumptions were determined by Eqs. (6) and (7), respectively.

Fig. 8 presents the results of calculated outlet moisture content compared with the experimental values taken from the conventional and pulsed FBD. Inlet moisture content of paddy in the experiments varied between 25.5% and 26.5% dry basis and inlet-air temperature was fixed at a temperature of 116 °C for the conventional dryer. For the PFBD, drying conditions were as shown in Table 1. The proposed model predicted outlet moisture content from the conventional FBD as lower than the experimental value, with a maximum error of prediction being 2.5% as shown in Fig. 8a.

When applying the same model to predict outlet moisture content from the PFBD, the pulsed airflow needed to be modified by taking the average velocity, determined by total airflow rate divided by the cross-sectional area of the drying chamber. It can be seen that the model described well the change in moisture content, in agreement with the experiment, as indicated by the estimated error lines of $\pm 2.7\%$ in Fig. 8b. The accuracy of the prediction of a simplified analysis clearly points out the negligible effect of pulsing the flow on diffusional mass transfer inside the kernel, although the convective heat transfer rate estimated by this approach was rather high due to the increase in local velocity.

The proposed model also reasonably quantified the amount of thermal energy consumed in the pulsed dryer, with a prediction error of $\pm 3.0\%$ of the measured quantity which ranged from 6.3 to 7.8 MJ/kg water evaporated. These calculated results are not presented here.

The simulation was then used to compare pulsed and conventional FBD. Inlet moisture content was set at 28% d.b., bed depth was fixed at 12 cm and all exhaust air was conveyed to atmosphere. Pulsation frequency was fixed at 25 cycles/min and maximum pulse velocity in the PFBD was limited to 3.0 m/s, equivalent to an average superficial velocity of 1.5 m/s throughout the bed, since kernels had a chance of being entrained out of the chamber at pulse speeds higher than 3.0 m/s. For the conventional FBD, air speed was fixed at 2–2.5 m/s. Other drying conditions were identical for both dryer types. Simulation results (Fig. 9) show that the PFBD used slightly less energy, in terms of heat and electricity, than the conventional dryer, whilst its ability to remove water was less (due to the lower average airflow rate). Lower water removal rate in the pulsed-flow dryer can be attributed to higher humidity inside the environmental drying chamber. The corresponding moisture content at the paddy surface became higher, reducing the driving force of moisture concentration difference between the centre and surface. The resulting water movement inside the kernel decreased.

Experimental and simulation results indicated that the pulsed-flow dryer had a great potential for drying paddy. Since the total airflow rate used was relatively lower in the pulsed-flow dryer than the conventional FBD, electrical energy consumption was reduced by at least 30%. In addition, transfer of heat from air to the grain bed was more effective, reducing thermal energy consumption and thus increasing drying efficiency. The main drawback of this dryer was the slightly lower drying capacity, which may not be favoured by the grain industry which strives for high capacity. The general situation found in industry, however, indicated that the initial moisture content in grain obtained from fields varied from 21% to 33% dry basis, depending upon harvesting season. The pulsed-dryer type is suitable for this wide range of moisture content since at lower moisture contents, heat utilisation in the PFBD is more efficient than the conventional FBD because using a higher air volume does not increase drying rate for the low moisture range.

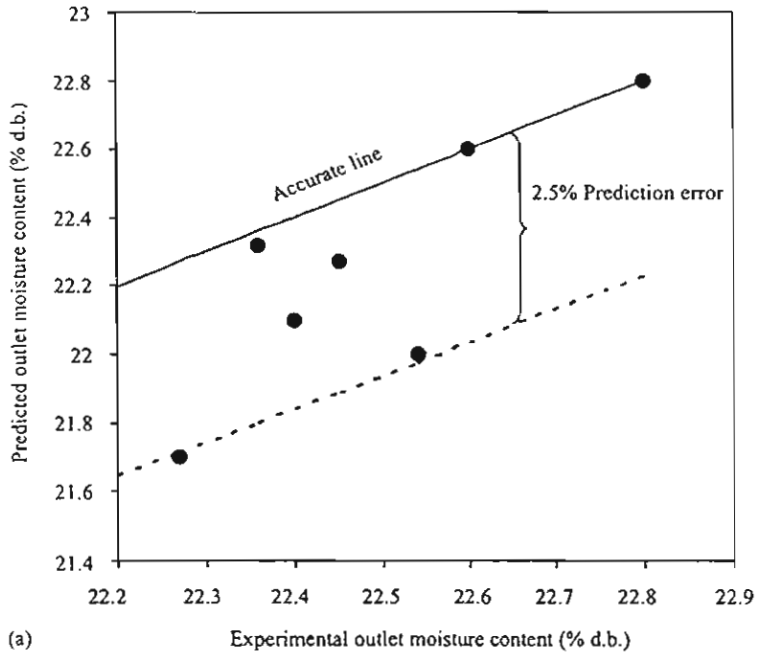

Fig. 8. Experimental and predicted values of outlet moisture content. (a) Conventional fluidised bed with a capacity of 9.5 tonnes/h (inlet-air temperature of 116 °C and superficial velocity of 2.2 m/s, Wangji, 1996). (b) Pulsed fluidised bed with a capacity of 15–16 tonnes/h (inlet-air temperature of 145–154 °C and superficial velocity of 1.5 m/s and frequency of 25 cycles/min).

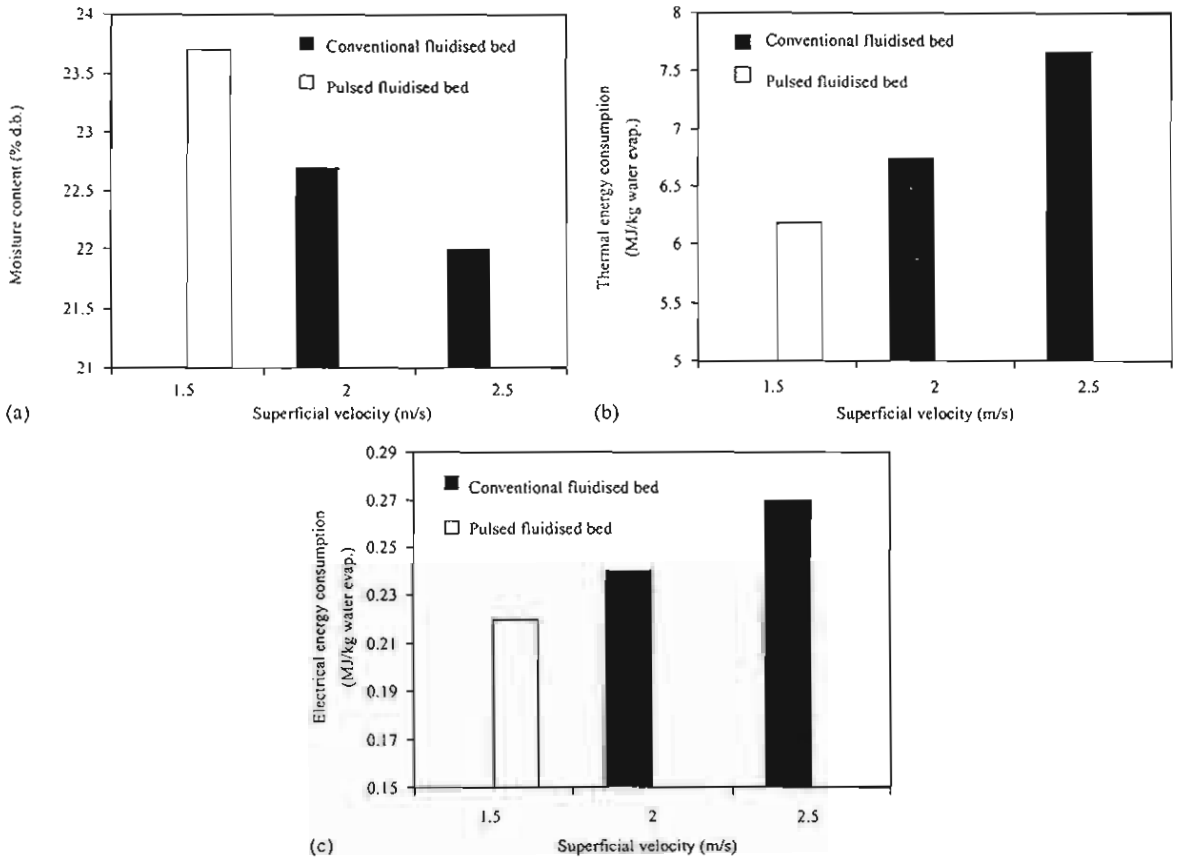

Fig. 9. Simulated performance of pulsed and conventional fluidised-bed dryers (inlet temperature of 145 °C, drying capacity of 20 tonnes/h and initial moisture content of 28% dry basis).

5. Conclusions

The moisture content of grain leaving pulsed and conventional fluidised-bed dryers did not differ greatly. Thermal energy consumed was between 6.5 and 7.8 MJ/kg water evaporated at moisture contents higher than 24% dry basis for both dryer types, without air recirculation. Below 24% dry basis, where internal water transport was restricted by diffusion, the thermal energy requirement was rapidly increased. When exhaust air was recycled, heat utilisation became more effective, with a 50% thermal energy reduction at 70–80% of recycled air. Electrical energy consumed by the pulsed fluidised bed was at least 30% lower than conventional FBD, and drying efficiency was higher. The mathematical model reasonably predicted the moisture change observed in the experiments. Simulation results showed better performance, in terms of energy consumption per unit moisture extracted, for the pulsed flow dryer than for the conventional FBD, whilst its ability to remove moisture was reduced. Head-rice yield and colour of white rice samples after drying were almost identical to those which were dried gently as a control over the whole range of moisture reduction from 24–30% dry basis down to 21–24% dry basis At an initial

moisture content lower than 28% dry basis, it was shown that inlet-air temperature should not be higher than 145 °C in order to avoid unacceptable change in colour of white rice. Hardness of cooked rice for samples dried at high temperature increased by about 8–12%, relative to the gently dried control sample.

Acknowledgements

The authors would like to thank The Thailand Research Fund for their financial support.

References

Gawrzynski, Z., Glaser, R., 1996. Drying in pulsed–fluid bed with relocated gas stream. Drying Technology 14, 1121–1172.

Gawrzynski, Z., Glaser, R., Zgorzalewicz, J., Pelech, Z., Stanislawski, J., Rogula, G., Pieczaba, B., 1996. Operational tests of a pulsed fluid bed dryer/cooler for granulated sugar. In: Strumillo, C., Pakowski, Z. (Eds), Proceedings of the 10th International Drying Symposium, Krakow, Poland, 30 July–2 August 1996, pp. 771–777.

Giner, S.A., Bruce, D.M., Mortimore, S., 1998. Two-dimensional simulation model of steady-state mixed-flow grain drying, part 1: the model. Journal of Agricultural Engineering Research 71, 37–50.

Gujral, H.S., Kumar, V., 2003. Effect of accelerated aging on the physicochemical and textural properties of brown and milled rice. Journal of Food Engineering 59, 117–121.

Inprasit, C., Noomhorm, A., 2001. Effect of drying air temperature and grain temperature of different types of dryer and operation on rice quality. Drying Technology 19, 389–404.

Kobayashi, H., Miwa, Y., Ishikowa, M., 1972. On the mechanism of cracking in rice kernels during drying of paddies; particularly moisture distribution and drying strain in one kernel. Research Bulletin of the Faculty of Agriculture of Gifu University 33, 279–293.

Kunze, O.R., Choudhury, M.S.U., 1972. Moisture adsorption related to the tensile strength of rice. Cereal Chemistry 49, 684–696.

Meeso, N., Soponronnarit, S., Wetchacama, S., 2000. Evaluation of drying system performance of rice mills in the central part of Thailand. Engineering Journal Kasetsart 14, 81–93 (in Thai).

Moussa, N.A., Fowle, A.A., 1985. Exploratory study of pulsed atmospheric fluidized-bed combustion. Proceedings of Eighth International Conference on Fluidized-Bed Combustion, vol. III, Texas, USA, pp. 1300–1310.

Nie, Y., Liu, D., 1998. Dynamics of collapsing fluidised beds and its application in the simulation of pulsed fluidised beds. Powder Technology 99, 132–139.

Soponronnarit, S., Yapha, M., Prachayawarakorn, S., 1995. Cross-flow fluidised bed paddy dryer: prototype and commercialization. Drying Technology 3, 2207–2216.

Soponronnarit, S., Prachayawarakorn, S., Sripawatakul, O., 1996a. Development of cross-flow fluidized bed paddy dryer. Drying Technology 14, 2397–2410.

Soponronnarit, S., Prachayawarakorn, S., Wangji, M., 1996b. Commercial fluidised-bed paddy dryer. In: Strumillo, C., Pakowski, Z. (Eds), Proceedings of the 10th International Drying Symposium, vol. (A), Krakow, Poland, 30 July–2 August 1996, pp. 638–644.

Soponronnarit, S., Amatachaya, P., Prachayawarakorn, S., Nathakaranakule, A., Inchan, S., 1997. Field trial of in-store drying and storage. The Kasetsart Journal 18, 86–100.

Soponronnarit, S., Rordprapat, W., Wetchacama, S., 1998. Mobile fluidised bed paddy dryer. Drying Technology 16, 1501–1513.

Soponronnarit, S., Wetchacama, S., Trutassanawin, S., Jariyatontivait, W., 2001. Designing, testing and optimization of vibro-fluidised paddy dryer. Drying Technology 19, 1891–1908.

Sripawatakul, O., 1994. Study of drying paddy by cross-flow fluidization technique. Master's Thesis, King Mongkut's University of Technology Thonburi, Bangkok, Thailand, 108pp.

Srzednicki, G.S., Driscoll, R.H., 1995. Adoption of in-store drying technology in Southeast Asia. Proceedings of the 17th ASEAN Technical Seminar on Grain Postharvest Technology, Lumut, Malaysia, 25–27 July 1995, 8pp.

Sungareeyakul, K., Wetchacama, S., Pongpullponsak, A., Soponronnarit, S., 2002. Evaluation of status of paddy dryers in Thailand. Thai Society of Agricultural Engineering Journal 9, 32–41 (in Thai).

Swasdisevi, T., Soponronnarit, S., Chujinda, A., Wetchacama, S., Thepent, V., 1997. Rice husk furnace for fluidised bed paddy dryer. Proceedings of the Second Asean Renewable Energy Conference, Phuket, Thailand, 6–9 November 1997, pp. 603–612.

Wangji, M., 1996. Development of industrial scale fluidised bed paddy dryer. Master's Thesis, King Mongkut's University of Technology Thonburi, Bangkok, Thailand, 197pp.

Available online at www.sciencedirect.com
SCIENCE DIRECT®
Journal of Food Engineering 71 (2005) 28–36
JOURNAL OF FOOD ENGINEERING
www.elsevier.com/locate/jfoodeng

Comparative study of fluidized bed paddy drying using hot air and superheated steam

Wathanyoo Rordprapat *, Adisak Nathakaranakule, Warunee Tia, Somchart Soponronnarit

School of Energy and Materials, King Mongkut's University of Technology Thonburi, 91 Pracha u-tid Road, Bangkok 10140, Thailand

Received 18 February 2004; accepted 7 October 2004
Available online 7 December 2004

Abstract

This research investigated the physical properties of paddy, i.e., head rice yield, whiteness, white belly, viscosity of rice flour and change of microstructure of rice kernel. The experimental results showed that, for the same duration of drying, drying rates of paddy dried by superheated steam were lower than those dried by hot air due to an initial steam condensation during the first few minutes of superheated steam drying. This initial condition, however, promoted starch gelatinization making head rice yield of paddy dried by superheated steam higher than that dried by hot air. However, the values of whiteness of paddy dried by superheated steam were lower than those dried by hot air, especially during the first few minutes of drying due to a higher degree of Maillard reaction. Nevertheless, no obvious difference between the percentage of white belly of paddy dried by superheated steam and hot air was noted. Measured pasting properties indicated that gelatinization occurred more in paddy dried by superheated steam than that dried by hot air.

Keywords: Condensation; Gelatinization; Physical properties; SEM

1. Introduction

Recently, it has been shown by various investigators that paddy dried by a high-temperature fluidized bed drying technique (140–150 °C) has high-head rice yield (Soponronnarit & Prachayawarakorn, 1994; Taweerattanapanish, Soponronnarit, Wetchacama, Kongseri, & Wongpiyachon, 1999); the technique has thus become an increasingly more popular technique for paddy drying. In addition, it is reported that higher drying air temperature results in a higher grain temperature and longer tempering time leads to partial gelatinization of starch granules inside paddy affecting the grain qualities in a similar way to parboiled rice (Inprarsit & Noomhorm, 2001). Fluidized bed drying parameters affecting the various properties of paddy are moisture content, drying air temperature and bed thickness (Sutherland & Ghaly, 1992; Tumambing & Driscoll, 1993). Moreover, changing the medium in paddy drying from hot air to superheated steam affects the various qualities of paddy including the head rice yield and color. In addition, paddy dried by superheated steam has cooking and eating qualities similar to those of parboiled rice as well (Taechapairoj, Dhuchakallaya, Soponronnarit, Wetchacama, & Prachayawarakorn, 2003).

From the above reasons, a comparative study of paddy drying with hot air and superheated steam is interesting and was performed in this study. The qualitative indicators used for comparing the paddy quality

* Corresponding author. Tel./fax: +662 470 8663.
E-mail address: r_wathanyoo23@yahoo.com (W. Rordprapat).

0260-8774/$ - see front matter © 2004 Elsevier Ltd. All rights reserved.
doi:10.1016/j.jfoodeng.2004.10.014

from both drying methods are head rice yield, whiteness, percentage of white belly, viscosity of rice flour and microstructure of the starch granules.

2. Materials and methods

A schematic diagram of a hot air fluidized bed dryer and its accessories is shown in Fig. 1. The system consists of three major components: a cylindrical drying chamber with an inner diameter of 20 cm and a height of 140 cm, a 12 kW electrical heater with a temperature controller, and a backward-curved-blade centrifugal fan, which was driven by a 1.5 kW motor. Exhaust air could be recycled, if needed, by means of two butterfly valves.

A batch superheated steam fluidized bed dryer is shown in Fig. 2. It consists of five major components: a cylindrical drying chamber with an inner diameter of 15 cm and a height of 100 cm, a 13.5 kW steam superheater, which was used to heat up saturated steam to become superheated steam, a backward-curved blade centrifugal fan driven by a 2.2 kW motor, a cyclone, and a small boiler capable of generating steam at a rate of 31 kg/h. A perforated sheet, with 10 holes per cm^2, was used for distributing the drying medium in the dryer. Superheated steam temperature was controlled by a PID controller with an accuracy of ±1 °C. To minimize the initial steam condensation inside the superheated steam dryer, hot air was first used to warm up the system until the temperature in all parts of the system reached the desired level (higher than 100 °C). Then, hot air was replaced by superheated steam. The steam generator generated saturated steam at 106 kPa (absolute) corresponding to a saturation temperature of around 100 °C.

Long grain rough rice (Supanburi 1 variety) from Pathum Thani Rice Research Center in Pathumthani Province, Thailand was used in all experiments. Rice

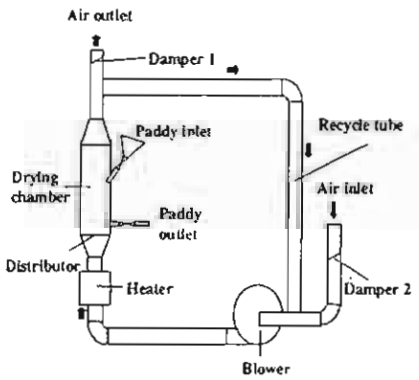

Fig. 1. A schematic diagram of a batch hot air fluidized bed dryer.

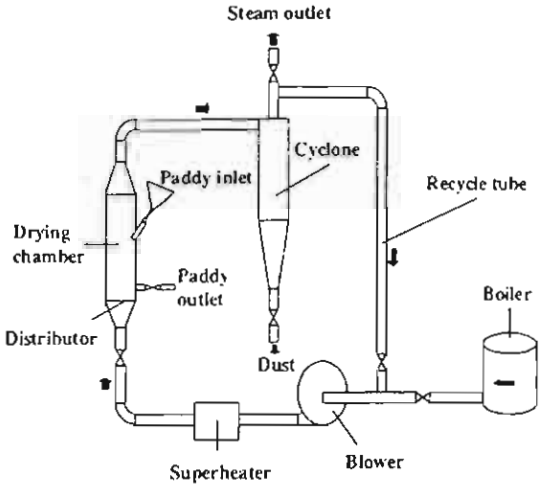

Fig. 2. A schematic diagram of a batch superheated steam fluidized bed dryer.

was cleaned and soaked in water with an initial temperature of 80 °C for 3 or 4 h, before being tempered for another hour. The experiments were conducted within the following ranges: initial bed depth of paddy of 10 cm medium temperature of 150 °C, superficial medium velocities of $1.3U_{mf}$ and $1.5U_{mf}$ (U_{mf} of hot air = 1.65 m/s, as reported by Soponronnarit & Prachayawarakorn (1994) and U_{mf} of superheated steam = 2.6 m/s, as reported by Taechapairoj et al. (2003)). Grain and drying medium temperatures were measured by type K thermocouples connected to a data logger having an accuracy of ±1 °C (COMARK Model 8510, England).

Dried paddy kernels were gently ventilated by ambient air until their temperatures become ambient and their moisture content reached 16% (d.b.). Finally, two samples, weighed 300 and 250 g, were taken from the bulk of dried kernels. The first 300 g sample was kept in a seal plastic bag for two weeks before testing for its head rice yield, whiteness and percentage of white belly. Another 250 g sample was shelled by a rubber roll husk (THU, Japan), polished by a Satake rice polisher (TM05, Japan) and graded by a rice grader (TRG, Japan) to measure the head rice yield. In this case, head rice yield is defined as milled rice having kernel length of at least 75% of its original length. The color of polished rice was measured by Kett digital whiteness meter (Model C-300, Japan), which was calibrated with a white reference color. The individual head rice kernels after milling were graded manually to check for the white belly. Kernels which had an opaque white area of more than 50% of the total area were deemed to be in the white belly category, according to the Thai Standard Rice (Ministry of Commerce Thailand, 1997).

The moisture content of paddy was determined by drying paddy in a hot air oven at a temperature of 103 °C for 72 h, according to the approved method of

the American Association of Cereal Chemists (AACC, 1995).

The changes in the microstructure of sample dried by hot air and superheated steam were observed by using a scanning electron microscope (SEM) (JSM-5600LV/ JSM-5600, Japan). The sampled rice kernel was cut along its cross-sectional axis, attached to an SEM stub, coated with a gold layer using a sputter-coater and photographed at an accelerator potential of 10 kV. The inspected location was between the kernel surface and its endosperm center.

Pasting properties of rice flour were determined by using a Rapid Visco Analyzer, RVA (Newport Scientific, Model RVA-4, Australia) and the approved method 61-02 (AACC, 1995). Rice flour (3 g on dry basis) was poured into distilled water (25 mL) in a canister and mixed thoroughly. The mixture was stirred at 960 rpm for 10 s and then changed to 160 rpm. Its temperature was first maintained at 50 °C for 1.5 min and then raised to 95 °C at a rate of 12 °C/min. After that the temperature was maintained at 95 °C for 2.5 min, followed by a cooling down to 50 °C at 12 °C/min and was maintained at 50 °C for 2.1 min. These tests were done in duplicate. A plot of pasting viscosity in an arbitrary RVA unit (RVU) versus time was used to determine the peak viscosity, temperature at peak viscosity, trough final viscosity, breakdown viscosity and setback viscosity. Peak viscosity indicates the water-biding capacity of the mixture. It is often correlated with the final product quality, and also provides an indication of the viscous load likely to be encountered by cooking. Breakdown viscosity measures the degree of disintegration of the granules or paste stability. Setback viscosity is a measure of gelling or retrogradation tendency of rice flour (Dengete, 1984).

3. Results and discussion

Drying behavior and physical properties of paddy, i.e., drying rate, grain temperature, head rice yield, whiteness, percentage of white belly, pasting properties and microstructure of rice kernel dried by superheated steam and hot air are discussed in the following sections.

3.1. Drying kinetics and grain temperature

Fig. 3 shows the evolutions of moisture content and temperature of paddy (soaked for 3 h) dried by superheated steam and hot air at 150 °C; an initial bed height was set at 10 cm and the superficial velocities of the drying medium were set at $1.3U_{mf}$ (Fig. 3a) and $1.5U_{mf}$ (Fig. 3b).

Fig. 3a indicates that during the first five minutes of drying moisture content of paddy dried by superheated steam decreased slower than that dried by hot air. This

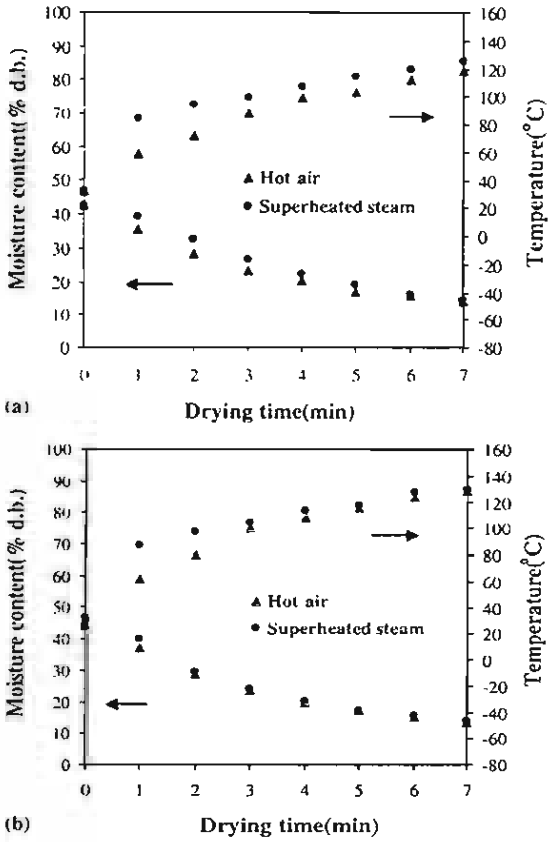

Fig. 3. Drying curves and temperature of paddy dried by superheated steam and hot air (drying temperature of 150 °C; bed depth of paddy of 10 cm; soaking time of 3 h). (a) superficial velocity of $1.3U_{mf}$, (b) superficial velocity of $1.5U_{mf}$.

is because paddy dried by superheated steam gained some moisture due to an initial steam condensation, which noticably occurred during the first few minutes of drying. This early stage condensation was also reported by Iyota, Nishimura, Onuma, and Nomura (2001) and Taechapairoj et al. (2003). After 5 min, the drying curves of both drying methods were almost the same. Temperature of paddy dried by superheated steam, however, increased faster than that dried by hot air during the first few minutes of drying. This phenomenon was due to the latent heat released to paddy from steam during an initial condensation mentioned earlier as well as due to the superior heat transfer properties of superheated steam compared with hot air (Mujumdar, 1995). The trends of moisture content evolution of paddy dried by superheated steam and hot air when using a superficial velocity of $1.5U_{mf}$ (Fig. 3b) were almost similar to those in the case of using a superficial velocity of $1.3U_{mf}$. Slightly higher rate of increase of temperature and decrease of paddy moisture content when using a superficial velocity of $1.5U_{mf}$ was a consequence of the higher heat transfer rate at higher

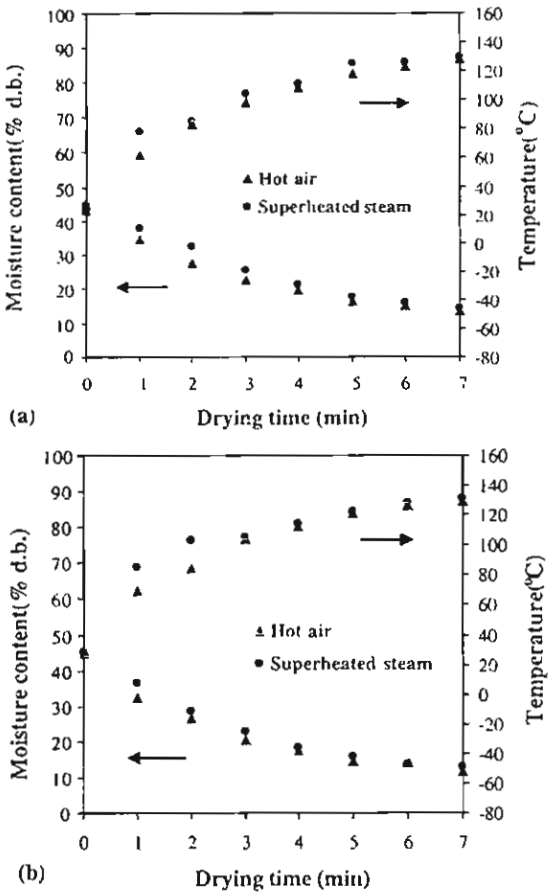

Fig. 4. Drying curves and temperature of paddy dried by superheated steam and hot air. (Drying temperature of 150 °C; bed depth of paddy of 10 cm; soaking time of 4 h). (a) Superficial velocity of $1.3U_{mf}$, (b) superficial velocity of $1.5U_{mf}$.

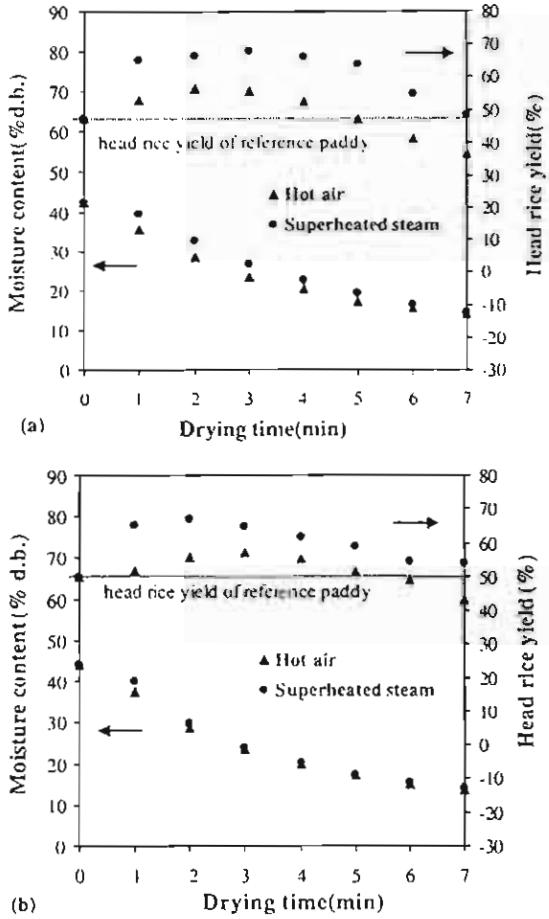

Fig. 5. Drying curves and head rice yield of paddy dried by superheated steam and hot air (soaking time of 3 h). (a) Superficial velocity of $1.3U_{mf}$, (b) superficial velocity of $1.5U_{mf}$.

superficial medium velocity (Looi, Mao, & Rhodes, 2002). The drying and temperature curves of paddy dried by both drying methods were almost the same after 3 min of drying.

Fig. 4 shows the evolutions of moisture content and temperature of paddy (soaked for 4 h) dried by superheated steam and hot air at the drying temperature of 150 °C, a paddy bed depth of 10 cm, and superficial velocities of $1.3U_{mf}$ (Fig. 4a) and $1.5U_{mf}$ (Fig. 4b). The experimental results were found to be similar to the case of 3-h soaking time (Fig. 3), and could be explained by the same reasons. Different soaking times, therefore, had no significant effect on the drying rate and the rate of change of temperature of paddy dried by both media in the ranges of our study.

3.2. Head rice yield

The evolutions of head rice yield and moisture content of paddy dried by superheated steam and hot air are presented in Figs. 5 and 6 for 3 and 4-h soaking conditions, respectively. The reference head rice yield of paddy dried by ambient air is also shown in these figures for comparison.

Head rice yields of paddy dried by both drying media (Fig. 5a) increased beyond that of the reference sample within the first few minutes of drying because starch granules inside the paddy kernels were partially gelatinized (Inprarsit & Noomhorm, 2001; Taweerattanapanish et al., 1999). The gelatinization process of starch inside the paddy kernels helped joining cracks inside the kernels and, consequently, led to an increase in the head rice yield. The gelatinization process is activated at different temperatures and moisture contents depending on the type of material dried. For paddy the proper temperature and moisture content for the gel formation are approximately 73–86 °C and 24–25% w.b., respectively (Taweerattanapanish et al., 1999; Zhou, Robards, Helliwell, & Blanchard, 2002). In the case of paddy dried with superheated steam, paddy temperature increased rapidly to the gelatinization temperature at an early stage of drying, while the moisture content of paddy was still in a suitable range for the gel formation.

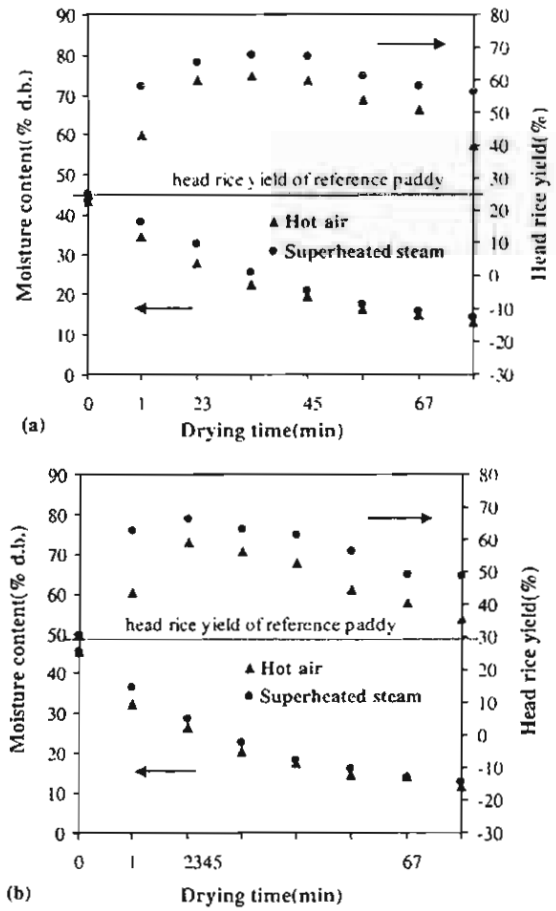

Fig. 6. Drying curves and head rice yield of paddy dried by superheated steam and hot air (soaking time of 4 h). (a) Superficial velocity of $1.3U_{mf}$, (b) superficial velocity of $1.5U_{mf}$.

This allowed the gel forming process to be longer in the case of superheated steam drying than in the case of hot air drying, which had lower rate of temperature rise but higher initial rate of drying. Therefore, head rice yield of paddy dried by superheated steam was higher than that dried by hot air. The slower gelatinization process in hot air drying compared to that in superheated steam drying was also reported by Iyota et al. (2001).

After 2 min of drying, head rice yield of paddy dried by superheated steam was almost constant and started to drop after 5 min of drying because paddy kernels had higher temperature and moisture gradients; these gradients led to the development of stress inside the kernels, which damaged the kernels. Head rice yield of hot air dried paddy was similar to that of superheated steam dried samples except that its value increased slower and decreased faster than in the case of superheated steam drying. The fast drop in head rice yield was due to the fast development of moisture gradient inside paddy kernel in hot air drying.

It can also be seen in these figures that a higher superficial velocity ($1.5U_{mf}$) resulted in a higher heat transfer from both media to the kernels. Paddy temperature in the case of using a superficial velocity of $1.5U_{mf}$ therefore rose to the gelatinization temperature faster than in the case of using a lower superficial velocity. Paddy moisture content, however, dropped below the suitable value for gelatinization faster than in the case of using a superficial velocity of $1.3U_{mf}$. The trade-off between the two parameters resulted in similar head rice yields of paddy dried at both drying medium velocities. The higher heat transfer rate also resulted in a rapid drop of head rice yield due to a rapid increase of the paddy temperature and moisture gradient inside the kernels.

3.3. Whiteness

Color changes of polished rice dried by superheated steam and hot air at superficial velocities of $1.3U_{mf}$ and $1.5U_{mf}$ (soaking time of 3 h) are shown in Fig. 7a and b, respectively. The whiteness of rice during the first few minutes of superheated steam drying decreased much faster than that of hot air drying, which slightly

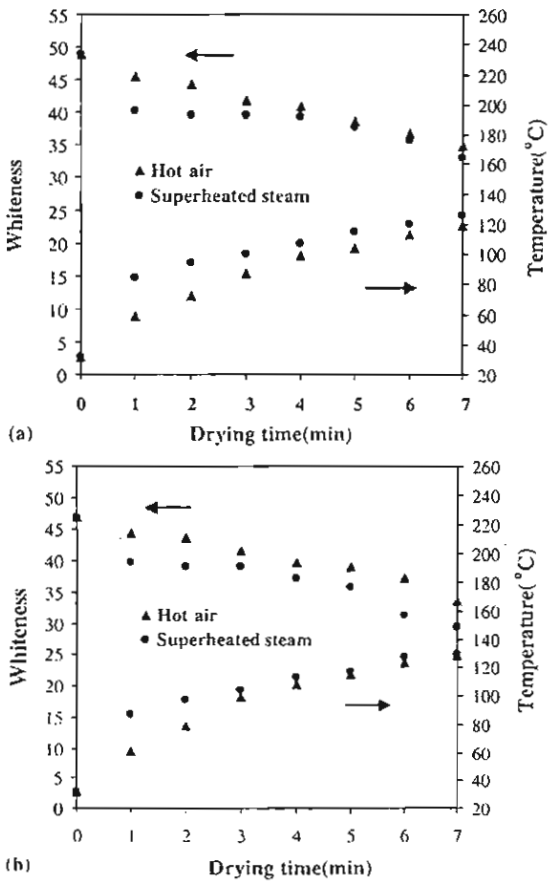

Fig. 7. Whiteness and temperature of paddy dried by superheated steam and hot air (soaking time of 3 h). (a) Superficial velocity of $1.3U_{mf}$, (b) superficial velocity of $1.5U_{mf}$.

but continuously dropped throughout the whole drying period. Such rapid drop in whiteness was a result of three phenomena, i.e., an initial steam condensation, which led to an increase in amount of free amino acid (Iyota, Nishimura, Komoshi, & Yoshida, 2002), a sharp increase in paddy temperature, which accelerated Maillard reaction and the transition of color substances from rice husk and rice bran into endosperm (Inprarsit & Noomhorm, 2001; Khan, Amilhussin, Arbolida, Manolo, & Chancellor, 1974; Yap, Juliano, & Pereze, 1988). After 1 min, the whiteness of rice dried by superheated steam was almost constant and started to drop after 3–4 min of drying. Paddy temperature increased with drying time in both drying methods; this induced Maillard reaction and caused whiteness of rice to drop slightly. The superficial velocity of the drying medium had no effect on the whiteness of rice.

The experimental results in the case of 4 h soaking time (Fig. 8a and b) were similar to those in the case of 3 h soaking time (Fig. 7a and b) and could be explained by the same reasons. Interestingly, it can be seen that in the case of using a superficial velocity of $1.5U_{mf}$ the whiteness slightly increased after 2 min of superheated steam drying (Fig. 8b). This phenomenon might be the consequence of the high-moisture diffusion rate, which moved the color substances out of the paddy kernels.

3.4. White belly

Paddy kernels having an opaque white area of more than 50% of the total area are categorized into the white-belly paddy category, according to the Thai rice standard (Ministry of Commerce Thailand, 1997). The changes of white belly of superheated steam and hot air dried paddy are shown in Fig. 9a and b, respectively. White belly was found to decrease with drying time in all experiments. The reduction of white belly was resulted from the gelatinization process. The trends of decreasing white belly of paddy dried by superheated steam were similar to those dried by hot air. At the end of drying, white belly was less than 2% for all drying conditions, which is an acceptable level for commercial parboiled rice.

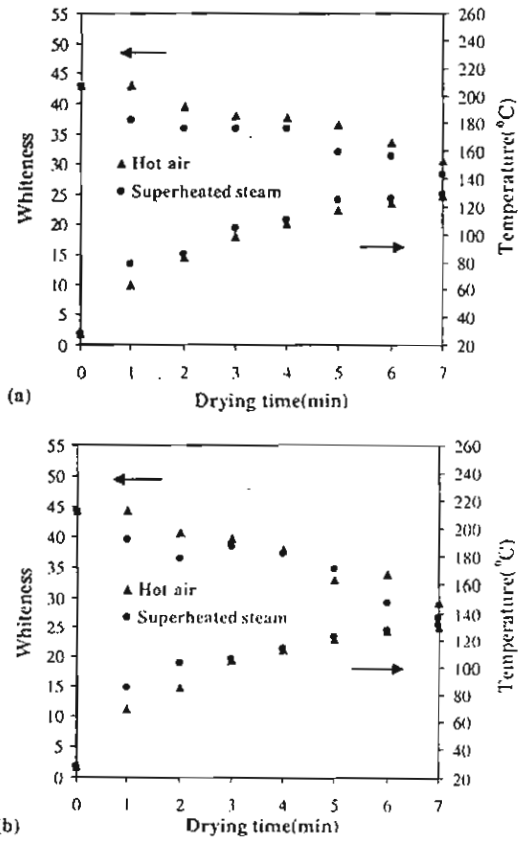

Fig. 8. Whiteness and temperature of paddy dried by superheated steam and hot air (soaking time of 4 h). (a) Superficial velocity of $1.3U_{mf}$, (b) superficial velocity of $1.5U_{mf}$.

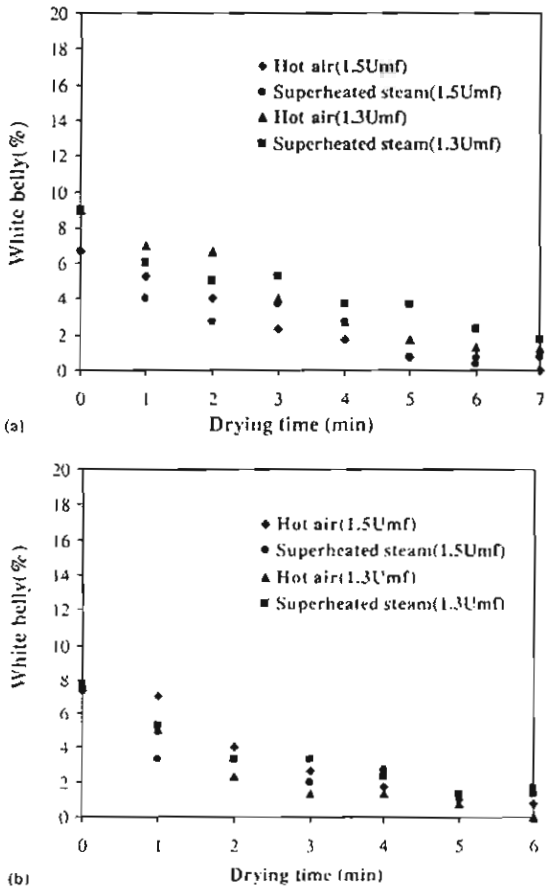

Fig. 9. White belly curves of paddy dried by superheated steam and hot air (soaking time of 3 and 4 h). (a) Paddy soaked of 3 h, (b) paddy soaked of 4 h.

3.5. Pasting properties

High-head rice yield of paddy dried either by superheated steam and hot air compared with that of the reference sample could be confirmed by the pasting properties of rice flour of the dried paddy measured by a Rapid Visco Analyzer (RVA). The measurement results are shown as RVA pasting curves in Figs. 10 and 11. It can be seen from Fig. 10a for the 1.3-U_{mf} and 3-h soaking condition that the pasting temperatures of paddy dried by both techniques were higher than those of the reference paddy, but the peak viscosities of paddy dried by both techniques were lower. In addition, it was observed that the pasting temperature of paddy dried by superheated steam was higher than that dried by hot air, but the peak viscosity was lower. Higher pasting temperature and lower peak viscosity indicated that more gelatinization occurred during both drying processes and this led to higher head rice yields of the processed paddy.

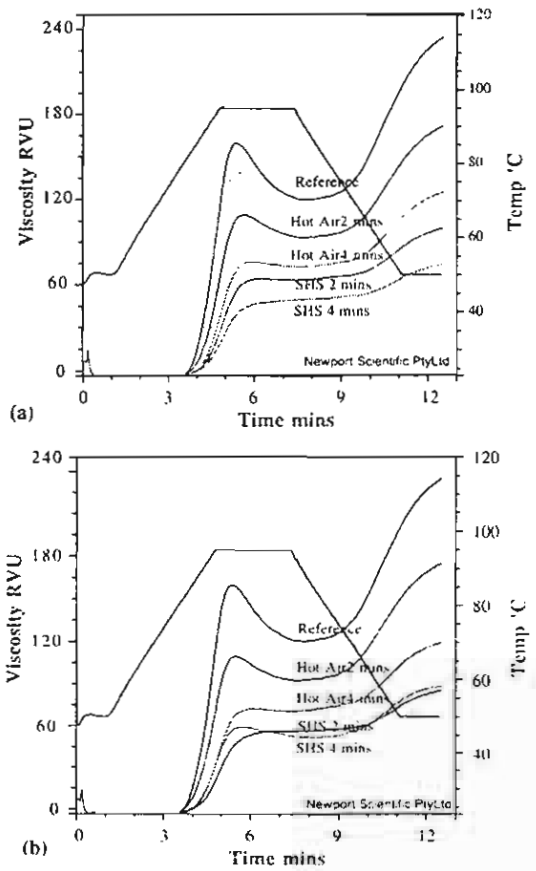

Fig. 10. Viscograph of rice flour dried by superheated steam and hot air (soaking time of 3 h). (a) Superficial velocity of 1.3U_{mf}, (b) superficial velocity 1.5U_{mf}.

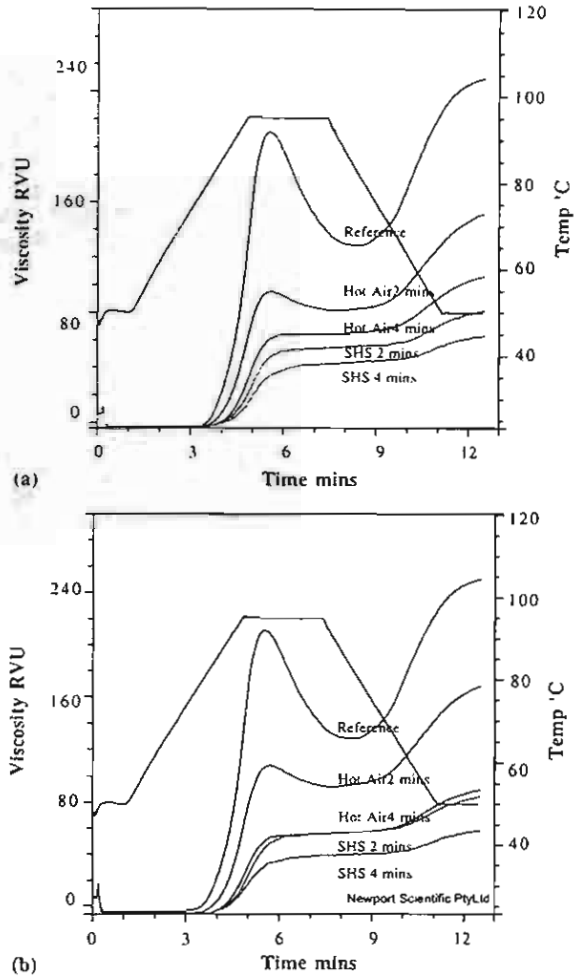

Fig. 11. Viscograph of rice flour dried by superheated steam and hot air (soaking of 4 h). (a) Superficial velocity of 1.3U_{mf}, (b) superficial velocity 1.5U_{mf}.

The final and setback viscosities of paddy dried by superheated steam and hot air were lower than those of the reference paddy and decreased with the drying time. When comparing with hot air, these properties

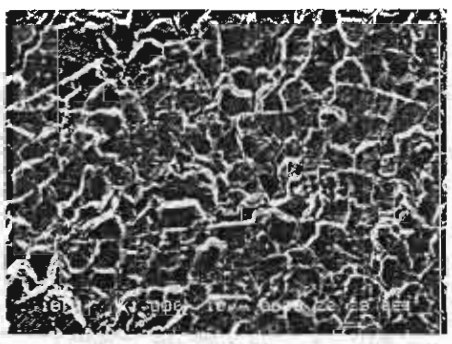

Fig. 12. SEM of cross-section of reference paddy.

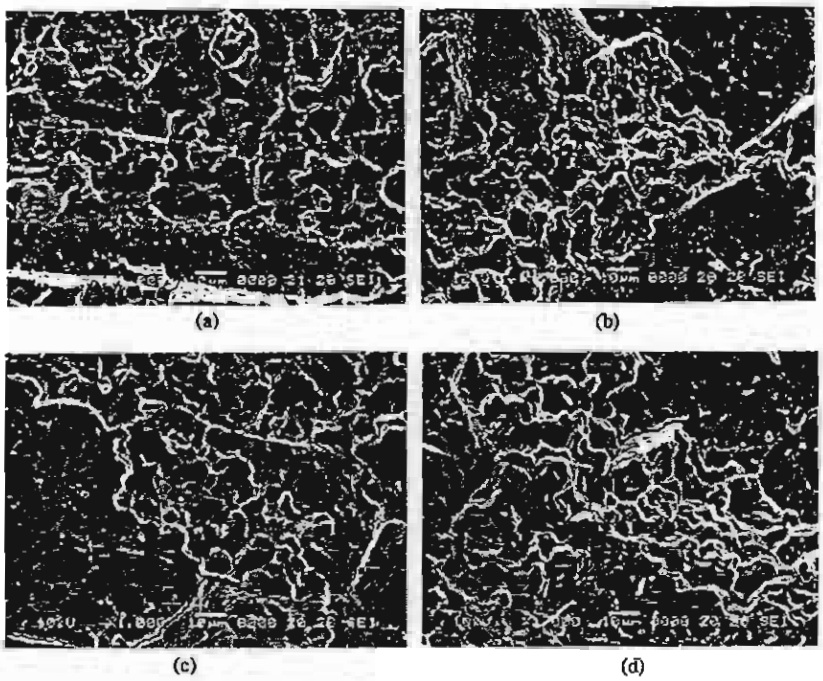

Fig. 13. SEM of cross-section of paddy dried by hot air and superheated steam for 4 min. (a) Hot air at $1.3U_{mf}$, (b) superheated steam at $1.3U_{mf}$, (c) hot air at $1.5U_{mf}$, (d) superheated steam at $1.5U_{mf}$.

of paddy dried by superheated steam were lower than that dried by hot air.

All pasting properties of paddy soaked for 3 h, dried at $1.5\text{-}U_{mf}$ condition, as shown in Fig. 10b, were similar to those at the $1.3\text{-}U_{mf}$ condition. This means that the medium velocity had no effect on the pasting properties of dried paddy. The same trends were observed for paddy soaked for 4 h, as can be seen in Fig. 10a and b.

3.6. Scanning electron microscopy (SEM)

SEM results of the reference paddy (soaked for 3 h and dried by ambient air) and paddy dried by superheated steam and hot air are shown in Figs. 12 and 13. Starch granules of the reference paddy (Fig. 12) spreaded throughout the cross-section of paddy with a loose crystal-like structure. On the other hand, starch granules of paddy dried by superheated steam and hot air (Fig. 13) were tightly packed. Comparing with the reference, starch granules of dried paddy obtained from both drying methods swelled and changed from crystallize to amorphous form due to the gelatinization effect. This structure transition made head rice yield of paddy dried by both media increased.

4. Conclusion

The superior heat transfer properties of superheated steam and the initial condensation occurred during an early stage of superheated steam drying increased the paddy temperature and maintained its moisture content at the level suitable for gelatinization, which changed the starch granules of rice kernels from the crystal-like structure to the amorphous form as revealed by SEM. As a result, head rice yield of paddy dried by superheated steam was found to be higher than that dried by hot air drying, which resulted in no condensation and slower increasing rate of paddy temperature. Measured pasting properties indicated that partial gelatinization occurred more in paddy dried by superheated steam than that dried by hot air and the reference paddy. Whiteness of paddy dried by superheated steam was lower than that of paddy dried by hot air due to an early stage condensation, which also resulted in a faster increase of the grain temperature. Percentage of white belly was reduced with the drying time; the value was less than 2% after 5 min of drying.

Acknowledgement

The authors would like to express their sincere appreciation to the Thailand Research Fund for financial support. Thanks are also due to the Pathum Thani Rice Research Center for testing physical qualities of rice and to the Institute of Food Research and Product Development, Kasetsart University for allowing the use of an RVA.

References

AACC (1995). *Approved method of the American association of cereal chemists* (9th ed.). MN: American Association of Cereal Chemists St. Paul.

Dengete, H. N. (1984). *Swelling pasting, and gelling of wheat starch. Advances in cereal science and technology* (vol. 6). MN: American Associated Cereal Chemistry, St. Paul (pp. 49–82).

Inprarsit, C., & Noomhorm, A. (2001). Effect of drying air temperature and grain temperature of different type of dryer and operation on rice quality. *Drying Technology, 19*(2), 389–404.

Iyota, H., Nishimura, N., Onuma, T., & Nomura, T. (2001). Drying of sliced raw potatoes in superheated steam and hot air. *Drying Technology, 19*(7), 1411–1424.

Iyota, H., Nishimura, T., Komoshi, Y., & Yoshida, K. (2002). Effect of initial steam condensation on color changes of potatoes during drying in superheated steam. In *Proceedings of the 13th International Drying Symposium* (pp. 1352–1359), Beijing China, B.

Khan, A. V., Amilhussin, A., Arbolida, J. R., Manolo, A. S., & Chancellor, W. J. (1974). Accelerated drying of rice using heat-conduction media. *Transactions of the ASAE, 17*, 949–955.

Looi, Y. A., Mao, Q. M., & Rhodes, M. (2002). Experimental study of pressurized gas-fluidized bed heated transfer. *International Journal of Heat and Mass Transfer, 45*, 255–265.

Ministry of Commerce, Thailand, Thai Standard Rice. Available from http://203.151.17.19/document/grain/english/standard.htm 1997, last revised on 20 June 2002.

Mujumdar, A. S. (1995). Superheated steam drying. In A. S. Mujumdar (Ed.), *Handbook of industrial drying* (2nd ed., pp. 1071–1086). New York: Marcel Dekker.

Soponronnarit, S., & Prachayawarakorn, S. (1994). Optimum strategy for fluidized bed paddy drying. *Drying Technology, 12*(7), 1667–1686.

Sutherland, J. W., & Ghaly, T. F. (1992). Rapid fluid-bed drying of paddy rice in the humid tropics. In *Proceedings of the 13th ASEAN Conference on Grain Post-harvest Technology*, Bruei Darussalam.

Taechapairoj, C., Dhuchakallaya, I., Soponronnarit, S., Wetchacama, S., & Prachayawarakorn, S. (2003). Superheated steam fluidized bed paddy drying. *Journal of Food Engineering, 58*, 67–73.

Taweerattanapanish, A., Soponronnarit, S., Wetchacama, S., Kongseri, N., & Wongpiyachon, S. (1999). Effect of drying on rice yield using fludization technique. *Drying Technology, 17*(1&2), 345–353.

Tumambing, J. A., & Driscoll, R. H. (1993). Modeling the performance of continuous fluidized bed paddy dryer for rapid pre-drying of paddy. In *Proceedings of the 14th ASEAN seminar on Grain Post-harvest Technology* (pp. 193–213), Manila, Philippines.

Yap, A., Juliano, O. B., & Pereze, C. M. (1988). Artificial yellow of rice at 60 °C. In *Proceedings of the 11th ASEAN Technical Seminar on Grain Post harvest Technology*, Kuala Lumpur, Malaysia, ASEAN Grain Post harvest Program, Bangkok, Thailand.

Zhou, Z. K., Robards, K., Helliwell, S., & Blanchard, C. (2002). Aging of stored rice: Changes in chemical and physical attributes. *Journal of Cereal Science, 35*, 65–78.

Biosystems Engineering (2006) **93** (2), 213–219
doi:10.1016/j.biosystemseng.2005.12.003
SE—Structures and Environment

Field Experiments and Economic Evaluation of an Evaporative Cooling System in a Silkworm Rearing House

C. Lertsatitthanakorn; S. Rerngwongwitaya; S. Soponronnarit

Faculty of Engineering, Mahasarakham University, Khantarawichai, Mahasarakham 44150, Thailand; e-mail of corresponding author: freeconvect@hotmail.com

(Received 10 November 2004; accepted in revised form 5 December 2005; published by 30 January 2006)

High ambient temperature has a negative effect on silk production. During heat stress, penalties to the efficient performance, production, reproduction, feed conversion, health and welfare of the animals can be severe. This research was aimed at investigating the feasibility of using direct evaporative cooling to improve the indoor air conditions in a silkworm rearing house. To this end, a silkworm rearing house of 32 m^2 floor area was fabricated and tested at Mahasarakham University. A cooling pad measuring 1·8 m by 3·6 m was placed on the north wall and a fan on the south wall. Experiments were performed through two seasons, namely: winter (November–December 2003) and summer (March–April 2004). Various operating airflow rates were considered to assess cooling performance and energy efficiency ratio (EER) of the evaporative cooling system. The results showed indoor dry bulb temperature drops of 6–13 °C could be achieved parallel with a 30–40% rise in relative humidity. The EER tends to be very high because the system consumes only fan and water pumping power. The economic analysis indicates that the payback period of the evaporative cooling system is about 2·5 years. Therefore, the direct evaporative cooling method demonstrates significant potential for silkworm rearing house cooling.

1. Introduction

Thailand is one of the countries well known for its silk fabrics and other fine silk products. During the period 1997–2001, the average annual value of the export of silk products was 1038·8 million Baht (40 Baht = 1 US$), compared to the average value of imports of 629·3 million Baht, or 54% of exports (Sericulture Extension Center No.1–9, 2002). It has been shown that Thai silk production is not sufficient to meet local demands. This situation has greatly obstructed the development of Thai silk industry. Among the strategies for silk production development during the Nine National Economic and Social Development Plan (2002–2006), was a plan to increase the silk yarn about 42% by the year 2006 (Chuprayoon *et al.*, 2002).

The ability of silkworms to produce is affected by seasonal factors such as temperature and humidity. It has been well established that efficiency in silkworm production is often lower during and after the hot season. One reason for the reduction in their productive performance might be elevated ambient temperatures, which induce heat stress. This is especially true in tropical areas such as Thailand where the temperature exceeds 30 °C for several months of the year (Suriyasomboon *et al.*, 2004) and, consequently, is not appropriate for rearing silkworms. Temperatures in the range of 21–27 °C with relative humidity (RH) of 70–85% (Tazima, 1978) are required. Most silkworm production in Thailand is performed in conventional stables which have an open air system with no walls. In recent years, a new housing system with a direct evaporative cooling system has been introduced to improve the microclimate for livestock in Thailand such as pigs (Boonyawattana *et al.*, 2003) and poultry (Ketjoy, 1999). Various other works on evaporative cooling systems applied to greenhouses had already been published such as Willits (2003), who presented a

cooling model that predicts axial gradients of temperature and humidity of a greenhouse evaporative cooling system. Kittas *et al.* (2003) reported on a large commercial greenhouse cooled with evaporative pads and partially shaded. Evaporative cooling is an adiabatic humidification process (Wiersma & Short, 1983) that does not involve heat gain or loss. Sensible heat from the air is used to evaporate the water that comes in contact with the air. This sensible heat is then converted into latent heat, resulting in a reduction of the dry bulb temperature with a complementary increase of the RH and water vapour content of the air. An evaporative cooling system might be one alternative way of reducing the impact of a harsh climate on silkworm production.

This paper presents an investigation of the feasibility of using evaporative cooling in a silkworm rearing house.

2. Analysis

2.1. *Cooling efficiency and enthalpy change in air*

Cooling efficiency η is an index used to assess the performance of a direct evaporative cooler. Cooling efficiency in percentage can be defined as follows (Koca *et al.*, 1994):

$$\eta = \frac{T_d - T_c}{T_d - T_w} \times 100 \qquad (1)$$

where: T_d and T_w are the dry and web bulb temperatures of the ambient air and T_c is the dry bulb of the cooled air in °C.

The enthalpy change in air ΔH, which can be calculated as follows:

$$\Delta H = MC_{pa}(T_d - T_c) \qquad (2)$$

where: C_{pa} is the specific heat of moist air in $kJ\,kg^{-1}\,K^{-1}$; and M is the air mass flow rate in $kg\,s^{-1}$.

2.2. *Energy efficiency ratio*

Energy efficiency ratio (EER) was developed by the industry to evaluate the rate of energy consumption for air conditioning units (El-Dessouky *et al.*, 2000). The EER represents a measure for rating air conditioning units. The energy efficiency ratio E_{ER} is defined as the net thermal energy removed from air for cooling purposes per watt of energy expended. That is

$$E_{ER} = \frac{\Delta H}{P}$$

where P is input electrical power in kW of the exhaust fan and water pump.

The value of EER is calculated by determining the difference in the enthalpy of the inlet and outlet air streams through the cooling pad and the input power.

3. Experimental silk worm rearing house and measurements

3.1. *Silk worm rearing house*

A roof type even span house with an effective floor area of 8 m by 4 m and a height of 2·5 m, with one access door and no windows has been considered for experimental purposes as shown in *Fig. 1*. The walls are made

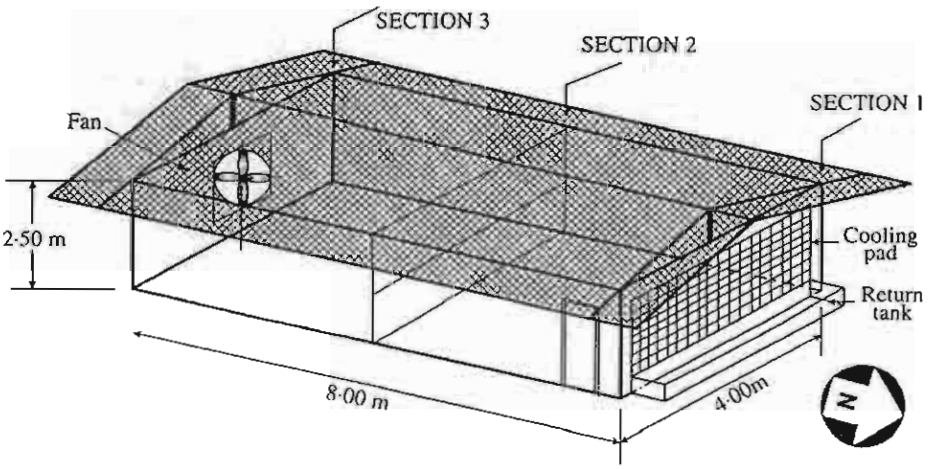

Fig. 1. Isometric view of silkworm rearing house

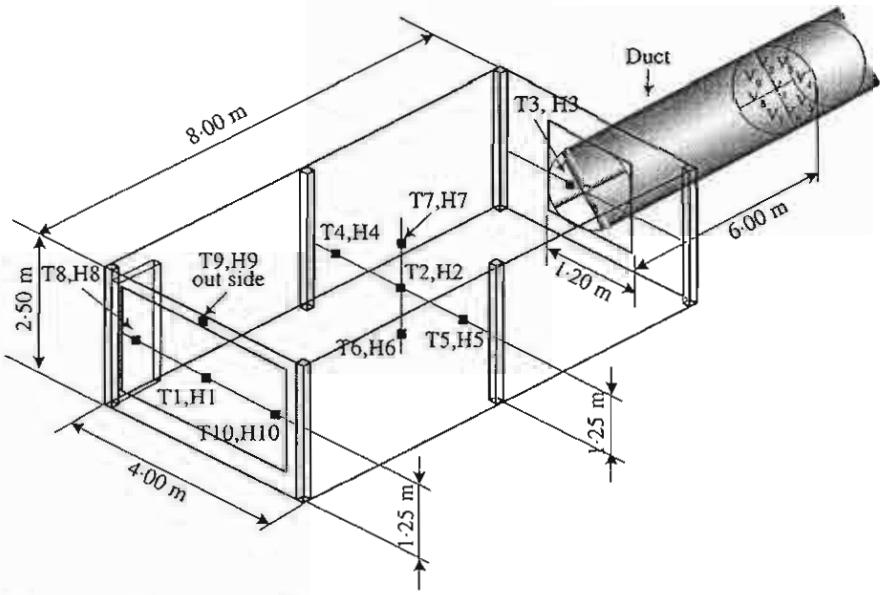

Fig. 2. Locations of temperature (T), humidity (H) and velocity (V) sensors in the experimental house

of asbestos-cement flat sheet. The roof gable, tilted at a 20°, is covered by Roman tiles. The horizontal ceiling is made of gypsum with 36 cm attic height. A cooling pad sized of 1·8 m by 3·6 m is located on the north wall and a 746 W exhaust fan is fitted at the south wall. The cooling pad is made of corrugated cellulose of 15 cm thickness has been impregnated with wetting agents. It was used to provide maximum surface area for evaporation. A water inlet is fitted on the top of the cooling pad. Several small holes of different diameters are made in the top solid part of the cooling pad to insure uniform distribution of the water throughout the cooling pad. A 373 W pump with water tank was attached to cooling pad for continuous water trickling.

3.2. *Measurements*

The silkworm rearing house temperature and humidity were measured at nine positions using nine calibrated temperature and humidity sensors (Testo model 175-H2, Germany, accuracy ±0·5 °C and ±3% RH) as shown in *Fig. 2*. The ambient temperature and humidity were also measured by Testo model 175-H2. A hot wire anemometer (Testo model 445, Germany, accuracy ±0·03 m s^{-1}) was used to measure air velocity (average of nine points as shown in *Fig. 2*). A variable voltage was used to drive the exhaust fan. A clamp on power meter [Hioki model 3286, Japan, accuracy ±2·3% reading (rdg) ±5 digit (dgt)] was used to measure the power consumption of the exhaust fan and water pump. The experiment started at 10 a.m. and ended at 5 p.m. with data recording at 15 min intervals.

4. Results and discussion

4.1. *Indoor temperature and humidity fluctuation*

Figure 3 shows that when the evaporative cooling system was not operating, the room temperature (average of nine points) was nearly the same as the ambient (before 14:00 h) because outdoor air infiltrates through the channels of the cooling pad. After 14:00 h, the room temperature was higher than ambient. This was due to the heat accumulated in the room. The maximum indoor temperature was about 33·1 °C. When the evaporative cooling system was turned on, the room temperature decreased from 32 to 22 °C while RH increased from 33% to 82% RH, which is appropriate for rearing the silkworm [suggest temperature in the range of 21–27 °C with RH of 70–85% (Tazima, 1978)] as shown in *Fig. 4*. The results in this study indicate that silkworms in the conventional system were exposed to higher temperatures than silkworms in the evaporative cooling system.

4.2. *Effect of seasonal variation*

In general, three different seasons in Thailand can be recognised as follows: the summer season is about 3

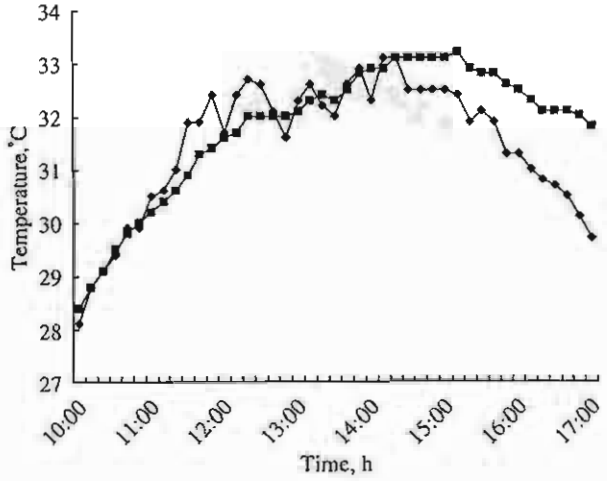

Fig. 3. Hourly variation of ambient and room temperatures when the evaporative cooling system was not operating (23/11/2003); –◆–, ambient temperature; –■– room temperature

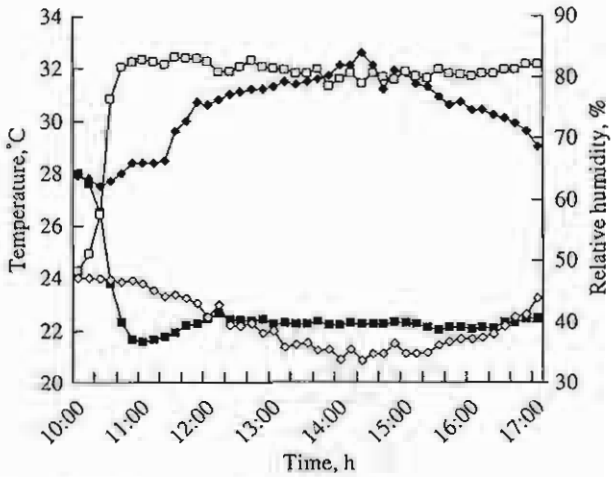

Fig. 4. Hourly variation of ambient and room temperatures and humidities of the open evaporative cooling system (4/12/2003); –◆–, ambient temperature; –■– room temperature; –◇–, ambient relative humidity; –□–, room relative humidity

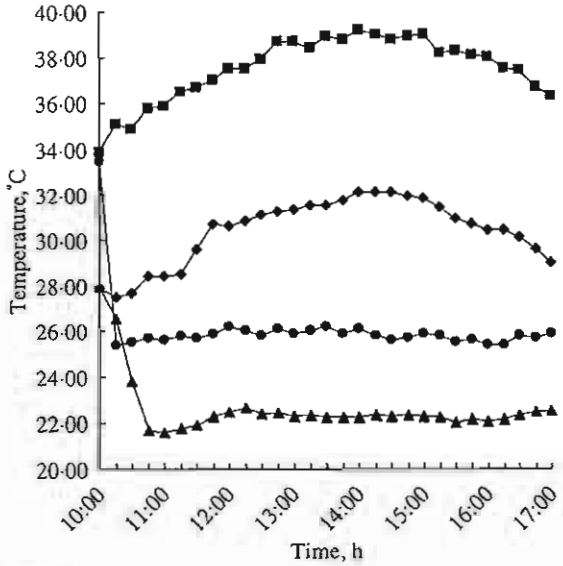

Fig. 5. Effect of seasons on room temperature (air mass flow rate = 6·3 kg s^{-1}); –◆–, outside temperature (4/12/2003); –■– outside temperature (25/3/2004); –▲–, room temperature (4/12/2003); –●–, room temperature (25/3/2004)

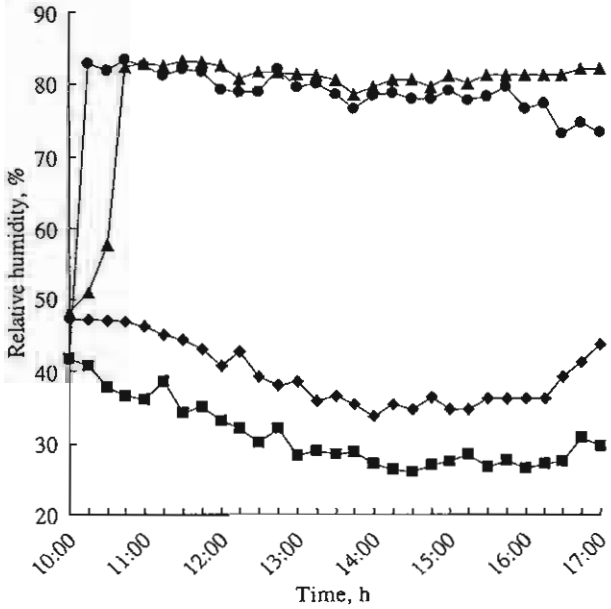

Fig. 6. Effect of seasons on room humidity (air mass flow rate = 6·3 kg s^{-1}); –◆–, outside relative humidity (4/12/2003); –■– outside relative humidity (25/3/2004); –▲–, room relative humidity (4/12/2003); –●–, room relative humidity (25/3/2004)

months long: from mid-February to mid-May. The rainy season occurs from mid-May to mid-October, and the winter season occurs from mid-October to mid-February (Khedari *et al.*, 2002). A comparison of ambient air inlet/outlet temperatures and humidity during different seasons of the year was undertaken during the winter season (4/12/2003) and the summer season (25/3/2004). It was seen that a lower outlet temperature of the processed air can be realised if the temperature and RH of the air is lower at the inlet. In the summer, the maximum outside air temperature was 39·2 °C at 14:00 h. The system reduced the air temperature by 13 °C and increased the RH by about 51·2%. In the winter the air temperature drops by about 10 °C as shown in *Figs 5* and *6*. This drop is because the ambient humidity in summer is lower than in the winter. In

summer there is a greater potential to absorb the moisture of the evaporative water. It is clear that evaporative cooling systems are efficient for dry conditions, but not as effective for humid conditions.

4.3. *Effect of air mass flow rate*

Testing of the effects of air mass flow rate on room temperature and humidity was undertaken on different days. Thus, it was not easy to draw a comparison amongst the results because of the various climatic conditions as presented in the above section. Nevertheless, general and subjective conclusions could be formulated. Tests were conducted at three different air mass flow rates: 4·4 kg s^{-1} (8/12/2003), 6·3 kg s^{-1} (4/12/2003) and 9·2 kg s^{-1} (3/12/2003). There is a little variation of RH with increase of air mass flow rate from 4·4 to 9·2 kg s^{-1} as shown in *Fig. 7*, whereas the temperatures are reduced with increase of air mass flow rate as shown in *Fig. 8*. The cooling efficiency is affected by several factors, such as pad design, thickness of pad, airflow rates and outside air temperature and RH. Using a fixed 15 cm thickness of pad, the cooling efficiency varies between 66% and 80·2%. This result agreed well with that presented in Watt (1986).

The power consumption in kWh and EER for the three air mass flow rates is shown in Table 1. The EER range of 24·4 to 59·9 at air mass flow rates increased from 4·4 to 9·2 kg s^{-1}. This is due to the cooling effect, which prevails over power consumption. However, in order to reduce the power consumption of the fan, an alternative scenario could be proposed by varying the airflow rate between summer and winter seasons. An example of temperature and humidity of the system are also shown in *Figs 5* and *6*. Where two airflow rates were considered, the air mass flow rate of 6·3 kg s^{-1} for summer and 4·4 kg s^{-1} for winter are shown.

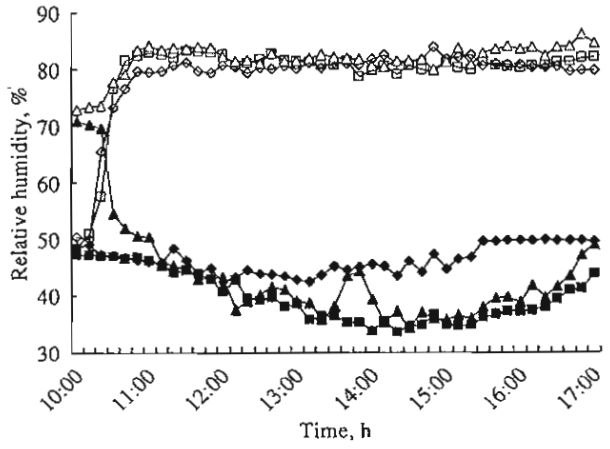

Fig. 7. Effect of ambient relative humidity and air mass flow rates on room humidity; –◆–, ambient relative humidity (4·4 kg s^{-1}); –■– ambient relative humidity (6·3 kg s^{-1}); –▲–, ambient relative humidity (9·2 kg s^{-1}); –◇–, room relative humidity (4·4 kg s^{-1}); –□–, room relative humidity (6·3 kg s^{-1}); –△–, room relative humidity (9·2 kg s^{-1})

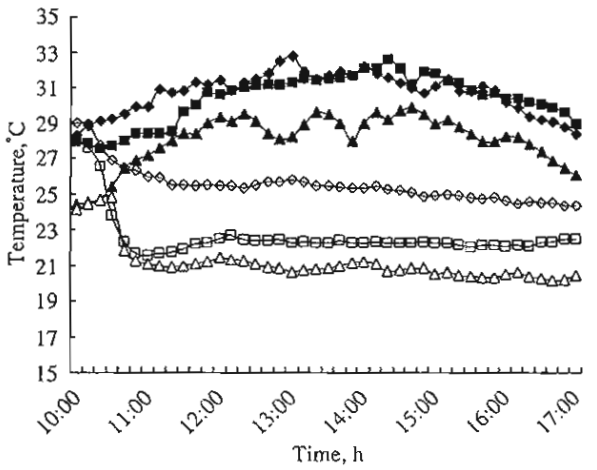

Fig. 8. Effect of ambient temperature and air mass flow rates on room temperature; –◆–, ambient temperature (4·4 kg s^{-1}); –■– ambient temperature (6·3 kg s^{-1}); –▲–, ambient temperature (9·2 kg s^{-1}); –◇–, room temperature (4·4 kg s^{-1}); –□–, room temperature (6·3 kg s^{-1}); –△–, room temperature (9·2 kg s^{-1})

Table 1
Input power and energy efficiency ratio at different airflow rate

Air flow rate, kg s^{-1}	*Input power, kW*	*Energy efficiency ratio*
4·4	1·14	24·4
6·3	1·15	51·2
9·2	1·23	59·9

4.4. *Rearing of silkworms—a demonstrative application*

The general question of the feasibility of a given application is not being addressed in this study. Instead, an experiment performed on the evaporative cooling system for rearing silkworms is used to illustrate a possible application. At this stage, two generations of Multi-voltine Thai silkworm 'Nanglai' (*Bombyx mori*) with 5000 larvae per generation were reared in the evaporative cooling house. The first and second generations were reared during November to December 2003 and March to April 2004, respectively. An interesting observation here is that, the percentage of survival of silkworms was 91% for the first generation and 93% for the second generation. Comparable conventional system percentage survival rates of silkworms were separated by

Table 2
Summary of economic evaluation of evaporative cooling system

Item	*Value, Baht*
Fixed cost	70 000
Variable cost	22 000
Income	49 420·8

season as follows: 46·5% for summer, 82·4% for rainy and 83% for winter (Attathom *et al.*, 2002). Obviously, the percentage of survival of the silkworms reared in the evaporative cooling system was higher than that obtained with the conventional rearing system, especially in summer. It could be concluded that the evaporative cooling system application could be an alternative in the silkworm rearing process.

4.5. *Economic evaluation*

In this section, a cost analysis of the evaporative cooling is evaluated. A payback period is employed to determine the period of time required for a profit that could be attributed to using the evaporative cooling. The payback period is defined as the investment of time required for the profit of an investment to equal the cost of the investment (Newnan, 1980). The life cycle of the Thai silkworm is approximately 25 days. Thus, 12 generations of silkworm can be raised per year with 44 000 larvae per generation. Assuming the percentage survival of silkworms was 90%, silkworm survival would be 39 600 larvae per generation. The average weight of a Thai silkworm cocoon was 1·3 g per larvae. The total weight for a survival of 39 600 larvae would be 51·48 kg per generation. During 2003, the purchase price of cocoon in the local market was 80 Baht per kg. The resulting annual income would have been 49 420·8 Baht. Fixed costs for the evaporative cooling house, including those for construction cost, suction fan, pump, piping and cooling pad, were 70 000 Baht. Variable costs, mainly the power cost, silkworm eggs and feed, were 22 000 Baht. These costs divided by the annual income of 49 420·8 Baht give a payback period of approximately 2·5 years. The summary of economic evaluation is given in Table 2. Therefore, the evaporative cooling system in a silkworm rearing house should be promoted as an alternative technology for the household farmer. Additional cost savings could be recognised in larger scale operations.

5. Conclusions

The feasibility of improving the indoor condition of a silkworm rearing house by using direct evaporative cooling was investigated experimentally. An experimental silkworm rearing house was built. The study was conducted during the summer and winter seasons in Mahasarakham, Thailand. It was found that the evaporative cooling system was capable of reducing the temperature and increasing the relative humidity as required for rearing the silkworm. An alternative scenario was also proposed that involved varying the air mass flow rate between summer and winter seasons to reduce operating costs. Consequently, as the experiment revealed, the evaporative cooling system should be recommended.

Acknowledgements

The authors would like to thank the Thailand Research Fund (TRF) for providing financial support to this study. Thanks are also due to Mr. N. On-uthai, Mr. M. Chinda, Mr. C. Sawasdee and Ms. S. Worrakhot for their assistance extended during data collection.

References

Attathom T; Saksirirat S; Pattanasethanon V (2002). Eri silkworm: potential culture on cassava leaf, factors affecting culturing and production cost analysis. Proceedings of XIXth Congress of the International Sericultural Commission, pp 274–278, Bangkok, Thailand

Boonyawattana K; Promwungkwa A; Terdtoon P; Rerkkriangkrai P (2003). The study of evaporative cooling pads performance and simulation of a swine house. Proceedings of the 17th Conference on Mechanical Engineering Network of Thailand

Chuprayoon S; Boonchoo S; Chuprayoon S (2002). Sericulture in Thailand. Proceedings of XIXth Congress of the International Sericultural Commission, pp 493–504, Bangkok, Thailand

El-Dessouky H T; Ettouney H M; Bouhamra W (2000). A novel air conditioning system membrane air drying and evaporative cooling. Transactions of the Institution of Chemical Engineering, 78(A), 999–1009

Ketjoy N (1999). Development of a mathematical model of changing temperature and relative humidity in the poultry house. Master Thesis 1999, Energy Technology Division, King Mongkut's University of Technology Thonburi, Bangkok, Thailand

Khedari J; Sangprajak A; Hirunlabh J (2002). Thailand climatic zones. Renewable Energy, 25(2), 267–280

Kittas C; Bartzanas T; Jaffrin A (2003). Temperature gradients in a partially shaded large greenhouse equipped with evaporative cooling pads. Biosystems Engineering, 85(1), 87–94

Koca R; Hughes W; Christiason L (1994). Evaporative cooling pads—test procedures and evaluation. Applied Engineering in Agriculture, 7(4), 485–490

Newnan D G (1980). Engineering Economic Analysis. Engineering Press Inc., California

Sericulture Extension Center No. 1-9 and Sericulture Sub-Division (2002). Silk yarn quality development by farmer groups in Thailand. Proceedings of XIXth Congress of the International Sericultural Commission, pp 568–574, Bangkok, Thailand

Suriyasomboon A; Lundeheim N; Kunavongkrit A; Einarsson S (2004). Effect of temperature and humidity on sperm production in Durco boars under different housing in Thailand. Livestock Production Science, **89**(1), 19–31

Tazima Y (1978). The Silkworm an Important Laboratory Tool. Kodansha Ltd., Tokyo, Japan

Watt J R (1986). Evaporative Air Conditioning Handbook, 2nd Edn. Chapman Hall, London, UK

Wiersma F; Short T (1983). Evaporative cooling. In: Ventilation of Agricultural Structures (Hellickson M A ed), pp 101–118. ASAE, St. Joseph, MI, USA

Willits D H (2003). Cooling fan-ventilated greenhouse: a modelling study. Biosystems Engineering, **84**(3), 315–329

Available online at www.sciencedirect.com
SCIENCE DIRECT®
Journal of Food Engineering 75 (2006) 423–432
JOURNAL OF FOOD ENGINEERING
www.elsevier.com/locate/jfoodeng

Parboiling brown rice using super heated steam fluidization technique

Somchart Soponronnarit [a], Adisak Nathakaranakule [a], Athikom Jirajindalert [a], Chaiyong Taechapairoj [b,*]

[a] *School of Energy and Materials, King Mongkut's University of Technology Thonburi, Suksawat 48 Road, Bangkok 10140, Thailand*
[b] *Faculty of Engineering and Industrial Technology, Silpakorn University, Sanamchandra Palace Campus, Nakorn Pathom 73000, Thailand*

Received 15 November 2004; accepted 27 April 2005
Available online 7 July 2005

Abstract

This research is a study of parboiling of brown rice using superheated steam fluidization technique. The influence of soaking temperature and time, steaming temperature, and bed depth on qualities of product: head rice yield, white belly, whiteness, and viscosity of rice flour were focused. The experiments were set up at the material initial moisture content of 12.8% dry basis (d.b.), soaking temperatures of 70–90 °C, soaking times of 0.5–2.0 h., steaming temperatures of 120–160 °C, velocity of 3.9 m/s and bed depths of 8–12 cm. The experimental result showed that gelatinization occurred while product moisture content decreased and final moisture content about 28% d.b. gave the acceptable levels of the whiteness and white belly. The final moisture content lower than 28% and 18% d.b. resulted in the lower percent of head rice yield and whiteness, respectively. Considering white belly, it was found that the white belly decreased with increasing drying time. Additionally, peak viscosity, breakdown viscosity and setback viscosity of rice flour were found lower than those of raw rice.

Keywords: Drying; Gelatinization; Grain; Head rice; Quality

1. Introduction

Parboiling of paddy is a hydro-thermal process aimed at improving milling, nutritional and organoleptic attributes of rice. It is an alternative method for prolonging rice storage. In addition, it reduces broken grain, increases head rice yield and reduces nutritional loss during polishing process (Bhattacharya, 1985). There are three steps of parboiling process consisting of soaking, steaming and drying. Paddy is moistened during the soaking process in which hot water is usually applied to enhance water diffusion into rice grain. Soaking process in warm water was found enhancing the effective cooking stage when the grain became saturated (Velupillai & Verma, 1982) because water makes starch granule sufficiently swell to be gelatinized. After soaking in hot water, paddy is left to cool down to environmental temperature for 2 h to allow water to enter the core part of rice grain.

The drying method is the key factor influencing the milling quality of rice (Bhattacharya & Indudhara Swamy, 1967). Several drying methods have been used for drying parboiled rice such as sun drying, hot air drying, vacuum drying and superheated steam drying (Bhattacharya, 1985; Soponronarit, Taechapairoj, & Prachayawarakorn, 2004; Taechapairoj, Prachayawarakorn, & Soponronarit, 2004).

Fluidization technique is an effective drying method, in which air and solid particles are rigorously mixed. It has been suggested that high moisture paddy should be dried quickly to approximate 23% d.b. to prevent the yellowing of rice kernels which is easily occurred at high moisture level and then subjected to ambient air

* Corresponding author. Fax: +66 34219360.
E-mail address: chaiyong_t@yahoo.com (C. Taechapairoj).

0260-8774/$ - see front matter © 2005 Elsevier Ltd. All rights reserved.
doi:10.1016/j.jfoodeng.2005.04.058

drying in a storage bin until its moisture content is down to 16% d.b. (Soponronnarit & Prachayawarakorn, 1994). Sutherland and Ghaly (1990) undertook an intensive investigation into the feasibility of using a hot air fluidized-bed drying technique for paddy. Their experiments showed that the head rice yield related to the final moisture content: the head rice yield was 58–61% when paddy was dried from 28.2% to 20.5% d.b. but was 15–24% for final moisture content lower than 20% d.b.

The drying medium which is used for carrying the evaporated water and fluidizing solid particles could be hot air or superheated steam. Superheated steam drying offers many important advantages over hot air drying. Firstly, the energy supplied to the dryer can be reduced economically by recycling the exhaust steam in a closed loop. Secondly, the energy from the exhaust steam resulting from the evaporation of moisture inside the solids can be recovered and used in the other sections. Lastly, environmental pollution or odour emission to the atmosphere can be eliminated since drying occurs in a closed chamber without air.

Parboiling of brown rice can save 40% of energy consumption compared to that of parboiled rice paddy. In addition, it prevents foreign matters and unsatisfied smell from rice paddy during soaking process. The cooking time is also reduced (Kar, Jain, & Srivastav, 1999).

The aim of this study is to determine the optimum parboiling process of brown rice using superheated steam fluidized bed. The physical properties of rice grain in terms of head rice yield, whiteness and white belly, rice flour viscosity and starch granule microstructure were compared with those of products dried in hot air under the same condition.

2. Materials and methods

Two fluidized-bed drying systems were used in the experiment. These are superheated steam and hot air systems (Fig. 1). The system of the superheated steam fluidized-bed dryer consists of five main components (Fig. 1a): a cylindrical chamber with a 15 cm inner diameter and a 100 cm height, a 13.5 kW electrical heater for converting saturated steam to the superheated steam, a backward-curved blade centrifugal fan driven by a 2.2 kW motor, a reverse flow cyclone and a small boiler with a 31 kg/h capacity of generated steam. A PID controller with an accuracy of ±1 °C was used to control steam temperature. Before using steam for drying, hot air was used for warming up the system until the temperature in every part reached the desired temperature. Then, the steam was replaced accordingly. The steam generator was generated the saturated steam at 106 kPa (absolute pressure) with the corresponding temperature of 100 °C. When the saturated steam was flowed through the electrical heaters, the additional heat

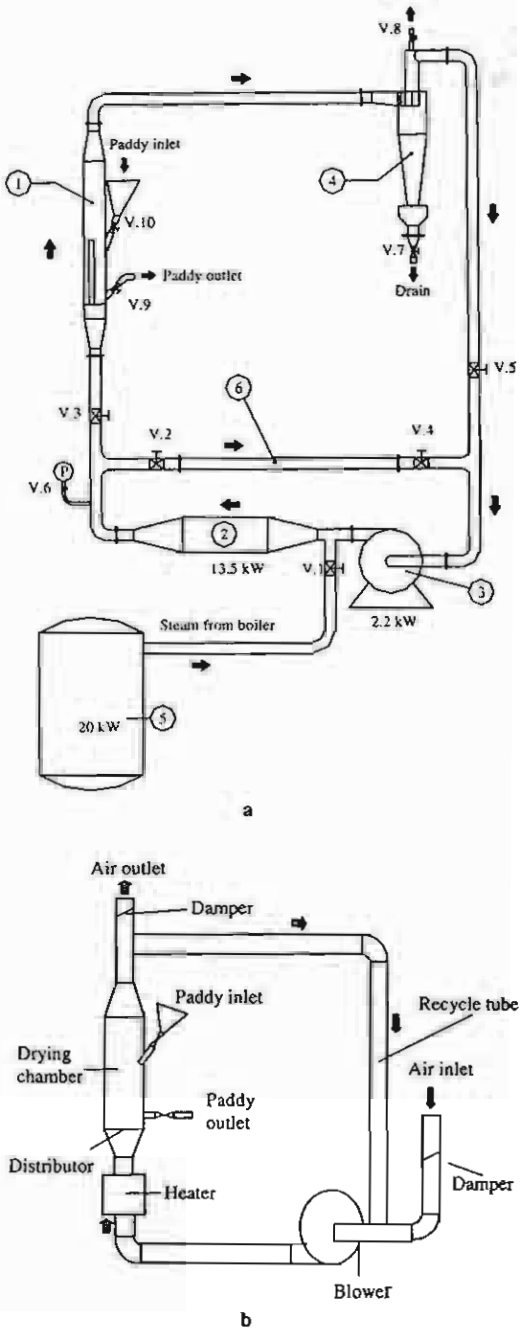

Fig. 1. Schematic diagrams of drying system. (a) Superheated steam fluidized-bed dryer. (b) Hot air fluidized-bed dryer.

was supplied to rise the steam temperature up to the required level. It was subsequently flowed through the fluidized-bed dryer. The dust particles and the immature grains being suspended in the exhaust steam were collected at the cyclone. Finally, the cleaning exhaust steam was reused again.

The hot air fluidized-bed dryer (Fig. 1b) consists of stainless steel cylindrical drying chamber of 20 cm

diameter and 140 cm height, a 12 kW heater with a PID controller with an accuracy of ±1 °C, a backward-curved blade centrifugal fan driven by a 1.5 kW motor.

Brown rice was prepared from long grain paddy of Chainat1 (CNT1) variety from Pathum Thani Rice Research Center, Pathum Thani Province, Thailand. The initial moisture of rice grain was 12.8% d.b. Brown rice was then soaked in hot water temperature of 70 °C for 0.5–2 h before draining and tempering to ambient temperature for 30 min. The drying condition was set at temperatures of 120, 140 and 160 °C, bed height of 8–12 cm at superficial velocity of 3.9 m/s under 106.1 kPa absolute pressure. The dried samples were then tempered to ambient temperature until the grain final moisture content was 16% d.b. before its quality was inspected.

The moisture content of paddy was determined by an electrical air oven at a temperature of 103 °C for 72 h. Paddy qualities in terms of head rice yield and whiteness were quantitatively determined and compared to the reference sample (paddy dried by the ambient air). The methods were followed with the guideline of the Ministry of Agriculture and Cooperatives, Thailand. Head rice is defined as milled rice having kernel length at least three-fourths of its original length. The head rice yield was calculated from the mass of white rice that remains as head rice after milling divided by the mass of paddy sample.

The colour of rice samples was measured by a Kett digital whiteness meter (Model C–300). Before measuring the colour of sample, the whiteness meter was calibrated with a white coloured reference, presenting a standard value of 86.3.

2.1. Scanning electron microscopy

Structural changes of kernels were investigated by scanning electron microscopy (SEM) (JSM-5600LV, Japan). The rice kernel was broken along the cross-sectional axis. Samples were placed on adhesive tape attached to a circular aluminum specimen stub, coated with gold layer using a sputter-coater and photographed at an accelerator potential of 10 kV.

2.2. RVA measurement

Pasting properties of rice flour were determined by a Rapid Visco Analyser model-4 (Newport Scientific Pty Ltd., Warriewood, Australia) utilizing thermocline. Following AACC Method 61-02 (AACC, 1995), the sample (3 g, 14% moisture basis) was mixed with distilled water in a RVA aluminum canister to make the total weight of slurry 28 g. The mixture was stirred at 900 rpm for 10 s and then changed to 160 rpm. The mixture was held at 50 °C for 1 min and then heated to 95 °C at 12 °C/min. After that, holding at 95 °C was 2.5 min, followed by cooling down to 50 °C at 12 °C/min and kept for 2.1 min. These tests were done in triplication. A plot of paste viscosity in arbitrary RVA unit (RVU) versus time was used to determine the peak viscosity (PV), temperature at peak viscosity (P_{Temp}), trough, final viscosity (FV), breakdown viscosity (BKV = PV − trough) and setback viscosity (SBV = FV − trough). The first point at which the viscosity increases to 1 RVU/s or faster is defined as the onset gelatinization temperature of rice flour (P_{Temp}). Peak viscosity (PV) indicates the water-binding capacity of mixture. It is often correlated with the final product quality, and also provides an indication of the viscous load likely to be encountered by a cook. Breakdown viscosity measures the degree of disintegration of the granules or paste stability. Setback viscosity is a measure of gelling or retrogradation tendency (Dengate, 1984).

3. Results and discussions

3.1. Drying curve

3.1.1. Effect of superheated steam temperature and bed depth

Fig. 2a shows the relationship between brown rice grain moisture content and temperature, and drying

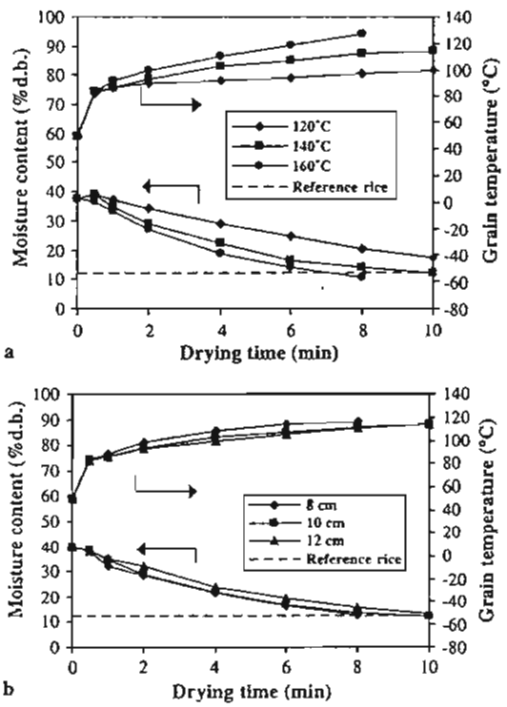

Fig. 2. Effect of superheated steam temperature and bed depth on moisture content and grain temperature at soaking temperature of 70 °C and soaking time of 1 h. (a) Bed depth 10 cm and (b) superheated steam temperature 140 °C.

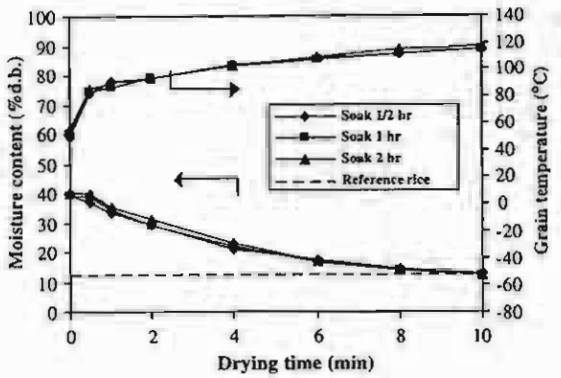

Fig. 3. Effect of soaking time on moisture content and grain temperature at superheated steam temperature of 140 °C and bed depth of 10 cm.

time. During the initial stage of drying, flowing water vapor was condensed due to its sudden contact with a low initial temperature of brown rice grain. This rapid release of heat vaporisation by condensation resulted in rapid increase in grain temperature. As shown in Fig. 2a, the grain temperature is slightly above 80 °C in the first minute of drying time and then relatively rises to 100 °C in 3 or 4 min. The grain temperature rapidly increases and higher grain temperatures follow with higher steam temperatures, resulting in the relative difference of moisture content.

The effect of bed depth on drying rate and grain temperature were of less significant than that of superheated steam temperature (Fig. 2b).

3.1.2. The effect of soaking time

Fig. 3 shows the relationship between soaking and drying rate. It was found that moisture content of grain increased with increasing soaking time due to water uptake of rice grain. However, its impact on drying rate of rice grain was not significant.

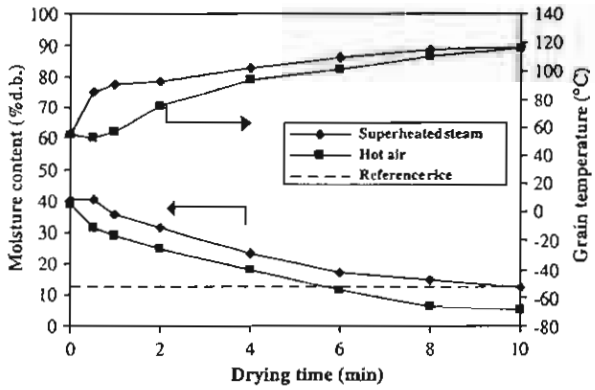

Fig. 4. Effect of heating media on moisture content and grain temperature at drying temperature of 140 °C, bed depth of 10 cm and soaking time of 2 h.

3.1.3. Comparison between superheated steam and hot air drying

Fig. 4 indicated that moisture content of rice grain dried by hot air dropped more rapidly and kept lower through the drying period. In contrast, the temperature of rice grain dried by superheated steam during the first minutes of drying increased faster than that dried by hot air. This phenomenon was due to latent heat from steam condensation added to rice grain during the initial stage of drying and superior heat transfer properties of superheated steam over hot air (Mujumdar & Menon, 1995).

3.2. Mathematical model of superheated steam drying

Fig. 5 shows drying curve predicted by the mathematical model in comparison with that from experimental data at various superheated steam temperatures and bed depths. It was found that the predicted curve was in accordant with experimental data. There were two drying periods in the predicted mathematical model as following.

3.2.1. Constant drying rate period

At the initial stage of drying, the drying rate of rice grain was constant due to the vaporization of water at grain surface. This period is indicated by the linear curve

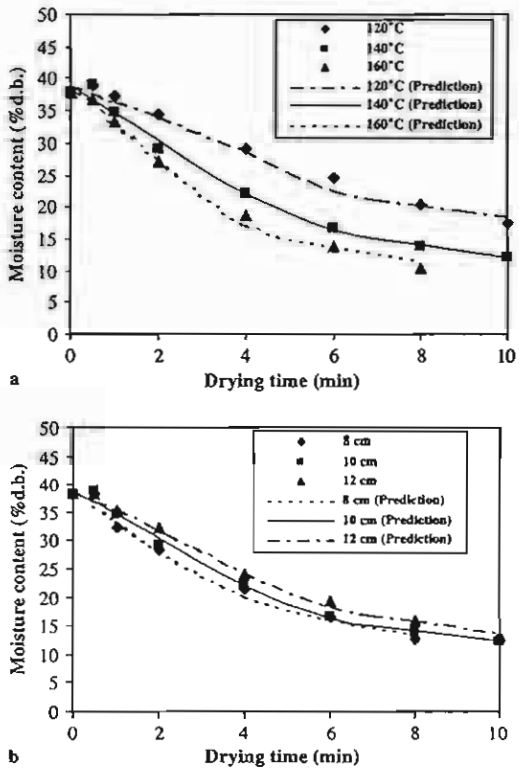

Fig. 5. Experimental data and the predicted drying curve under superheated steam. (a) Bed depth 10 cm and (b) superheated steam temperature 140 °C.

of grain moisture versus drying time. The drying rate is explained by the following equation:

$$MR = (-1.9594 \times 10^{-3} VT + 0.7586V + 4.004 \times 10^{-5} T - 0.016268)t + 1.030765 \ (R^2 = 0.92) \quad (1)$$

where V is specific mass velocity ($kg_{steam}/s\ kg_{drymatter}$), T is the inlet steam temperature (K) and t is drying time (s).

This equation is applicable in the range of temperature of 120–160 °C and specific mass velocity of 0.035–0.053 $kg_{steam}/s\ kg_{drymatter}$, and until the grain moisture reaches the critical moisture content of brown rice (about 25.5–26% d.b.) at which the falling drying rate period begins.

3.2.2. Falling drying rate period

After rice grain reaches its critical moisture content, the loss of moisture was at an exponential rate due to internal water diffusion to the grain surface at which the vaporization occurs. The effective diffusion coefficient of spherical shape brown rice grain was determined by analytical solution as Eq. (2).

$$\frac{M_t - M_{eq}}{M_{cr} - M_{eq}} = \frac{6}{\pi^2} \sum_{n=1}^{\infty} \frac{1}{n^2} \exp\left[\left(\frac{n\pi}{R}\right)^2 D_{eff}(t - t_{cr})\right] \quad (2)$$

where D_{eff} is the effective diffusion coefficient (m^2/s), R is the radius of brown rice (m) and t_{cr} is the drying time at the critical point (s)

Fig. 6 shows the relationship between the effective diffusion coefficient and bed depths, and superheated steam temperature. At drying temperature of 120–160 °C, the effective diffusion coefficient was between 1.0497×10^{-10}–2.4672×10^{-10} m^2/s. The effective diffusion coefficient increased with increasing drying temperature as indicated in the following Arrhenius equation.

$$D_{eff} = 9.95289 \times 10^{-7} \exp\left(\frac{-32915.126}{RT}\right) \ (R^2 = 0.86) \quad (3)$$

where T is the inlet steam temperature (K) and R is universal gas constant.

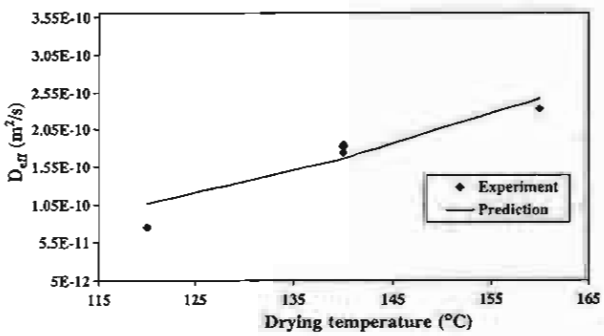

Fig. 6. Experimental and the predicted values of effective diffusivity (superheated steam).

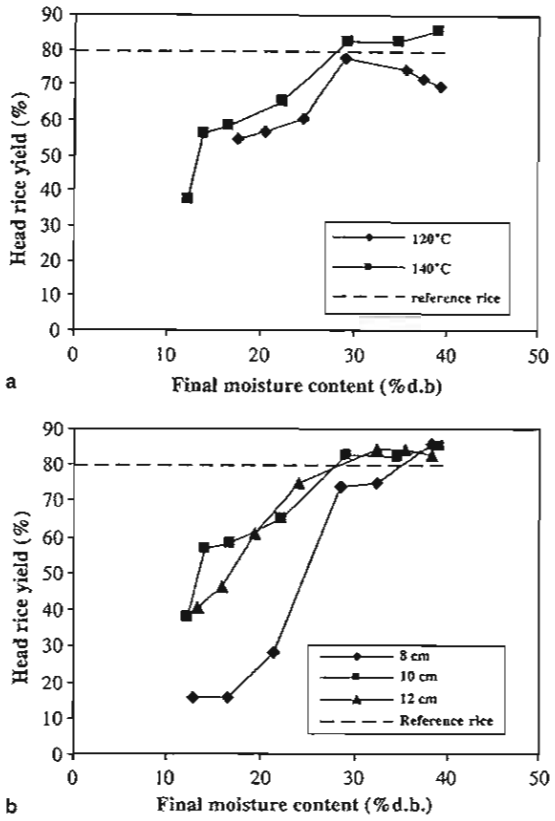

Fig. 7. Relationship between head rice yield and final moisture content during drying in superheated steam at different bed depths and superheated steam temperatures. (a) Bed depth 10 cm and (b) superheated steam temperature 140 °C.

3.3. Head rice yield

The relationship between head rice yield and final moisture content of brown rice grain at various

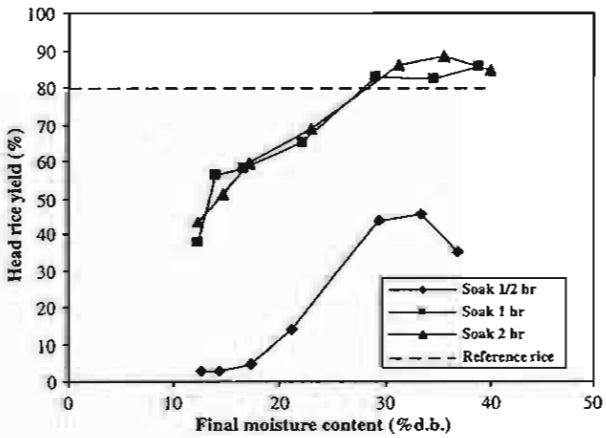

Fig. 8. Relationship between head rice yield and final moisture content at superheated steam temperature of 140 °C and bed depth of 10 cm.

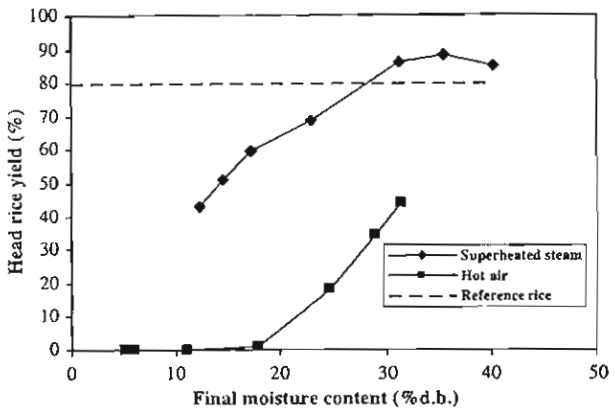

Fig. 9. Relationship between head rice yield and final moisture content of brown rice dried by superheated steam and hot air at drying temperature of 140 °C and bed depth of 10 cm.

superheated steam temperatures and bed depths are presented in Fig. 7.

Drying brown rice with superheated steam at an initial stage provided higher head rice yield compared to that of reference sample. An increase in head rice yield closed to that of reference rice was apparent at the final rice moisture content of 28–29% d.b. This improvement was caused by stronger structure of rice starch as a result of gelatinization process (Fig. 10c). Furthermore, the denaturation of protein and diffused into inter-granular space of starch increase the binding effect. With higher moisture content, rice starch dried by superheated steam was more rapidly gelatinized, thus, stronger structure was obtained. When rice grain with moisture content of lower than 28% d.b. was exposed to longer heat, rice grain temperature will be increased resulting in more porosities within rice starch, high moisture and temperature gradient causing stress development inside the kernels. As a result, rice kernel are more susceptible to physical damage during milling process leading to lower head rice yield. At given final moisture content, head rice yield increased with increasing superheated steam temperature and bed depth.

The relationship between head rice yield and final moisture content of rice grain at different soaking times is presented in Fig. 8. It was found that an increase in soaking time prompted an increase in head rice yield because of higher initial moisture content of rice grain. Soaking rice for less than 1 h is insufficient for rice to uptake water for gelatinization process resulting in lower head rice yield with white belly appearance.

Fig. 9 shows the relationship between head rice yield and final moisture content of brown rice grain comparing superheated steam drying and hot air drying. It was

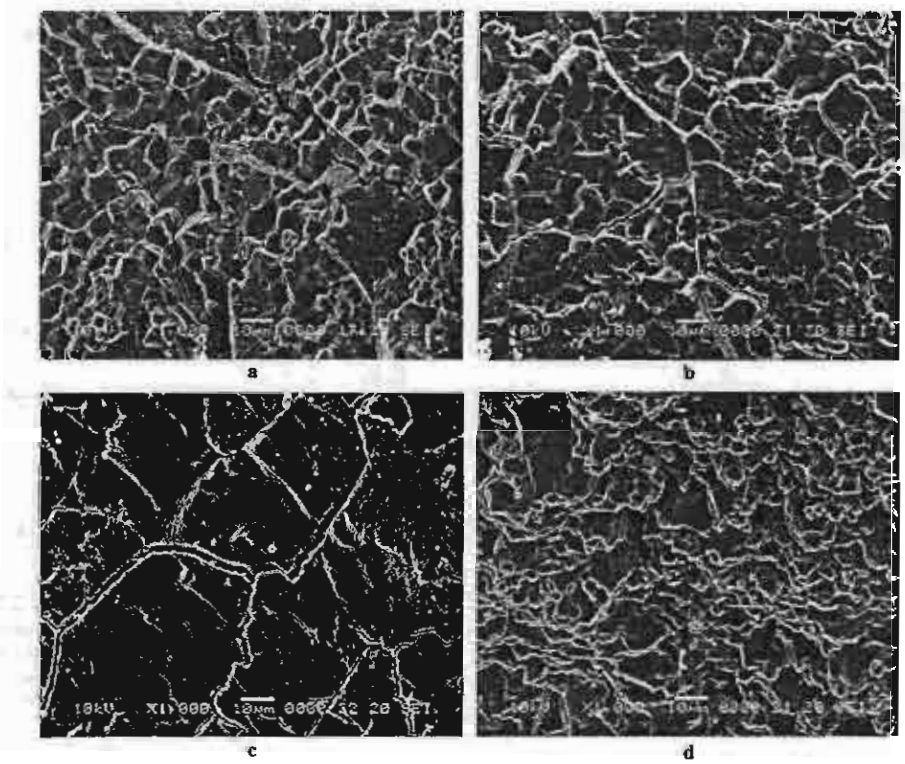

Fig. 10. Scanning electron micrographs of rice at different processes. (a) Raw rice, (b) soaked rice dried by ambient air, (c) soaked rice dried by superheated steam at temperature of 140 °C and (d) soaked rice dried by hot air at temperature of 140 °C.

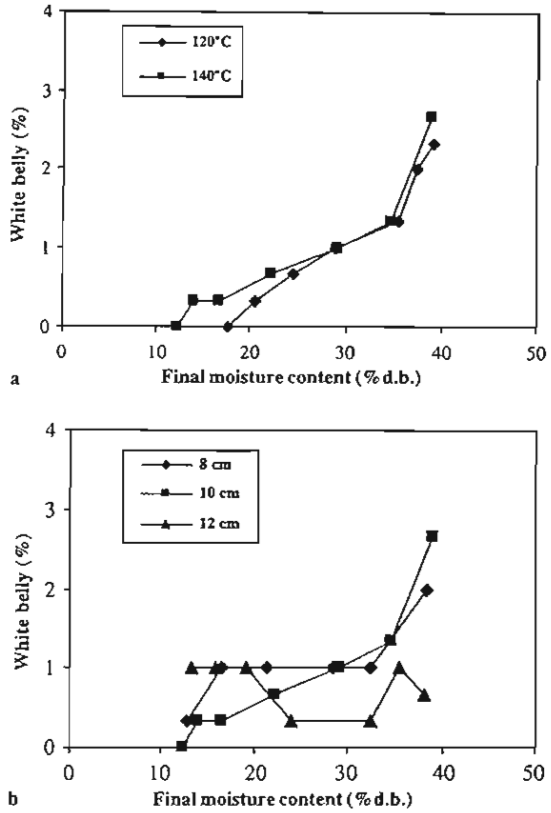

Fig. 11. Relationship between white belly percentage and final moisture content during drying in superheated steam at different drying temperatures and bed depths (white belly percentage of reference rice = 20%). (a) Bed depth 10 cm and (b) superheated steam temperature 140 °C.

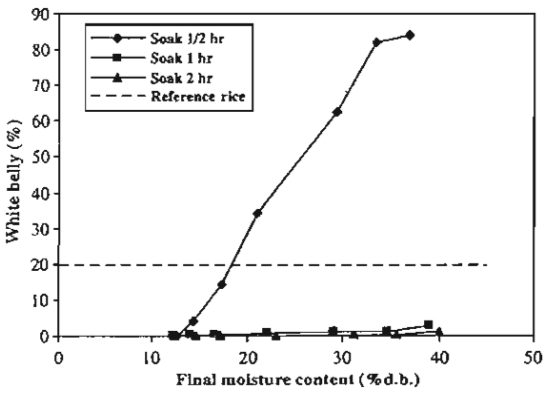

Fig. 12. Relationship between white belly percentage and final moisture content during drying in superheated steam temperature of 140 °C and bed depth of 10 cm at different soaking times.

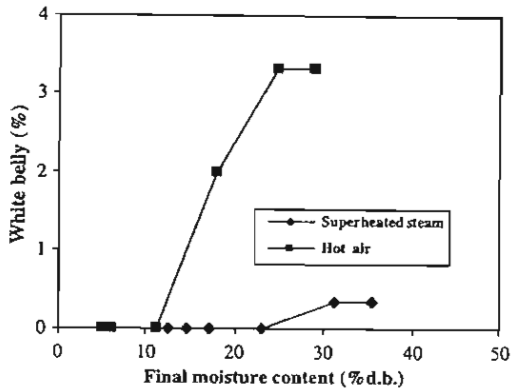

Fig. 13. Relationship between white belly percentage and final moisture content of brown rice dried by superheated steam and hot air at drying temperature of 140 °C and bed depth of 10 cm (white belly percentage of reference rice = 20%).

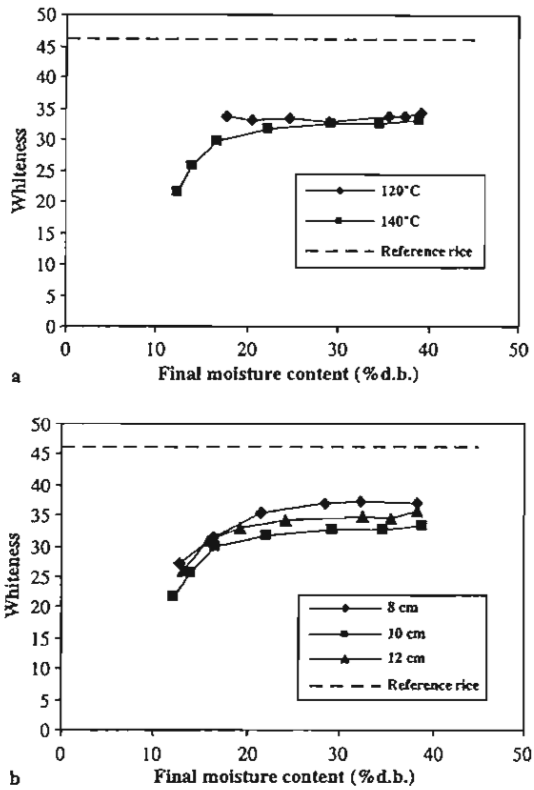

Fig. 14. Relationship between whiteness and final moisture content during drying in superheated steam at different drying temperatures and bed depths (whiteness of reference rice = 44.6). (a) Bed depth 10 cm and (b) superheated steam temperature 140 °C.

found that brown rice dried by superheated steam provided higher head rice yield than that dried by hot air. High head rice yield was still found at final moisture content of rice grain at 28% d.b. An improvement of head rice yield at initial stage of drying with superheated steam could be explained by suitable condition for gelatinization. Slow gelatinization process in hot air compared with superheated steam (Iyota, Nishimura,

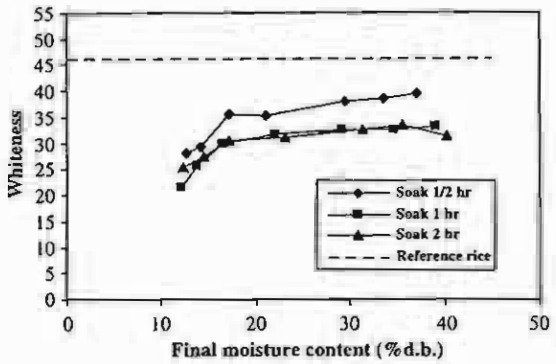

Fig. 15. Relationship between whiteness and final moisture content during drying in superheated steam temperature of 140 °C and bed depth 10 cm at different soaking times (whiteness of reference rice = 44.6).

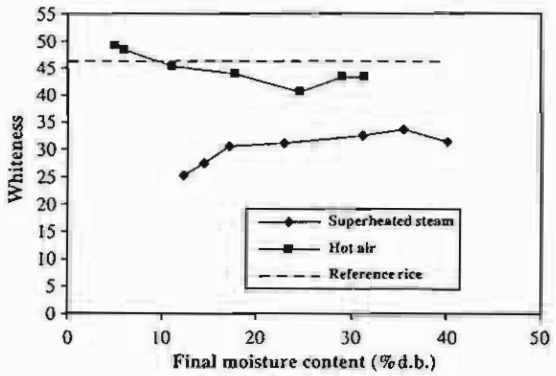

Fig. 16. Relationship between whiteness and final moisture content of brown rice dried by superheated steam and hot air at drying temperature of 140 °C and bed depth of 10 cm (whiteness of reference rice = 44.6).

Onuma, & Nomura, 2001) causes susceptible grain to damage during milling process; thus, lower head rice yield. Fig. 10c shows the completed gelatinization of rice starch obtained from superheated steam compared with incomplete gelatinized structure as indicated in Fig. 10d.

3.4. White belly

White belly is considered a poor characteristic of parboiled rice caused by incomplete gelatinization of rice starch. It is described as dully white spot with porosities between the starch granules. White belly is usually found at the core of rice kernel. Figs. 11 and 12 show the relationship between white belly and final moisture content of brown rice at various temperatures, bed depths and soaking times. The results indicated that soaking time influenced the white belly intensity. The longer soaking period, the less extent of white belly was the rice kernel. However, this association was obvious only at the soaking period of 0.5 h. When the soaking period was over half an hour, final moisture was not related to white belly. This could be explained that at soaking period of 0.5 h, the water uptake was found only at the surface of rice kernel resulting in uneven gelatinization of starch with the rice kernel.

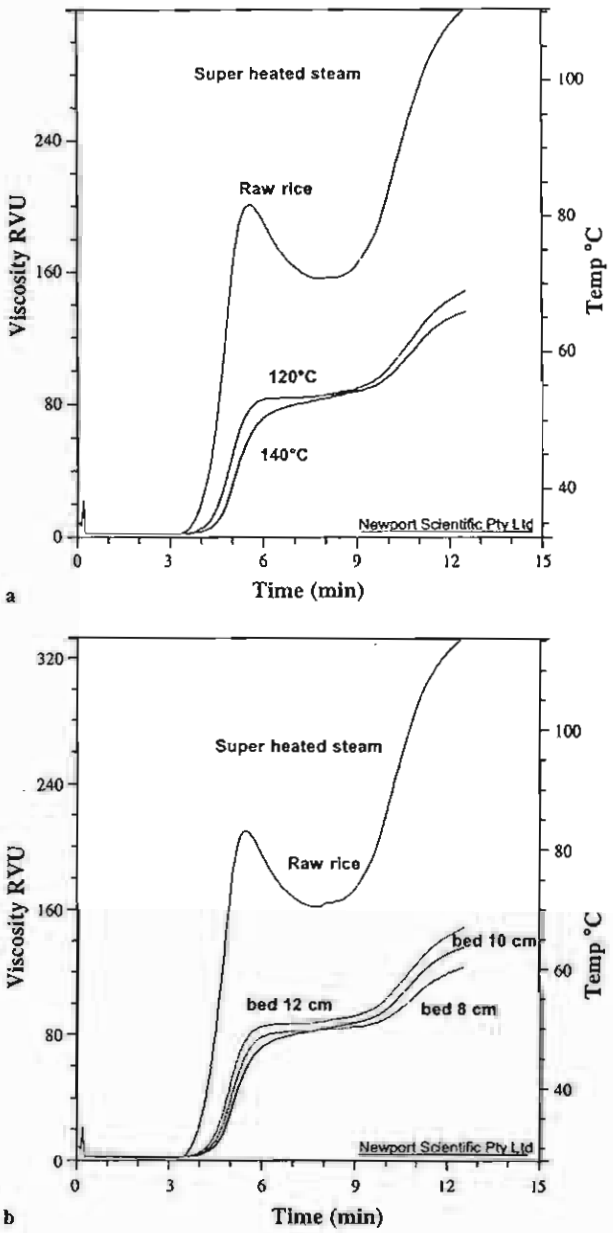

Fig. 17. Viscograph of raw rice flour and rice flour dried by superheated steam (soaking time 1 h). (a) Bed depth 10 cm and (b) superheated steam temperature 140 °C.

Fig. 13 shows the relationship between white belly and final moisture content of brown rice grain during drying with superheated steam and hot air. It was found that drying brown rice grain with superheated steam

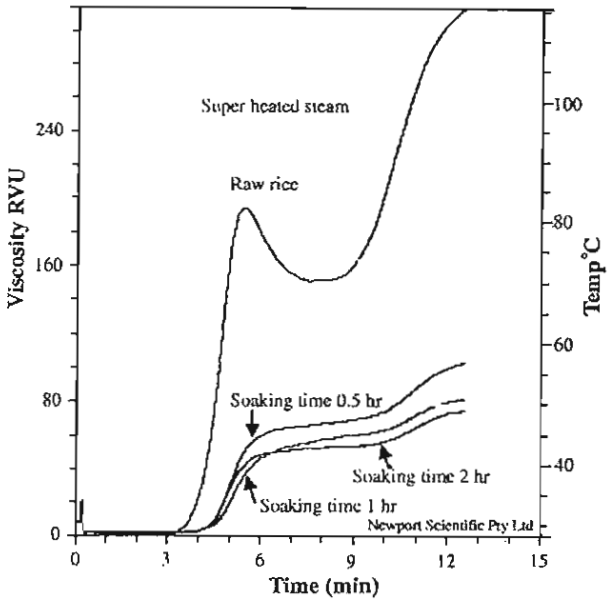

Fig. 18. Viscograph of raw rice flour and rice flour dried by superheated steam at drying temperature of 140 °C and bed depth of 10 cm.

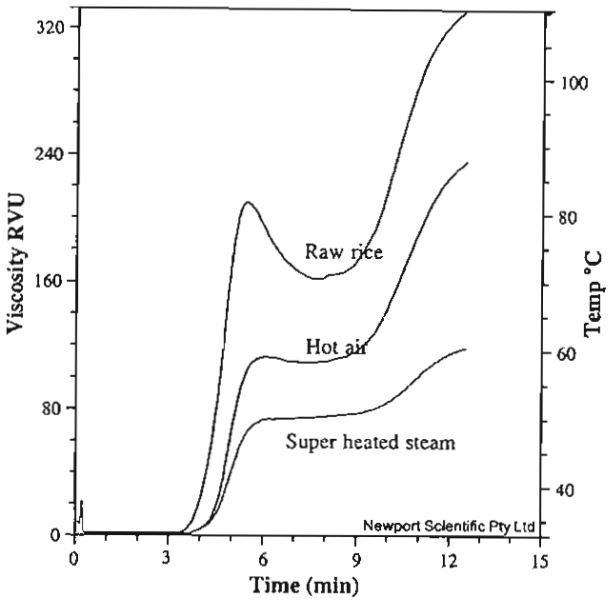

Fig. 19. Viscograph of raw rice flour and rice flour dried by superheated steam and hot air at drying temperature of 140 °C and bed depth of 10 cm.

gave less white belly kernel than that with hot air. This improvement was due to more complete gelatinization resulted from water condensation from superheated steam while no condensation was found in hot air drying.

3.5. Whiteness

Compared with reference rice, dried brown rice gave lower whiteness value (Figs. 14–16). The dark colour of dried grain was caused by maillard browning reaction between reducing sugar and amino acid activated by heat. Fig. 14 shows the relationship between the whiteness and final moisture content of brown rice at various temperatures and bed depths. It was found that whiteness of brown rice dried by superheated steam was higher in value compared to that of reference rice. Superheated steam temperature did not show significant effect on the whiteness. The decrease in whiteness was found only when the final moisture content of brown rice was lower than 20% d.b.

Whiteness of brown rice is associated bed depth. At bed depth of 8 cm, the whiteness of brown rice was highest in value. Soaking time was also related to whiteness of brown rice. However, there was significant effect only at soaking time of 0.5 h (Fig. 15). This was due to the short period of soaking allowing less moisture uptake into rice grain; thus, it was insufficient for complete

Table 1
Pasting properties of raw and dried rice flour

	Peak viscosity (rvu)	Trough 1 (rvu)	Breakdown viscosity (rvu)	Final viscosity (rvu)	Setback viscosity (rvu)	Pasting temperature (°C)
Raw rice	209.67	161.92	47.75	332.67	123.00	79
Hot air 140 °C, soaking time 2 h and bed depth 10 cm	112.92	109.33	3.58	236.67	123.75	89
Superheated steam 120 °C, soaking time 1 h and bed depth 10 cm	84.33	84.42	−0.08	148.58	64.25	89
Superheated steam 140 °C, soaking time 1/2 h and bed depth 10 cm	84.92	84.83	0.08	139.42	54.50	89
Superheated steam 140 °C, soaking time 1 h and bed depth 10 cm	80.08	80.50	−0.42	135.92	55.83	89
Superheated steam 140 °C, soaking time 2 h and bed depth 10 cm	77.75	77.58	0.17	125.08	47.33	89.9
Superheated steam 140 °C, soaking time 1 h and bed depth 8 cm	82.17	82.17	0.00	123.00	40.83	89
Superheated steam 140 °C, soaking time 1 h and bed depth 12 cm	87.17	87.17	0.00	148.58	61.42	89

gelatinization. This appearance was in accordant with white belly characteristic.

As shown in Fig. 16, the result indicated more whiteness of brown rice dried by hot air than that by superheated steam. The whiteness of brown rice dried by hot air increased when final moisture content of grain decreased. On the contrary, the whiteness of brown rice started to decrease at final moisture content of rice kernel lower than 20% d.b.

3.6. Pasting properties

Pasting properties of rice starch dried by superheated steam and hot air, and reference rice (not dried) are shown in Figs. 17–19 and Table 1. The result shows that pasting temperature of rice starch dried by superheated steam and hot air was higher than that of reference rice. On the other hand, PV, BKV and FV of rice starch dried by superheated steam and hot air was lower than that of reference rice (Figs. 17 and 18). Decrease in PV of dried rice was due to its loss of water-binding capacity as a result of partial gelatinization. Since rice dried by superheated steam gave more complete gelatinization, its PV was lower than that dried by hot air. FV and SBK indicate cooked rice hardness (Ali & Bhattacharya, 1980; Priestley, 1976; Ranghavendra & Juliano, 1970). Brown rice dried by superheated steam gave lower FV and SBK compared to those of hot air dried grain. Therefore, cooked rice obtained from superheated steam drying provided higher hardness than that of hot air dried rice and reference rice when cooked.

4. Conclusion

From the study of superheated steam fluidized-bed drying of parboiled brown rice, it was found that superheated steam temperature was the most significant effect on drying rate while bed depth and rice soaking period were of minor importance. The head rice yield considerately decreased when final moisture content of rice grain was lower than 28% d.b. When final moisture content of brown rice was lower than 18% d.b. the whiteness of rice decreased. Increasing soaking time improved head rice yield and reduced white belly due to increasing gelatinization. According to the viscosity properties of rice starch, superheated steam drying provided lower PV, BKV and SBV compared with hot air.

Acknowledgements

The authors would like to express their profound thanks to Thailand Research Fund for financial support and Institute of Food Research and Product Development, Kasetsart University for physical properties testing machine.

References

AACC. (1995). *Approved method of the American Association of Cereal Chemists*, 9th ed. St. Paul, MN: American Association of Cereal Chemists, AACC.

Ali, S. Z., & Bhattacharya, K. R. (1980). Pasting behaviour of parboiled rice. *Journal of Texture Studies, 11*, 239–245.

Bhattacharya, K. R. (1985). Parboiling of rice. In B. O. Juliano (Ed.), *Rice: Chemistry and technology* (pp. 289–348). St. Paul, MN, USA: American Association of Cereal Chemists.

Bhattacharya, K. R., & Indudhara Swamy, Y. M. (1967). Conditions of drying parboiled Paddy for optimum milling quality. *Cereal Chemistry, 44*, 592–600.

Dengate, H. N. (1984). Swelling pasting and gelling of wheat starch. In Y. Pomeranz (Ed.). *Advances in cereal science and technology* (vol. 6, pp. 49–82). St. Paul, MN, USA: American Associated Cereal Chemistry.

Iyota, H., Nishimura, N., Onuma, T., & Nomura, T. (2001). Drying of sliced raw potatoes in superheated steam and hot air. *Drying Technology, 19*(7), 1411–1424.

Kar, N., Jain, R. K., & Srivastav, P. P. (1999). Parboiling of dehusked rice. *Journal of Food Engineering, 39*(1), 17–22.

Mujumdar, A. S., & Menon, A. S. (1995). Drying of solids. In A. S. Mujumdar (Ed.), *Handbook of industrial drying* (2nd ed., pp. 1–46). New York: Marcel Dekker.

Priestley, R. J. (1976). Studies on parboiled rice. I. Comparison of the characteristics of raw and parboiled rice. *Food Chemistry, 1*, 5–14.

Ranghavendra, R. S. N., & Juliano, B. O. (1970). Effect of parboiling on some physicochemical properties of rice. *Journal Agricultural Food Chemistry, 18*, 289–294.

Soponronnarit, S., & Prachayawarakorn, S. (1994). Optimum strategy for fluidised bed paddy drying. *Drying Technology, 12*(7), 1667–1686.

Soponronarit, S., Taechapairoj, C., & Prachayawarakorn, S. (2004). New technique producing parboiled rice. *The Journal of the Royal Institute of Thailand, 29*(1), 78–86.

Sutherland, J. W., & Ghaly, T. F. (1990). Rapid fluid-bed drying of paddy rice in the humid tropics. Presented the 13th ASEAN seminar on grain postharvest technology, Bandar Seri Begawan, Brunei Darussalam (pp. 1–12).

Taechapairoj, C., Prachayawarakorn, S., & Soponronarit, S. (2004). Characteristics of rice dried in superheated steam fluidised bed. *Drying Technology, 22*(4), 719–743.

Velupillai, L., & Verma, L. R. (1982). Parboiled rice quality as affected by the level and distribution of moisture after the soaking process. *Transactions of the American Society of Agricultural Engineering*, 1450–1456.

Available online at www.sciencedirect.com
SCIENCE DIRECT®
Journal of Food Engineering 76 (2006) 411–419
JOURNAL OF FOOD ENGINEERING
www.elsevier.com/locate/jfoodeng

Modelling of parboiled rice in superheated-steam fluidized bed

Chaiyong Taechapairoj [a,*], Somkiat Prachayawarakorn [b], Somchart Soponronnarit [c]

[a] Faculty of Engineering and Industrial Technology, Silpakorn University, Sanamchandra Palace Campus, Rajamankha Nai Road, Amphoe Muang, Nakhon Phathom 73000, Thailand
[b] Faculty of Engineering, King Mongkut's University of Technology Thonburi, Suksawat 48 Road, Bangkok 10140, Thailand
[c] School of Energy and Materials, King Mongkut's University of Technology Thonburi, Suksawat 48 Road, Bangkok 10140, Thailand

Received 8 July 2004; accepted 21 May 2005
Available online 21 July 2005

Abstract

Mathematical model of paddy drying in superheated-steam fluidized bed has been developed to predict moisture content and temperature. The model was written based on mass and energy balance. The kinetics of gelatinization of paddy at fluidizing condition described by zero-order reaction was also included in the model. The operating parameters set in the model development included superheated-steam temperature, bed depth and superficial superheated-steam velocity. The numeric calculations from the model were in agreement with experimental investigations for different operating conditions. The model was then used to examine the effect of the operating conditions on the drying behavior and gelatinization of paddy.

Keywords: Fluidized bed; Gelatinization; Mathematical model; Superheated steam

1. Introduction

Traditional parboiling process consists of many steps. In the process, paddy is steeped in water overnight or longer until attaining the moisture content between 42% and 54% dry basis. Boiling or steaming the steeped rice at 100 °C is proceeded in order to gelatinize the starch. The parboiled rice is then cooled down to ambient environment and then dried before storage and milling. In the modern parboiling process, hot water is applied during steeping stage in order to eliminate the enzymatic activity that produces the sour odor and accelerate transport of water into the kernels. However, these processes are still not very convenient in practice since they still consist of many steps and take a long time. With the advent of using superheated steam for dehydrating foods (Blasco & Alvarez, 1995; Makowski, Cenkowski, Hatcher, Dexter, & Edwards, 2003; Tang & Cenkowski, 2000), it shows great potential to replace the hot air, particularly when used with starch-based materials. Recent studies have also reported on advantages of superheated-steam drying such as high drying rate and deodorization of products (Iyota, Nishimura, Nomura, Konishi, & Yoshida, 2002; Tatemoto, Mawatari, Sakurai, Noda, & Komatsu, 2002). Therefore, an attempt to use this medium for producing the parboiled rice is of particular interest in the present investigation. When using this medium type, both steaming and drying stages, required for the traditional method, are incorporated into a single stage.

In producing the parboiled rice, the translucent kernel, implying the starch available in the raw material to be gelatinized, is the most important feature that is concerned by the producer, in addition to the colour. The quality of parboiled rice is downed from the premium grade when the white belly, which is in part of ungelatinized starch, appears. The white belly problem is not very serious for the conventional method since the paddy is closely contacted with steam in a closed

* Corresponding author. Fax: +66 34219360.
E-mail address: chaiyong_t@yahoo.com (C. Taechapairoj).

0260-8774/$ - see front matter © 2005 Elsevier Ltd. All rights reserved.
doi:10.1016/j.jfoodeng.2005.05.040

bin for a sufficient long time and there is no moisture loss from the grains during steaming so that the starch is almost gelatinized completely. The gelatinization behaviour may be changed when the parboiled rice is made with superheated-steam drying where three stages i.e. heat, moisture transfer and gelatinization, are simultaneously occurred in the drying chamber. The gelatinization may not complete if the temperature is not adequately high and the grains held in the drying chamber too short. To obtain a good quality of parboiled rice, a mathematical model with incorporation of gelatinization kinetics is thus needed to simulate the drying of paddy in bed fluidized with superheated steam. This investigation is directed towards understanding the dehydration process associated with gelatinization of paddy occurring in the superheated-steam fluidized bed.

2. Mathematical model of drying system

As a model for the fluidized-bed dryer, the designation presented in Fig. 1 is used. To produce the parboiled rice, dry paddy is soaked in water until its moisture content reach 44–45% dry basis, at which it is almost uppermost holding capacity of kernel. When the soaked paddy is come into contact with steam, the corresponding steam condenses onto the paddy surface, thereby gaining moisture content. The increased moisture content may be present in the area near the exterior surface. Under such state together with the existing high initial moisture content, the evaporation rate is very fast, as evident from the experiment, and the moisture transport is governed by heat transfer control. As drying further proceeds, the surface dries and the available moisture in part of interior area is transported to the exterior by the Fick's law of diffusion. To predict the moisture content over the entire drying period, three distinct phases with different heat and mass transfer mechanisms are therefore identified and the energy balance for the components of steam, solid and water evaporated or contained in the grains are set up. To develop a mathematical model, it requires the following assumptions:

- Uniform moisture content throughout the bed.
- A plug flow of steam.
- Negligible heat loss of drying system.
- The temperature gradient inside single kernel and the grain shrinkage are negligible.
- Small Biot number, presenting unimportant heat conduction in paddy kernel.
- During period of condensation, the amount of steam flowing through the bed is totally condensed.

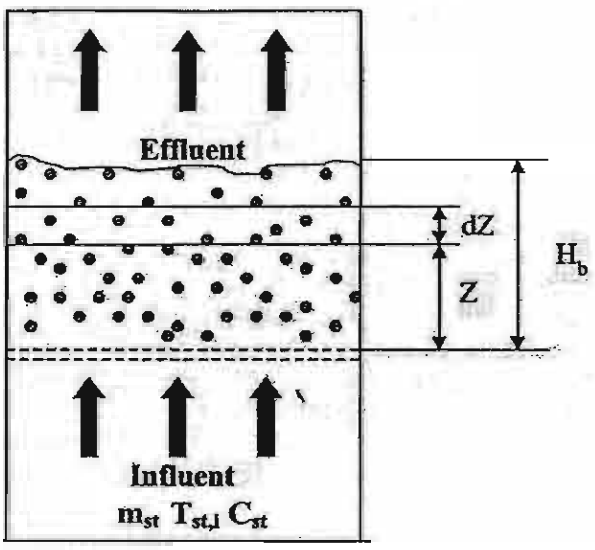

Fig. 1. Control volume of fluidised bed chamber.

2.1. Heating up period

At initial heating phase, superheated steam will thoroughly contact with cold surface of grain. As a result, the steam condensation will obviously occur onto the grain surface and the subsequent grain temperature rapidly increases from the initial temperature (room temperature) to the steam saturation temperature. The steam condensation is stopped when the grain temperature arrives at the saturation temperature which is 100 °C at the corresponding pressure of 106 kPa. To account for such change, the energy balance was made and the first term on the left side of Eq. (1) stands for the heat released by superheated steam, the second term represents heat of condensation and the last term characterizes the heat released from the saturated water to the temperature T_p, which is lower than the saturation temperature:

$$\dot{m}_{st}C_{st}(T_{st,i}-T_{sat})+\dot{m}_{st}h_{fg}+\dot{m}C_{fl}(T_{sat}-T_p) = m_{ds}(M_iC_{fl}+C_p)\frac{dT_p}{dt} \quad (1)$$

where $\dot{m}_{st}$ is the mass flow rate of steam (kg s^{-1}), m_{ds} is the dry mass of solid particles in the bed (kg), C_{st} is the specific heat of steam (J kg^{-1} K^{-1}), C_{fl} is the specific heat of water (J kg^{-1} K^{-1}), C_p is the specific heat of solid particle (J kg^{-1} K^{-1}), h_{fg} is the latent heat of vaporization (J kg^{-1}), $T_{st,i}$ is the temperature of steam at the inlet of drying chamber (K), T_{sat} is the saturated steam (K) and T_p is the temperature of particles (K), M_i is the initial moisture content and t is the drying time. To solve Eq. (1), it requires the initial condition which is the grain temperature equal to the room temperature.

While steam condenses in the bed of particles, paddy immediately adsorbs the condensing water and the resulting its moisture content is changed. The varying

quantities of moisture content of paddy can be can be calculated by the following equation:

$$\left(\frac{dM}{dt}\right)_{heat-up} = \frac{\dot{m}_{st}}{m_{ds}} \quad (2)$$

2.2. Constant rate period

Drying of paddy, with an initial moisture content of 41–42.5% dry basis, using superheated-steam fluidized bed existed the constant drying rate period, in addition to the falling rate period (Taechapairoj, Prachayawarakorn, & Soponronnarit, 2004). At the constant rate period, temperature of moist paddy keeps a constant value at the saturation temperature (T_{sat}) when using superheated steam as drying medium, whereas it is equal to the wet-bulb temperature for the hot air drying. The heat transfer rate from superheated steam to the grains, imposed by difference between steam temperature, T_{st}, and sample temperature, T_p, must be equal to the enthalpy change of superheated steam and it can thus be written for a small control volume in the fluidized-bed as

$$-\dot{m}_{st}C_{st}dT_{st} = h_p(T_{st} - T_p)dA \quad (3)$$

let

$$A = A_p\frac{Z}{H_b}$$

where h_p is the heat transfer coefficient (W m^{-2} K^{-1}), A_p is the surface area of a single kernel (m^2), Z is the distance along the bed height (m) at any time and H_b is the total solid bed height (m). Substitution of A into Eq. (3) yields

$$-\dot{m}_{st}C_{st}dT_{st} = h_p(T_{st} - T_p)d\left(A_p\frac{Z}{H_b}\right)$$

The above equation is rewritten as

$$\int_{T_{st,i}}^{T_{st}}\frac{dT_{st}}{T_{st} - T_p} = -\int_0^Z \frac{h_pA_p}{\dot{m}_{st}C_{st}H_b}dZ \quad (4)$$

Upon integrating Eq. (4) and then rearranging it, we obtain

$$T_{st} = (T_{st,i} - T_p)\exp\left(-\frac{h_pA_p}{\dot{m}_{st}C_{st}H_b}Z\right) + T_p \quad (5)$$

The average temperature of superheated steam in drying chamber can be determined by

$$T_{st,avg} = \frac{1}{H_b}\int_0^{H_b} T_{st}dZ \quad (6)$$

Substituting T_{st} in Eq. (5) into Eq. (6), the average steam temperature is thus

$$T_{st,avg} = \frac{\dot{m}_{st}C_{st}}{h_pA_p}(T_{st,i} - T_p)\left(1 - \exp\left(-\frac{h_pA_p}{\dot{m}_{st}C_{st}}\right)\right) + T_p \quad (7)$$

where $T_{st,avg}$ is the average steam temperature (K).

To determine the kernel moisture content, the energy balance is applied again by which the heat transferred from medium to the grains is equal to the heat of vaporization, plus sensible heat of the evaporated water, yielding

$$\{h_{fg} + C_{st}(T_{st,avg} - T_{sat})\}m_{ds}\left(\frac{dM}{dt}\right)_{cons} = -h_pA_p(T_{st,avg} - T_p)$$

and reporting:

$$\left(\frac{dM}{dt}\right)_{cons} = \frac{-h_pA_p(T_{st,avg} - T_p)}{m_{ds}\{h_{fg} + C_{st}(T_{st,avg} - T_p)\}} \quad (8)$$

2.3. Falling rate period

Drying rate starts reducing when moisture content of paddy is lower than the critical moisture content. Below the critical level, the paddy surface is rather dried and the moisture existing inside kernel will transport to the surface via chaotically void spaces by moisture diffusion mechanism and this mechanism is a main controlling step in dehydration process.

Similar to the energy balance as mentioned in the constant drying rate period, the average steam temperature is

$$T_{st,avg} = \frac{\dot{m}_{st}C_{st}}{h_pA_p}(T_{st,i} - T_p)\left(1 - \exp\left(-\frac{h_pA_p}{\dot{m}_{st}C_{st}}\right)\right) + T_p \quad (9)$$

where T_p is the grain temperature (K) and it is equivalent to the steam saturation temperature at the beginning of falling rate period. In the solid phase, the heat is transferred from steam and this provides energy to increase grain temperature and evaporate some amounts moisture from the grain. Hence, the grain temperature can then be calculated by

$$\frac{dT_p}{dt} - \frac{1}{m_{ds}C_p}\left[\{h_{fg} + C_{st}(T_{st,avg} - T_p)\}m_{ds}\left(\frac{dM}{dt}\right)_{fall} + h_pA_p(T_{st,avg} - T_p)\right] \quad (10)$$

where m_{ds} is the total dry matter of grains in the dryer. Eqs. (9) and (10) are solved using the iterative technique. The initial condition for Eq. (10) is the particle temperature equal to the temperature of saturated steam. Convective heat transfer coefficient (h_p) can be determined by the equation proposed by Shi-Jan-Fou, Romankov & Rashkovska and this equation is appeared in the article written by Ciesielczyk (1996) as follows:

$$Nu = 0.25Re\frac{d_s}{H_b(1 - \varepsilon_0)} \quad (11)$$

where d_s is the particle diameter, ε_0 is the void and Re is the Reynold number, $\frac{d_s u \rho_s}{\mu}$ (u is the superficial velocity of superheated steam (m s^{-1}), μ is the superheated steam viscosity (kg/m s)). Using Eq. (11), we assume that the void in the fluidized bed was equivalent to the void at the minimum fluidizing condition. The rate of water removal, $\frac{dM}{dt}$ in Eq. (10), can be determined from the theoretical diffusion equation, Eq. (12).

$$\mathrm{MR} = \frac{6}{\pi^2}\sum_{n=1}^{\infty}\frac{1}{n^2}\exp\left[-\frac{n^2\pi^2}{r}\left(\frac{D_{\mathrm{eff}}t}{r}\right)\right] \tag{12}$$

where MR is the dimensionless ratio of $\frac{M(t)-M_{eq}}{M_{cr}-M_{eq}}$, r is the radius of sphere (m), t is the time (s), M_{cr} is the critical moisture content, with a value of 25% d.b. (Taechapairoj et al., 2004) and M_{eq} is assumed to be zero since the high steam temperature is used.

The effective diffusion of paddy in superheated-steam fluidized-bed dryer (Taechapairoj et al., 2004) is given by

$$D_{\mathrm{eff}} = 2.4243\times10^{-6}\exp\left(-\frac{29100}{RT_p}\right) \tag{13}$$

where R is the universal gas constant (J/mol K) and D_{eff} is the effective diffusion coefficient (m/s^2). Eq. (13) is valid in the grain temperature range between 112 and 126 °C.

2.4. Gelatinization kinetics

During gelatinization, starch granules undergo hydration, formation of ghost remnants, swelling, exudation of amylose and amylopectin, loss of birefringence, loss of crystallinity and changes in viscosity. To develop mechanisms for starch gelatinization, Taechapairoj et al. (2004) measured the degree of gelatinization of samples, dried by superheated-steam fluidized-bed dryer at different temperatures, using a differential scanning calorimeter. The change in gelatinized starch was described by the zero-order reaction (Taechapairoj et al., 2004):

$$\frac{\mathrm{d}(\%\mathrm{USG})}{\mathrm{d}t} = k \tag{14}$$

and

$$k = 75.93504 - (933.9536 - (97.5594 * H_b) + (3.3496 * H_b^2))\exp\left(\frac{-21944.38}{RT_p}\right) \tag{15}$$

where H_b is the bed depth, USG is the ungelatinization (%) and t is the time (s). Eq. (15) is valid in the bed depth 10–15 cm and the grain temperature range between 112 and 126 °C.

2.5. Solution algorithm

The calculation procedure of moisture change and gelatinization development during simultaneous heat and mass transfer in superheated-steam fluidized-bed dryer is shown in Fig. 2. The input variables are an initial moisture content of paddy, a bed depth, a superficial superheated-steam velocity and a superheated-steam temperature. The calculation steps are as follows: the change of grain temperature in the heating up period is determined. If the grain temperature is lower than the boiling point temperature, the calculation procedure

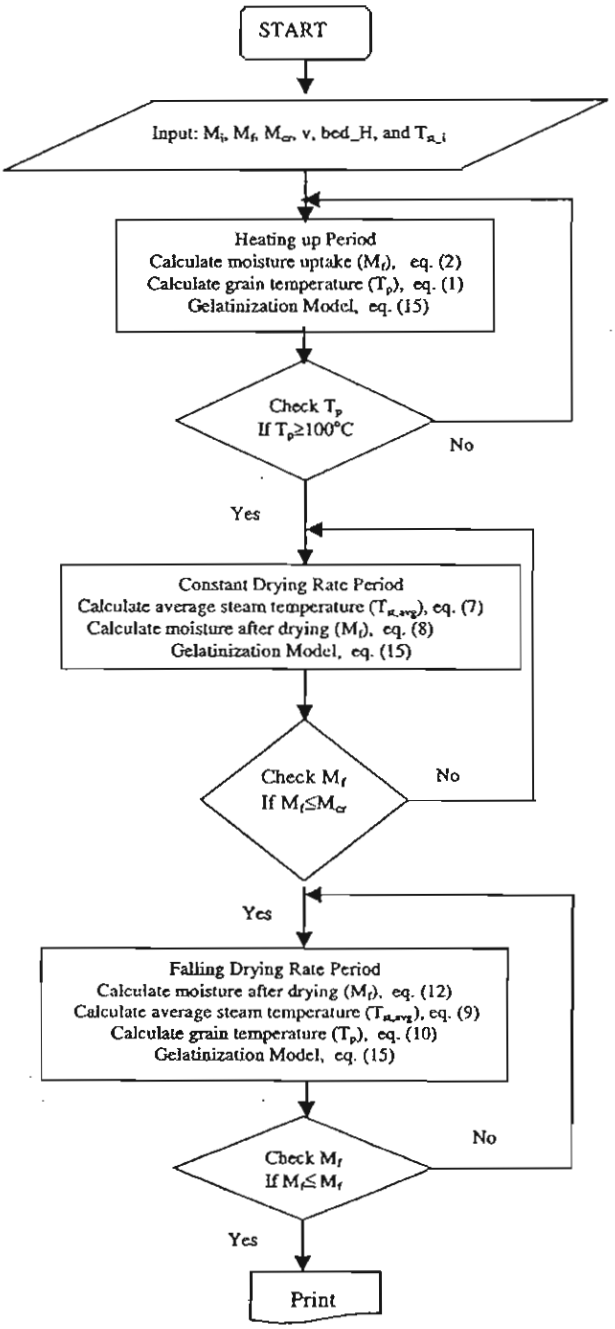

Fig. 2. Simulation flow chart of superheated-steam fluidized-bed dryer.

in this section is repeated until the grain temperature is higher or equal to the boiling point temperature. Next, the constant drying rate period is computed and then the moisture content is determined. If grain moisture content is higher than the critical moisture content, it will be used as an initial moisture content for the next calculation in this loop and the calculation continues until the moisture of paddy is lower or equal to the critical moisture content. Finally, the falling drying rate is calculated. The time step used in the calculation was set at 10 s and in each step, the degree of ungelatinization is determined by Eq. (14).

3. Material and methods

3.1. Sample preparation

Long grain paddy of Chainat1 (CNT1) variety from the Rice Experiment Station at Ayutthaya Province, Thailand, was used in the present investigation. In preparation, it was followed by a traditional method where paddy was cleaned and soaked at a temperature of 80 °C for 3.5 h. Then, water was drained out and the paddy was tempered at the same tank for 1 h prior to drying.

3.2. Drying

After soaking, paddy samples were dried with a batch superheated steam fluidized bed dryer as shown in Fig. 3. The system of the fluidized-bed dryer consists of five main components: a cylindrical chamber with an 15 cm inner diameter and a 100 cm height, a 13.5 kW electrical heater for converting saturated steam to the superheated steam, a backward-curved blade centrifugal fan driven by a 2.2 kW motor, a reverse flow cyclone and a small boiler with a 31 kg/h capacity of generated steam. A PID controller with an accuracy of ±1 °C was used to control steam temperature. Before using steam for drying, hot air was used for warming up the system until the temperature in every part reached the desired temperature. Then, the steam was replaced accordingly. The steam generator generated the saturated steam at 106 kPa (absolute pressure), a pressure slightly above the atmospheric pressure. When the saturated steam flew through the electrical heaters, the additional heat was supplied to raise the steam temperature up to the desired level. It was subsequently flowed through the fluidized-bed dryer. Paddy was loaded into the dryer by opening valve no. 10 and while loading the sample, valves no. 3 and 5 were closed and valves nos. 2 and 4 were opened. After loading the material, valve nos. 10, 2, and 4 were closed whereas valve nos. 3 and 5 were opened. During operation, all valves were manually controlled. The dust particles and the immature grains being suspended in the exhaust steam were collected at the cyclone. Finally, the cleanning exhaust steam was reused again.

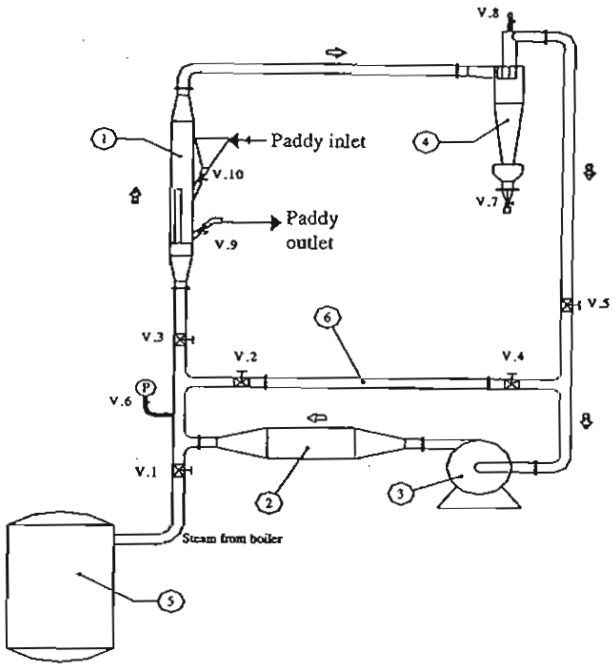

Fig. 3. A schematic diagram of the superheated-steam fluidized bed dryer: (1) fluidised bed dryer, (2) heater, (3) fan, (4) cyclone, (5) boiler, (6) bypass line, (V) = valve, and (P) = pressure gauge.

All drying conditions were performed at a superficial velocity of 3 m/s and static bed depths of 10–15 cm. To determine the moisture content and grain temperature, samples were taken out from the drying chamber at valve no. 9. For measuring grain temperature, the sample was collected in a well-insulated container. Grain temperature and drying superheated steam temperature were measured by Chromel-Alumel thermocouples (Type K) connected to a data logger with an accuracy of ±1 °C. The moisture content of paddy was determined by an electrical air oven at temperature of 103 °C for 72 h. Error of measurement was approximately ±0.1% dry basis. In the experiments, two experiments were carried out under each set of conditions, so as to confirm the reproducibility of the experiments. Good reproducibility was found as shown by moisture content in Fig. 4, grain temperature in Fig. 5 and degree of starch gelatinization in Fig. 6.

Gelatinization properties of parboiled rice flours were analyzed using a differential scanning calorimeter (DSC Pyris-I, Perkin–Elmer, Norwalk, CT, USA). The calibration was periodically performed using indium (heat of fusion of 28.41 J/g and 156.66 °C of melting temperature). Flour samples (~3 mg each) were weighed in sample pans, mixed with distilled water (~9 μL). The sample pan was sealed and allowed to stand for 1 h at

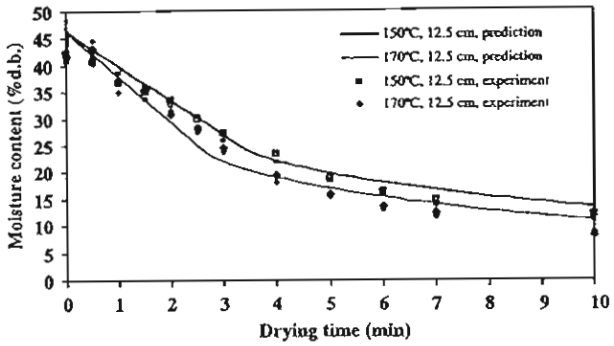

Fig. 4. Comparison between simulated moisture profile and experimental data of paddy at two temperatures and initial moisture content of 42% dry basis (superheated-steam velocity of 3 m/s).

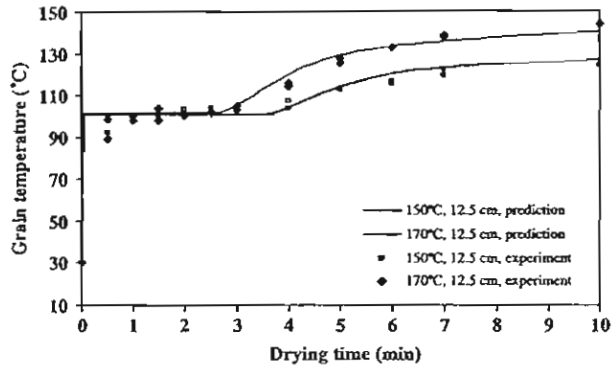

Fig. 5. Variation in grain temperature at different inlet temperature superheated-steam temperatures and initial moisture content 42% dry basis (superheated-steam velocity of 3 m/s).

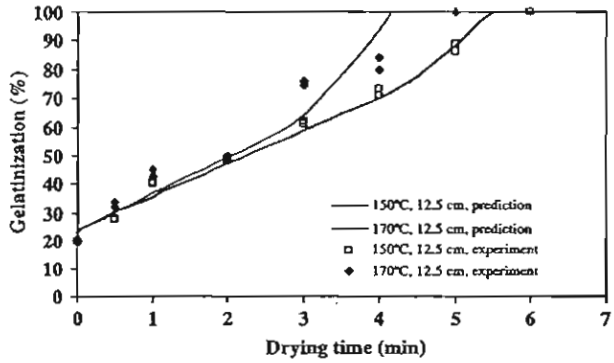

Fig. 6. Gelatinization of rice at different inlet temperatures (superheated-steam velocity of 3 m/s and initial moisture content 42% dry basis).

room temperature (Normand & Mashall, 1989). The sample was held isothermally at 30 °C for 1 min, and then scanned at a heating rate of 5 °C/min until the temperature raise to 100 °C. The calorimetric measures were made by duplications. The enthalpy change (ΔH) was evaluated using Thermal Analyzer (TA) Instruments analysis software program. The degree of gelatinization (SG) of rice flour was calculated by the following equation (Marshall, Wadsworth, Verma, & Velupillai, 1993):

$$SG(\%) = [1 - (\Delta H_{pg}/\Delta H_{raw})] \times 100 \quad (16)$$

where ΔH_{pg} and raw ΔH_{raw} are the enthalpies of gelatinized and raw rice grains, respectively.

4. Results and discussion

4.1. Validation of the model

4.1.1. Moisture content and grain temperature

The experimental data on moisture content and grain temperature are compared with those obtained from the simulations. In Fig. 4, the comparison between calculation and experiment for the moisture content is presented, indicating that the prediction from the model proposed is relatively consistent to the experimental data for a wide range of drying conditions. After the experiments are started, the superheated steam comes into contact with kernels that have a lower temperature. Hence, the steam is condensed and the condensed water is correspondingly adsorbed by grains, leading towards the increase in moisture content of paddy at the early drying stage as evident in Fig. 4, and this condensation results in a rapid rise in grain temperature as shown in Fig. 5. This temperature and the amount of water containing in kernels are sufficiently high enough to promote the starch granules to be gelatinized.

From the calculation, the water adsorption process of paddy together with the increase of grain temperature occurs rapidly: its moisture content is increased to a value higher than 45% dry basis, corresponding to the saturated steam temperature, in a few seconds (Fig. 4). The grain temperature prediction at this period slightly overestimates, as compared to the measured grain temperatures in Fig. 5 that shows the grain temperatures of 93 and 97 °C at the drying time of 30 s for the inlet steam temperatures of 150 and 170 °C, respectively. The over prediction of temperature is probably due to the steam flow entering into the bed of grains to be partly condensed whilst the total condensation is assumed for the calculations throughout which the grain temperature is below the saturation temperature. However, the partial condensation may probably occur when the grain temperature is nearing the saturation point.

After the elapsed time of 1 min, as observed from Fig. 5, the grain temperatures reach the saturation temperature at the operating pressure and stay at that temperature for a certain time. At the saturation temperature, the moisture content of paddy linearly decreases with drying time, representing the constant dry-

ing rate. When the drying rate is reduced, the grain temperature is increased. As shown in Fig. 5, the higher grain temperature is found with a higher steam inlet temperature because of a greater heat transfer rate from the superheated steam to the grains.

4.1.2. Gelatinization

Fig. 6 shows the progression of paddy gelatinization over time for two superheated steam temperatures. Before drying paddy kernels with superheated steam, some starch granules previously soaked with hot water were gelatinized, to a certain degree of 20%. The prediction from the kinetic model in conjunction with heat and mass transfer equations generally agrees with the experimental data for a wide range of experimental conditions. The rate of gelatinization was increased with increased temperature. As shown in Fig. 6, the complete gelatinization is accomplished in 6 min at 150 °C and 5 min at 170 °C.

4.2. Simulation results

The model was employed to predict moisture change, temperature and degree of gelatinization when paddy was dried at different operating conditions. The operating conditions we were interested in this study were the bed depth, drying temperature and superficial velocity. Throughout the simulations, the operating pressure was fixed at the atmospheric pressure and the operating conditions simulated were limited at the bed depth between 10 and 15 cm, and superficial velocity between 2.5 and 3.5 m/s. This is because if the bed depth is too thick and superficial velocity is too high, the quality of fluidization will become very poor, characterizing the large bubble sizes in the bed. This behaviour accordingly impedes the transfer of heat from medium to the kernels, and hence, the kernels throughout the bed do not uniformly receive the heat, leading to the subsequent non-uniformity of starch gelatinization for each kernel.

4.3. Effect of variables on drying rate and grain temperature

4.3.1. Effect of bed depth

Fig. 7 shows the effect of bed depth on the changes of moisture content and grain temperature. In the heating up period, because of steam condensation, the moisture content of paddy is increased from the initial moisture content of 42% dry to approximately 46% dry basis, for all bed depths. When the grain temperature arrives the saturation temperature, the evaporation period starts with a rate depending upon the bed depth. The calculated results present a faster drying rate following with a decrease of bed depth. The faster evaporation rate at thinner bed may possibly be related

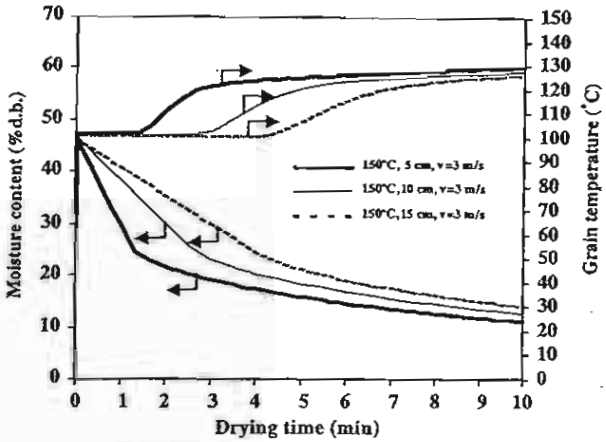

Fig. 7. Simulated results of effect of bed depth on moisture content and grain temperature (initial moisture content 42% dry basis).

to particle collision where the impaction amongst solid particles is very intensive for thin bed, thus reducing the laminar boundary layer near the heated particle surface. This effect is remarkable during which surface water is eliminated, and becomes less important when proportion of water inside the kernel is removed as indicated by moisture reduction, in which the drying curves at different bed depths are relatively closer at the later drying time than at the early drying time. For example, at the elapsed time of 1.5 min which still appeared the available surface moisture, the moisture content of paddy was reduced from the peak to approximately 25% dry basis for the bed depth of 5 cm and to 37% dry basis for 15 cm while the moisture content at the elapsed time of 5 min (no available surface moisture) was 18% for 5 cm bed depth and 23% for 15 cm bed depth.

As observed from the experiment, the falling rate period started when the surface water was completely evaporated, corresponding to the critical moisture content of ~25% dry basis, so that this critical value was used as input parameter for determining the moisture reduction in the falling rate period. During the falling rate period, the temperature starts increasing due to limitation of water transport. After the drying time of about 7 min, the grain temperature is slightly increased and seems to be slightly affected by bed depth.

4.3.2. Effect of superficial superheated-steam velocity

Fig. 8 shows the effect of superficial velocity on the changes of moisture content and grain temperature at bed depth of 15 cm and superheated temperature of 150 °C. Rate of moisture removal is accelerated by increasing the superficial velocity. In this case, the moisture transfer rate is governed by the heat transfer characteristics between solid surface and bulk stream. The steam velocity also influences on grain temperature, with

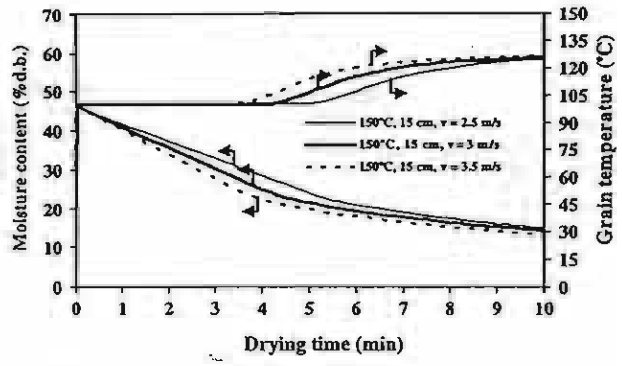

Fig. 8. Simulated results of effect of superficial superheated-steam velocity on moisture content and grain temperature (initial moisture content 42% dry basis).

more rapid rise in grain temperature in relation to higher steam velocity.

4.3.3. Effect of superheated steam temperature

As shown in Fig. 9, when the superheated steam temperature changes from 140 to 180 °C, the rate of moisture reduction, along with the progression of grain temperature, is increased with increased steam temperature, because of a greater difference of temperature between grain and superheated steam. Reducing the moisture content from 42% dry basis to approximately 19% dry basis requires drying times of 3.7, 4.5 and 5 min for the corresponding steam temperatures of 180, 160 and 150 °C. These calculated drying times included the initial condensation period.

It is note that paddy should not be dried below 19% dry basis by using superheated steam otherwise the drop in head rice yield is enormous (Taechapairoj, Prachayawarakorn, & Soponronnarit, 2003). To maintain high head-rice yield, the slow-drying technique is necessary for reducing the moisture content from the critical level.

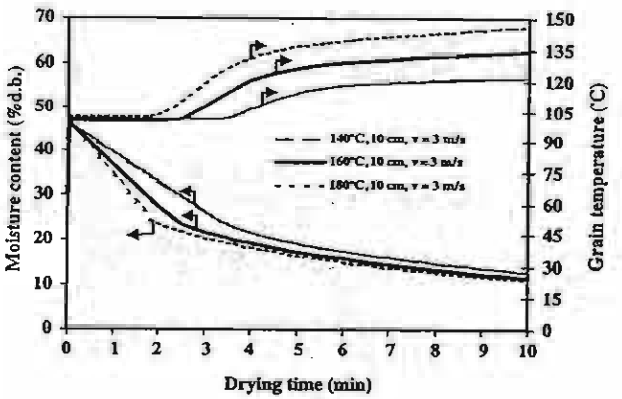

Fig. 9. Simulated results of effect of superheated-steam temperature on moisture content and grain temperature (initial moisture content 42% dry basis).

4.4. Effects of operating parameters on grain gelatinization

Good quality of parboiled rice should have a characteristic of translucent kernel or less amount of white belly. The appearance of white belly in kernel, which is usually found at the central area of kernel, intrinsically implies some starch granules inside kernel to be not fully gelatinized. This is in part affected by insufficient time for gelatinization. According to this, it is important to know the time required for complete gelatinization under different operating conditions i.e. temperature, bed depth and velocity. This useful information provides us to choose the suitable condition for producing high-quality parboiled rice, along with a high production capacity.

4.4.1. Bed depth

Fig. 10, on the left axis, shows the calculated time of complete gelatinization by plotting against the superheated–steam temperature at different bed depths, indicating that the processing time is shorter using higher temperature and thinner bed depth. This is because paddy experiences a higher heat transfer rate, resulting in more rapid rise in grain temperature and hence stimulating the starch to be gelatinized with a higher rate.

Although the gelatinization time at higher bed depth is apparently increased, this is not disadvantageous since the holding capacity is increased and it is more compensated than the increase of spent time for complete gelatinization. When the productivity, defined as the ratio of holding capacity to the reaction time, were consequently plotted against the steam temperature as shown in Fig. 10 on the right axis, the result represents the higher production at higher bed depth.

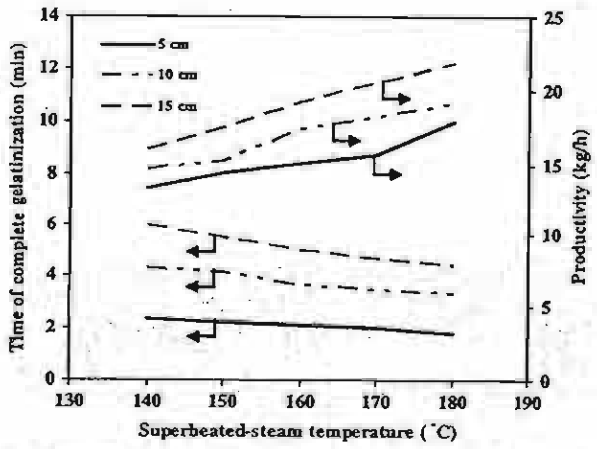

Fig. 10. Simulated results of effect of bed depth on the time of complete gelatinization and productivity of paddy during drying (initial moisture content 42% dry basis, final moisture content 19.9 ± 0.7% dry basis and superficial superheated-steam velocity = 2.5 m/s).

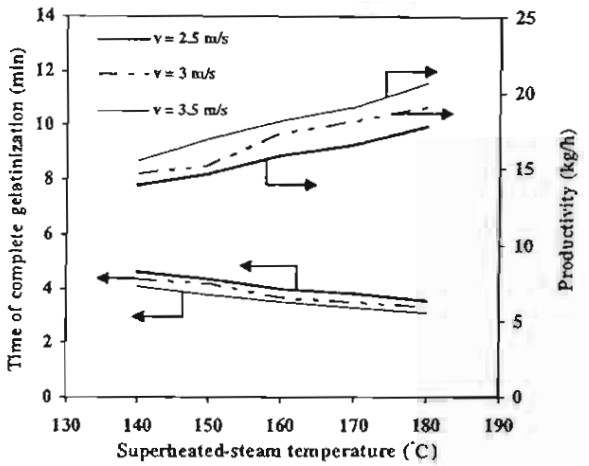

Fig. 11. Simulated results of effect of superficial superheated-steam velocity on the time of complete gelatinization and productivity of paddy during drying (initial moisture content 42% dry basis, final moisture content 19.9 ± 0.7% dry basis and bed depth 10 cm).

4.4.2. Superficial superheated-steam velocity

Fig. 11 shows the time of complete gelatinization as affected by superficial superheated-steam velocity at different superheated-steam temperatures. At a given temperature, increasing superficial velocity leads to shorter time to complete gelatinization due to higher convective heat transfer from heating medium to the grains. However, the effect of superficial superheated-steam velocity on the reaction time is relatively less important than the effects of bed depth and temperature.

According to these simulated results, they suggest that an efficient way to improve the productivity can be made by increasing the bed thickness and temperature.

5. Conclsions

Superheated-steam showed a high possibility of producing parboiled rice. A mathematical model for the drying of paddy in superheated steam had been developed and tested against the experimental results. The validation showed that the developed model had the capability to predict moisture content, temperature and degree of gelatinization. The validated model was then used to explore the suitable operating condition for producing parboiled rice and the simulated results showed that the times for complete gelatinization and evaporating water were shorten by increasing superficial superheated-steam velocity and temperature as well as decreasing bed depth, the first factor being least important. To obtain high productivity of parboiled rice, it was recommended from the simulations that the superheated-steam fluidized bed dryer should be operated at the bed depth of 15 cm and temperature of 180 °C.

Acknowledgement

The authors would like to express their sincere thanks to the Thailand Research Fund for financial support.

References

Blasco, R., & Alvarez, P. I. (1995). Flash drying of fish meals with superheated steam: isothermal process. *Drying Technology, 17*, 775–790.

Ciesielczyk, W. (1996). Analogy of heat and mass transfer during constant rate period in fluidized bed drying. *Drying Technology, 14*(2), 217–230.

Iyota, H., Nishimura, N., Nomura, T., Konishi, Y. & Yoshida, K. (2002). Effect of initial steam condensation on color changes of potatoes during drying in superheated steam. In *Proceedings of the 13th international drying symposium* (Vol. B, pp. 1352–1359). Beijing, China.

Makowski, M., Cenkowski, S., Hatcher, D. W., Dexter, J. E., & Edwards, N. M. (2003). The effect of superheated-steam dehydration kinetics on textural properties of Asian noodles. *Transactions of the American Society of Agricultural Engineers, 46*, 389–395.

Marshall, W. E., Wadsworth, J. I., Verma, L. R., & Velupillai, L. (1993). Determining the degree of gelatinization in parboiled rice: comparison of a subjective and an objective method. *Cereal Chemistry, 70*, 226–230.

Normand, F. L., & Mashall, W. E. (1989). Differential scanning calorimetry of whole grain milled rice and milled rice and milled rice flour. *Cereal Chemistry, 66*(4), 317–320.

Taechapairoj, C., Prachayawarakorn, S., & Soponronnarit, S. (2003). Superheated steam fluidized bed paddy drying. *Journal of Food Engineering, 58*, 67–73.

Taechapairoj, C., Prachayawarakorn, S., & Soponronnarit, S. (2004). Characteristics of rice dried in superheated-steam fluidized-bed. *Drying Technology, 22*(4), 719–743.

Tang, Z., & Cenkowski, S. (2000). Dehydration dynamics of potatoes in superheated steam and hot air. *Canadian Agricultural Engineering, 42*, 43–49.

Tatermoto, Y., Mawatari, Y., Sakurai, K., Noda, K. & Komatsu, N. (2002). Drying characteristics of pours material in superheated steam fluidized bed. In *Proceedings of the 13th international drying symposium* (Vol. A, pp. 624–633), Beijing, China.

Drying Technology, 24: 65–75, 2006

ISSN: 0737-3937 print/1532-2300 online
DOI: 10.1080/07373930500538717

Taylor & Francis
Taylor & Francis Group

Effects of Peeled and Unpeeled Garlic Cloves on the Changes of Drying Rate and Quality

Somkiat Prachayawarakorn[1], Narongsak Kaewnin[2], Adisak Nathakaranakule[2], and Somchart Soponronnarit[2]

[1]*Faculty of Engineering, Thonburi, Bangkok, Thailand*
[2]*School of Energy and Materials, King Mongkut's University of Technology, Thonburi, Bangkok, Thailand*

Reducing moisture content as fast as possible, together with minimizing loss of quality, is important to food processing. To reach these objectives, experimental investigations were conducted to examine the effects of both peeled and unpeeled garlic cloves as well as operating parameters such as temperature and superficial velocity on the drying rate and quality of dried product. Peel resistance to moisture diffusion is considerably dominated and yields the longer drying time. Drying at high temperature shows the shrinkage of garlic clove to be lower than that at low temperature, whereas the product color is browner and the sizes of produced pores as revealed by scanning electron microscope are larger. The loss of volatile oil is insignificantly different among low- and high-temperature drying. The peel effect exhibits negative results on the product color, giving lower luminosity than the peeled sample, in particular at low temperature, because of longer drying time.

Keywords Dehydration; Garlic; Shrinkage; Volatile oil

INTRODUCTION

Garlic (*Allium sativum* L.), one of the most important *Allium* species, is well known in folk medicine for prevention of stroke and coronary thrombosis[1] and is commonly used as a primary ingredient in food formulations and a flavoring agent. The flavor, mainly containing sulphur aromatic volatiles, is produced when garlic cloves are disrupted, enabling alliinase enzyme to come in contact with alliin.[2,3] With this enzymatic reaction, the alliin is converted to 2-propenyl-2-propenethiol-sulphinate and eventually decompose to disulfides and thiosulfinates. The diallyl disulfide has been identified as the main component in garlic oil.[4]

Garlic after harvesting contains a large amount of water with an approximately 1.8–2.0 g water/g dry matter and the considerable loss in quantity, due to infection of microorganisms, is unavoidable. The garlic, with high moisture, will also quickly sprout if the environmental condition is suitable. When this event takes place, the nutritional qualities of garlic become degradable, besides the loss of commercial value. To eradicate such problems, drying is therefore needed. Drying is an important food process that causes the physical and chemical changes of products, such as in the physical properties, i.e., color, shrinkage, microstructure, and the quality of products.[5–7] Garlic is a biological material that is very sensitive to heat, and when dried, the volatile oil in the garlic is lost, consequently reducing the flavor intensity.[8,9] This may degrade the quality of dried garlic. Therefore, choice of drying condition to obtain high-end product quality is an important issue to investigate in the present work. In addition, the physical pretreatment of garlic clove by eliminating peel before drying is another matter to explore to find how it affects the moisture diffusion rate and the subsequent qualities compared to no pretreatment, which is commonly practiced in factory. The quality parameters of dried garlic cloves are characterized by color, volatile oil, and shrinkage. The microstructure of the dried garlic tissue is also examined. In addition, the series diffusion model, describing the transport of water through two composite layers, garlic tissue and peel, is developed to determine their effective diffusion coefficients.

Correspondence: Somkiat Prachayawarakorn, Faculty of Engineering, King Mongkut's University of Technology Thonburi, Suksawat 48 Road, Bangkok 10140, Thailand; E-mail: somkiat.pra@kmutt.ac.th

MATERIALS AND METHODS

Equipment

The experimental setup is schematically shown in Fig. 1. Ambient air, which is heated by electrical heater, flows with a constant mass flow rate through samples lying on a screen metal sheet within the drying chamber. The air speed could be changed by setting a frequency inverter connected with a 1/2 hp motor to drive a forward curved blade centrifugal

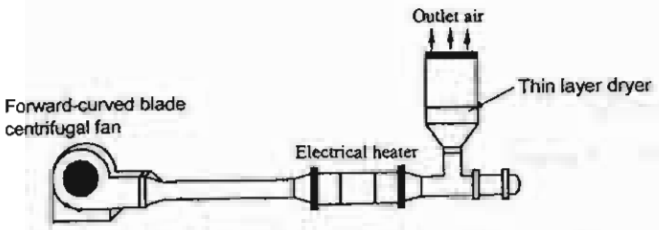

FIG. 1. Experimental thin-layer drying equipment.

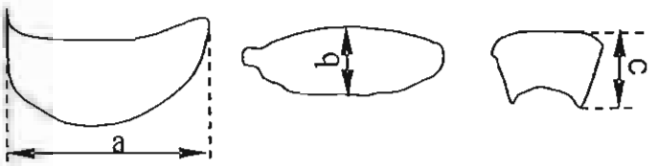

FIG. 2. Garlic clove dimension.

fan. A hot-wire anemometer, with a precision of ±0.1 m/s of reading, was used to measure the velocity. A PID-type controller was chosen for controlling heating system and the variation of inlet air temperature was in the range of ±1°C from the setting temperature. In the experiment, the temperature at different positions, i.e., dryer inlet, outlet, and grain, was measured by a K-type thermocouple connected with a Yogokawa data logger with an accuracy of ±1°C. To measure garlic temperature while being dried, the thermocouple was inserted into the middle position of the sample.

Drying

The dryer was operated at the three temperatures, 50, 60, and 70°C, and two air velocities, 0.7 and 1.7 m/s. The relative humidity of inlet air was not controlled in this study. Garlic bulbs obtained from local markets had a moisture content of 181–203% (dry basis). Before drying, the bulbs were manually cracked and the subsequent garlic cloves including the thin peel were obtained and divided into two groups in order to study the drying kinetics. The garlic cloves with peel were taken to dry immediately and another group was physically treated by peeling the shell before drying. Since the garlic clove was not a well-defined geometrical shape, the equivalent sphere diameter, calculated from its volume, was employed. The original size of the garlic cloves was given as a range of 12.9 to 13.6 mm. The moisture curve was determined by weighing the sample every hour during the early drying period, where the moisture content loosed rapidly, and every 5 h afterwards. In addition to moisture, shrinkage of garlic was measured. At the drying end, the samples were taken to determine moisture content using a hot air oven at temperature of 103°C,[10] volatile oil, and color, and also to characterize the microstructure of garlic tissue.

Shrinkage

To investigate the behavior of material shrinkage, the experiment was conducted separately from the drying experiment and the material shrinkage in this work was defined as the volume of material at time t divided by the volume at the beginning. The solid volume was obtained by measuring each garlic clove dimension, shown in Fig. 2, and then calculated by the following equation:

$$V = \frac{\pi}{6}(a \cdot b \cdot c) \tag{1}$$

where a is the longest intercept, b is the longest intercept normal to a, and c is the longest intercept normal to a and b. Five samples were measured and the average value was represented.

Color

A tristimulous colorimeter (Juki model JP-700), which could be specified by three coordinates in the color space, i.e., L-value, a-value, and b-value, was used to measure the product color. The L-value is a measure of lightness with a scale of 0 to 100, the a-value indicates the change of the color from green to red, and the b-value the change from blue to yellow, both latter indicators being in the scale of −60 to +60. Before measuring the sample, the colorimeter was examined with a standard pure white having Hunter values of 97.76 for L-value, −0.06 for a-value, and −0.31 for b-value.

Volatile Oil

The volatile oil content of garlic mainly consisting of sulphur compounds was determined by chloramine-T method.[11] Five grams of the finely ground sample (fresh and dried) was homogenized with water for 5 min, with a wait period of 30 min for fresh garlic and 60 min for dried garlic, in order to completely release the flavor. An aliquot of the slurry was distilled and oxidised by chloramine-T. The amount of excess chloramine-T in the experiment and the blank were determined. The volatile oil content in the samples was expressed as mg oil/g dry matter.

Microstructure

Samples of garlic cloves dried at different temperatures were taken to examine the microstructure. The samples were cut in cross section with sieve tubes using a sharp razor blade. The samples were then placed on adhesive tape attached to a circular aluminum specimen stub, followed by gold coating using a sputter-coater. The samples were finally viewed in a transmission electron microscope (Leica Cambridge Tld, model Stereosoan 206) at an accelerating voltage of 10 kV.

Mathematical Model of Drying Kinetics

Drying of porous media is a simultaneous process of heat and mass transfer and the models are written, based on energy and mass balance, to describe the transport process.[12,13] Under certain conditions, drying can be approximately treated as an isothermal process. In this case, the problem is reduced to a single differential equation, describing specifically the water transport inside porous solid. The transport of water in most agricultural products is governed by the diffusion and its change is simply described by Fick's second law of diffusion, where the expression for spherical shape is given by

$$\frac{\partial M}{\partial t} = D\left(\frac{\partial^2 M}{\partial r^2} + \frac{2}{r}\frac{\partial M}{\partial r}\right) \tag{2}$$

where the moisture content, M (dry basis decimal), is a function of both the radial coordinate, r (m), and drying time, t (s). The effective diffusivity, D (m^2/s), as a transport property of material, is a lumped parameter that is taken into account the several transport mechanisms, i.e., capillary, film flow, and vapor diffusion.

While material is being dehydrated, the physical change such as shrinkage causes the transport of water inside the porous solid to be changed, hence, the diffusivity.[14,15] To determine the effective diffusivity of the shrinkable material, the shrinkage effect must be included in the diffusion model and Eq. (2) is discretized by the finite difference method. In this work, the explicit method was used. Throughout the calculation, the volume of peeled garlic clove is divided into a constant number of elements, while the size of each element volume is changed following the shrinkage expression.

Since the garlic clove is a heterogeneous material consisting of peel and tissue, both of which are connected in series, the moisture transporting through each particular part may exhibit different characteristics of diffusion property, and the components of garlic are modeled as concentric layers of materials as shown in Fig. 3. Equation (2) is applied for predicting the moisture change in the tissue ($0 < r < R_1$) and the peel ($R_1 < r < R_2$) where the corresponding D_t and D_p present the effective moisture diffusion in the tissue and peel, respectively.

First Falling Rate Period

Kinetics of the garlic drying can be divided into two drying periods, namely first and second falling rate periods. At the first falling rate period, the evaporation of water always occurs near the material surface and the moisture removal rate depends on air velocity, temperature, and water concentration between the surface and air stream. At this period, the drying rate of garlic clove at any time t is decreased and can simply be calculated from the mass flux at the surface, which is expressed by

$$D_p \left.\frac{\partial M}{\partial r}\right|_{r=R_2} = k(M|_{r=R_2} - M_{eq}) \qquad t > 0 \tag{3}$$

where k is the experimentally determined drying constant (m/s), R_2 is the radius of garlic clove (m), and M_{eq} is the equilibrium moisture content. The thickness of peel measured by a digital micrometer was approximately 96 μm. To predict the moisture change from Eq. (2), it is also

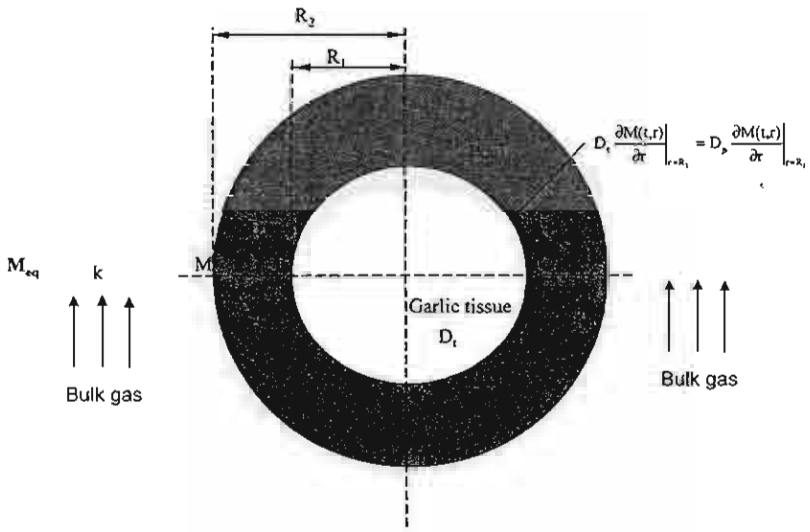

FIG. 3. Schematic diagram of idealized model of garlic clove with peel surrounded with gaseous film.

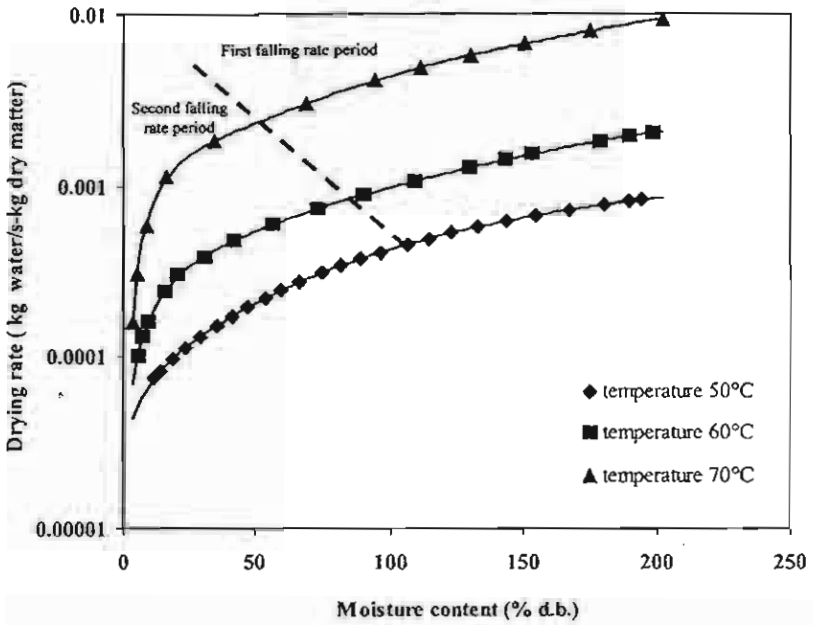

FIG. 4. Drying rate of peeled garlic clove as functions of moisture content and drying temperature (superficial velocity of 0.7 m/s).

assumed that the moisture content throughout the size range is spatially uniform at the beginning and the moisture gradient at the center is zero at $t > 0$.

Second Falling Rate Period

When moisture content reaches a certain level, the drying kinetics fall to the second falling rate period, characterizing the nonlinear drop of rate with moisture content, as will be shown in Fig. 4. At this period, we assume that the surface moisture equilibrates with the environmental drying condition and the moisture transport is governed by pure diffusion mechanism[16] and the following boundary condition is given by

$$M(R_2, t) = M_{eq} \qquad t > 0 \tag{4}$$

In addition to above-mentioned boundary conditions, another boundary is given at the interface between the innermost peel and outermost tissue by equating the mass flux of water diffusing through the tissue at any time to that diffusing through the peel.

$$D_t \left.\frac{\partial M(t,r)}{\partial r}\right|_{r=R_1} = D_p \left.\frac{\partial M(t,r)}{\partial r}\right|_{r=R_1} \qquad t > 0 \tag{5}$$

From the known moisture profile, the average moisture content of garlic clove is calculated by

$$\overline{M} = \frac{\int_0^{R_2} 4\pi r^2 M(r,t)dr}{V_p} \tag{6}$$

where $\overline{M}$ is the average moisture content and V_p is the particle volume (m^3).

The behaviour of garlic clove shrinkage during dehydration is explained by the following exponential equation:

$$\frac{V}{V_0} = a \exp\left(-b\frac{\overline{M}}{M_{in}}\right) \tag{7}$$

where V is the particle volume (m^3) at moisture M, with subscript 0 presenting the volume at the beginning. The constant parameters of a and b are obtained by the statistical fit with experimental data using a linear regression method.

When garlic clove is peeled, its drying process can be mathematically described by accounting for the moisture diffusion in the garlic tissue and the water vapor in gaseous film surrounding the garlic clove. Equation (2), together with the boundary conditions (Eqs. (3–4)), were used to determine the effective diffusivity of garlic tissue, D_t, and drying constant, k. A trial-and-error approach was used to estimate the transport parameters, and the estimated parameters were supposed to be correct when the mean residual square of moisture content, MRS_M, was less than 0.002. MRS is generally defined as

$$\text{MRS} = \frac{\sum_{i=1}^{n} (\text{observed data} - \text{calculated data})^2}{n} \tag{8}$$

where n is the number of experimental data.

To determine D_p and k for drying garlic clove with peel, the aforementioned calculation procedure, with an

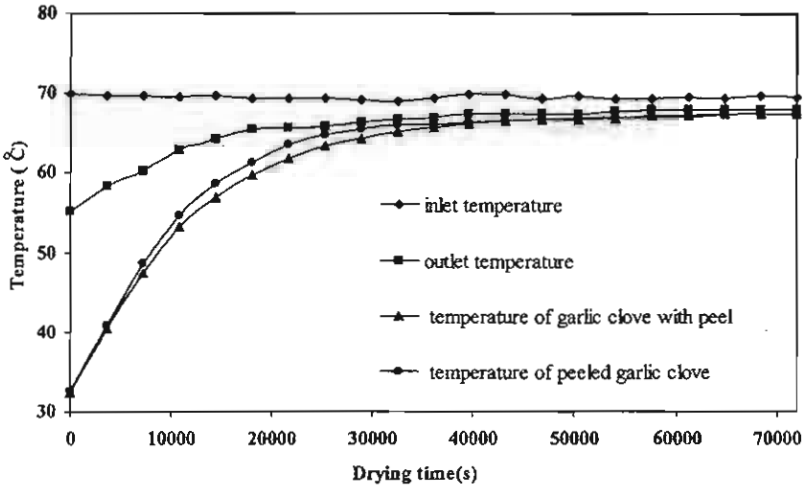

FIG. 5. Evolution of temperatures in thin-layer drying system (inlet air temperature of 70°C and superficial velocity of 0.7 m/s).

additional Eq. (5), was used. In this calculation step, D_t was already known.

RESULTS AND DISCUSSION

Temperature Change in Drying System

Temperature at several positions in the thin-layer dryer was recorded during the experiments and their changes are illustrated in Fig. 5, in which the operating parameters were controlled at the inlet-air temperature of 70°C and the superficial velocity of 0.7 m/s. The temperatures of the garlic cloves with and without peels were initially at 32°C and were increased by a different rate; the increase of the peeled garlic temperature was slightly faster. When the time was elapsed for 8 h, the change of both product temperatures was not very sensitive as well as the product temperatures appeared closer together. The temperature of the materials kept constantly at the temperature of 66°C for the inlet temperature of 70°C. This clearly indicates that the heat transfer rate approaches the equilibrium state faster than the moisture transfer rate.

Moisture Change

Some experimental results of moisture change of garlic clove at temperatures of 50, 60, and 70°C are shown in Fig. 6, indicating that increasing the drying temperature

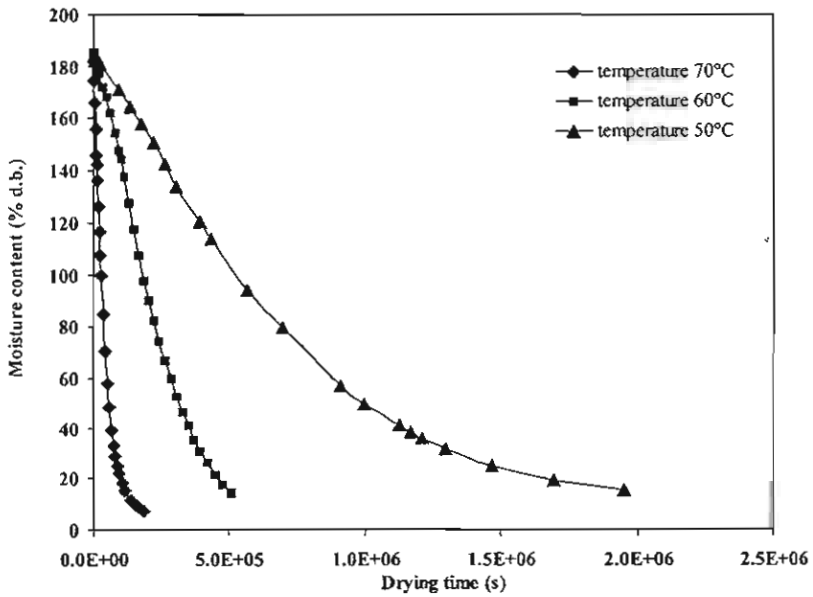

FIG. 6. Moisture change of garlic clove with peel at different temperatures (superficial velocity of 0.7 m/s).

causes an important increase in the drying rate. Drying garlic clove at a temperature of 50°C can not obtain the moisture content of finished product required at 5% dry basis. At this drying temperature, the moisture content of dried garlic, as observed from the drying curve, equilibrates with the flowing air at 19.2% dry basis. To reach the required moisture content of product, the higher temperature of 60°C is needed.

Figure 4 illustrates the drying rates as functions of moisture content and temperature. Each drying rate curve presented was obtained by differentiating the suitable empirical equation with respect to time. The suitable form that predicted the moisture change was in exponential relation as indicated by R^2, of which the value obtained from fitting was given above 0.98 for each experiment. As can be seen in Fig. 4, it appears that two well-defined drying zones where the linear decrease of drying rate followed with nonlinearity behavior with moisture content are found. These drying rate curves also suggest that drying at high temperature provides more potential capability to remove moisture than that at low temperature and the drying efficiency is possibly improved because the enhanced removal rate is more compensated than the energy consumed: drying rate at 70°C increases approximately 10 times of that at 50°C at the remaining moisture content above 50% dry basis, whereas the drying temperature used increases only 1.4 times. At the lower moisture content, however, the use of high temperature may not get potential benefit since the drying rate is not largely different among low and high temperature.

TABLE 1
Pseudo-critical moisture content of garlic at different operating parameters

Temperature (°C)	Air velocity (m/s)	Pseudo-critical moisture content (% dry basis)	
		Unpeeled garlic clove	Peeled garlic clove
50	0.7	123	120
	1.7	121	118
60	0.7	109	98
	1.7	107	95
70	0.7	69	58
	1.7	67	58

It is also shown in Fig. 4 that the moisture content at which the drying rate changes from linear to nonlinear is pseudo-critical moisture content in this work and this value is relied on the drying condition. Table 1 presents the pseudo-critical moisture content of unpeeled and peeled garlic cloves, indicating the dependence of pseudo-critical moisture content upon the drying temperature and characteristics of garlic clove, the first factor playing more important role, whereas it is independent on velocity.

Drying Constant

The drying constants estimated from the first falling rate period for the peeled and unpeeled garlic cloves are shown in Fig. 7 and the result indicates that the drying constant

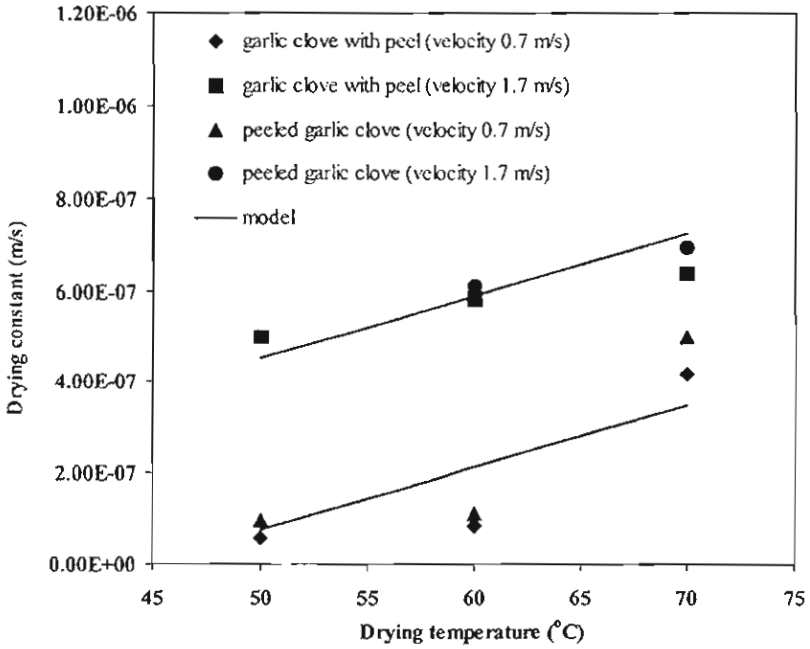

FIG. 7. Change of drying constants as functions of drying temperature and air velocity.

increases as the superficial velocity and temperature increase, whereas it is not affected by surface characteristics (peeled and unpeeled garlic cloves). Correlation of the drying constant to the involved parameters is thus given by

$$k = -2.87 \times 10^{-5} + 4.20 \times 10^{-6} V^{0.100} + 8.65 \times 10^{-6} T^{0.182} \quad (9)$$

where V is the superficial velocity (m/s) and T is the drying temperature (K). R^2 and MRS_k of the drying constant obtained from the statistical fitting of Eq. (9) are 0.90 and 5.2×10^{-15}, respectively, implying the suitability of proposed equation in predicting the drying constant at condition studied. The constant parameters in Eq. (9) indicate that the drying constant is rather more influenced by temperature than by the air velocity.

Effective Diffusivity

The effective diffusivity of moisture moving through the garlic tissue and the peel are shown in Fig. 8 and the values presented were estimated from the drying characteristic curve. The temperature renders a strong contribution to the effective diffusivity, where the higher effective moisture diffusivity is shown up as temperature is increased. As shown in Fig. 8, transport of water through the garlic clove with peel is governed by the peel resistance, of which the value of effective diffusivity is remarkably lower than that found in the garlic tissue. The dependence of moisture diffusivity on temperature is explained by a well-known Arrhenius relationship and the results from statistical fitting for the effective diffusivities of the garlic tissue and peel is expressed by

$$\text{Garlic tissue: } D_t = 6.97 \times 10^9 \exp\left(-\frac{131,221}{RT}\right) \quad (10)$$
$$R^2 = 0.99, \quad \mathrm{MRS}_{D_t} = 3.6 \times 10^{-24}$$

$$\text{Peel: } D_p = 1.47 \times 10^9 \exp\left(-\frac{133,671}{RT}\right) \quad (11)$$
$$R^2 = 0.98, \quad \mathrm{MRS}_{D_p} = 3.3 \times 10^{-25}$$

where R is the universal gas constant (kJ/kmol) and T is the absolute temperature (K). The calculations of effective diffusivities of moisture transporting through the garlic tissue and the subsequent garlic peel using the respective Eqs. (10) and (11) agree well with the experiments, as shown by solid lines against the experimental data in Fig. 8. From the Arrhenius equation, it is also seen that the energy required for driving the moisture through the peel is slightly larger than through the tissue.

Shrinkage

When foods undergo volumetric changes during water loss, this is referred as shrinkage, which has a negative result for the quality of dehydrated product. These physical modifications, taking place continuously while material is being dried, influence the physical properties of the solids and the diffusive transport properties. The shrinkage of material is generated from a pressure unbalance between the inner material and the external pressure that leads to material shrinkage or collapse. Figure 9 shows the relation of shrinkage of garlic tissue to the remaining moisture content at temperatures, indicating that the size of garlic is rapidly and almost linearly reduced with moisture content at early period drying period and then followed with a slow

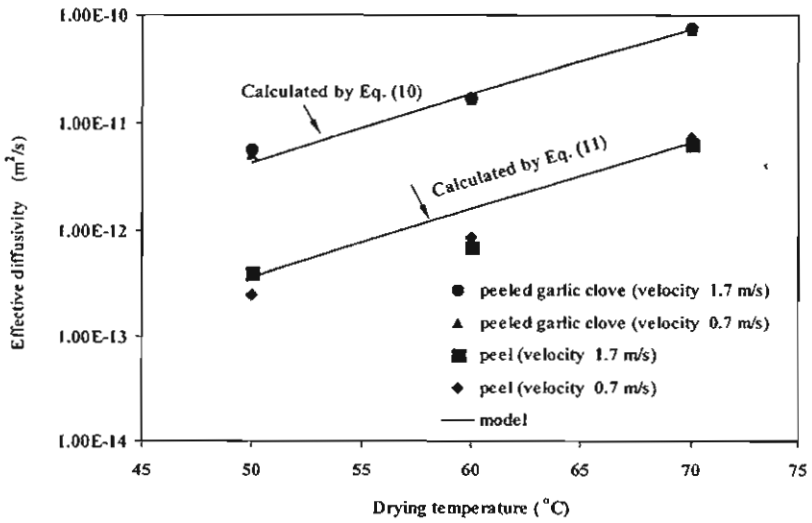

FIG. 8. Effective moisture diffusivities of garlic tissue and peel at temperatures.

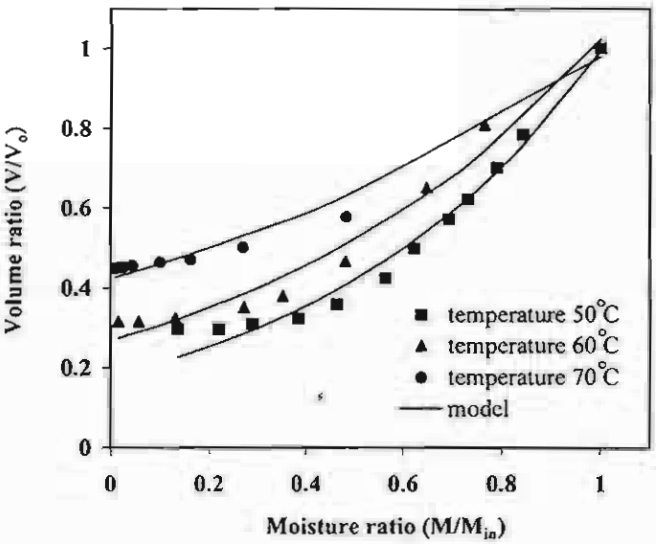

FIG. 9. Shrinkage behavior of garlic tissue during drying at different temperatures.

shrinking rate. The rapid decrease of size occurs while garlic has high moisture content, and tissue characteristics at this moisture level are rather soft. As the moisture content is decreased, the surface of garlic becomes more rigid, allowing the slower decrease of its size until no further shrinkage occurs, although the drying continues. This phenomenon was also found in some foods, i.e., potato and apple.[17,18]

It was found that the garlic dried at temperatures of 60 and 70°C possessed a rigid crust at the outer surface, whereas the outer surface was rather softer for drying garlic at temperature of 50°C. The difference of physical characteristics of dried garlic clove may produce different shrinkage rates, in which the shrinkage is relatively lower for drying garlic at high temperature than one dried at low temperature, as presented in Fig. 9. The lower shrinkage at higher temperature may possibly be attributed to the rigid crust formation at external garlic surface that fixes the volume of garlic.

The constant parameters in Eq. (7), a and b, were correlated with the temperature in the empirical forms, which are given by

$$a = 684171.98 \exp\left(-\frac{4907.86}{T}\right) \qquad (12)$$
$$R^2 = 0.99,\ \mathrm{MRS}_a = 0.0000225$$

$$b = 0.043884\mathrm{T} - 15.92 \quad R^2 = 0.99, \mathrm{MRS}_b = 0.000868 \qquad (13)$$

Equations (12) and (13) are limited to the temperature range of 50 to 70°C. The predictions from the proposed shrinkage model presented by solid lines in Fig. 9 show good agreements with the experimental ones. It is noted that the value of volume shrinkage ratio at the ratio of M/M_{in} equal to unity is, in fact, always unity, but the calculated values under the studied temperature range are slightly different from unity, with a maximum difference being 2.0% for a temperature of 70°C.

Validation of Moisture Content

The constant parameters for diffusive Eqs. (9), (10), and (11), together with shrinkage Eqs. (12) and (13), were used to calculate the moisture changes of the peeled and unpeeled garlic cloves at temperatures and the calculated results are shown in Fig. 10, indicating that the agreement between the experiments and simulations is good for a wide range of experimental conditions and the difference of moisture content between experiment and prediction at

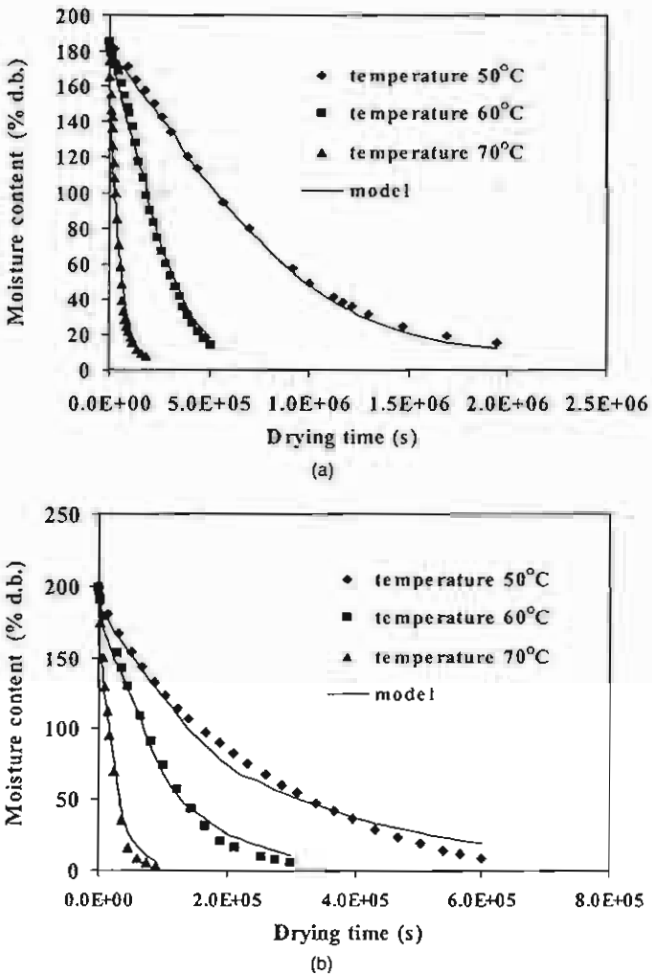

FIG. 10. Comparison of moisture content obtained from the experiments and prediction. (a) Garlic clove with peel and (b) peeled garlic clove.

the drying end for each drying condition was less than 4%, except only for the peeled garlic clove dried at 50°C with the difference being up to 10%. Compared to the effect of peel on temperature development as illustrated in Fig. 5, the effect of peel on retarding the moisture movement is considerably more dominant. Particularly, when the garlic was dried at temperature of 50°C, the time employed for drying garlic clove takes much longer than the peeled one: for example, requiring the drying time of 470 min for the unpeeled garlic clove and of 167 min for the peeled garlic clove in reducing moisture content from 180–200% dry basis to 19.2% dry basis.

Morphology of Dried Garlic

Different drying conditions may produce diverse structures of material. Figure 11 shows modifications of garlic tissue in the course of drying at temperatures of 50, 60, and 70°C. A small number of pores, with small sizes, are formed at the temperature of 50°C and the pore sizes, along with degree of porosity, are increased as temperature is increased. According to the SEM photographs, such pore formation is possibly induced by moisture stresses developed during drying, with larger moisture stresses as the rate of drying is accelerated. The larger stresses generally result in larger decrease of pasta size.[19] For the garlic drying, however, the smaller decrease of the size, when the moisture removal rate became faster, was found. This is because at higher temperature, the rigidity of the external surface exists and the volume of the sample becomes fixed, and it can thus withstand the moisture-induced stress forces, yielding a reduced degree of shrinkage.

Color

Figure 12 shows L-, a-, and b-values of garlic cloves with and without peels dried at different temperatures and the samples taken to examine the color had final moisture content of 19% dry basis for garlic dried at 50°C and 5% dry basis for the drying temperatures of 60 and 70°C. Garlic initially possesses creamy white color as interpreted by L-value ranging from 67.5 to 67.6, a-value ranging from -3.3 to -3.4, and b-value ranging from 11.3 to 11.7. As the garlic was thermally dried, the L-, a-, and b-values changed dissimilar ways, in which the L-value was decreased while the a- and b-values were increased. The change in their values in such direction implies the color of garlic becoming brown, with least degree of browning being at 50°C and increasing with higher temperature. At a temperature of 60 or 70°C, however, the dried garlic color is insignificantly different as indicated by the L-, a-, and b-values in which the value of each Hunter parameter of the finished product is almost equal. In addition, the color of product obtained by drying garlic with and without peels is not different. On the contrary, the effect of peel on the color of garlic is evident for drying at temperature of 50°C, especially for the L-value,

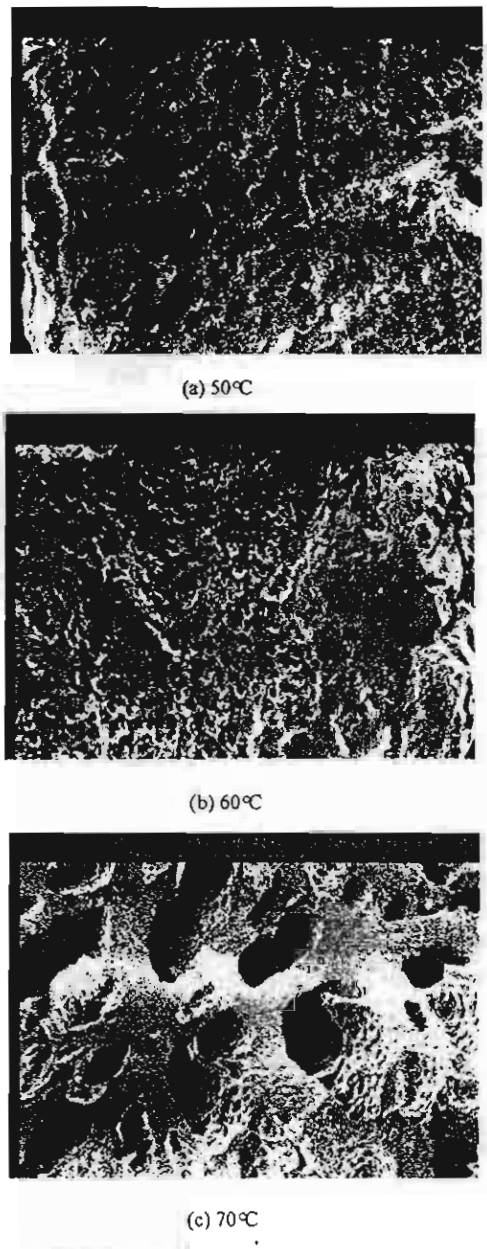

(a) 50°C

(b) 60°C

(c) 70°C

FIG. 11. Morphology of peeled garlic clove dried at different temperatures.

which shows 61 for the garlic clove and 52 for the peeled one, the lower value presenting the darker color. The darker color of unpeeled garlic clove is due to slower drying rate compared to that of the peeled sample, resulting in longer drying time. From Fig. 12 it can be seen that because of the wrinkles and roughness on the shrunken surface, there is a deviation of measuring the color of samples, indicated by the error bar, and the deviation becomes smaller when the powdered garlic is employed.[5]

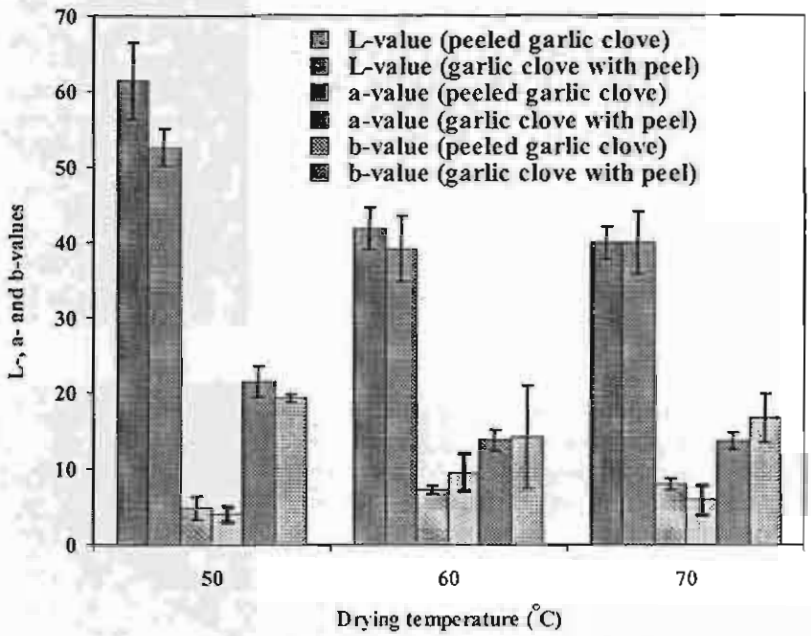

FIG. 12. Comparison of color of garlic with and without peel dried at different temperatures.

Volatile Oil

From the view points of color quality of the finished product and moisture reduction, garlic clove should be peeled before drying. Further examination was made with the peeled garlic clove by evaluating the loss of volatile oil content. Total volatile oil content of raw garlic ranges between 7.2 and 10.8 mg oil/g dry matter and the loss of volatile oil content after drying at different conditions is summarized in Table 2. The loss of volatile oil is not very different for samples dried at low or high temperature.

TABLE 2
Volatile oil content of peeled garlic cloves dried at different operating conditions

Temperature (°C)	Superficial velocity (m/s)	Volatile oil (mg oil/g dry matter) Before drying	After drying	% Loss
50	0.7	10.8	2.7	75
	1.7	7.2	1.5	79
60	0.7	9.6	3.3	65
	1.7	10.7	3.4	68
70	0.7	9.6	2.8	71
	1.7	10.6	3.2	70

CONCLUSIONS

Drying of unpeeled and peeled garlic cloves exhibited a linear reduction in water removal rate to moisture content at the early period of drying, followed by a nonlinear decrease. The effective diffusivity of garlic tissue and peel showed the drying rate of garlic clove to be limited by the peel resistance, giving lower drying rate of garlic clove with peel than that of the peeled one. Drying at high temperature provides the advantage of lower shrinkage compared to low-temperature drying, while disadvantageously producing browner and larger damage of garlic tissue, which is characterized by large pore sizes. It is recommended that garlic cloves should be peeled before drying and further tests indicated that the loss of volatile oil of peeled samples was not different among the samples dried at low or high temperature.

ACKNOWLEDGEMENTS

The authors thank King Mongkut's University of Technology Thonburi and The Thailand Research Fund for their financial support.

REFERENCES

1. Block, E.; Ahmad, S.; Catalfamo, J.L.; Jain, M.K.; Apitz-Castro, R. Antithrombotic organosulfur compounds from garlic: Structure, mechanic and synthetic studies. Journal of the American Chemical Society **1986**, *108*, 7045–7055.

2. Schwimmer, S.; Weston, W.J. Enzymatic development of pyruvic in onion as measure of pungency. Journal of Agricultural Food Chemistry **1961**, *9*, 301–304.
3. Brodnitz, M.H.; Pascale, J.V.; van Derslice, L. Flavour components of garlic extract. Journal of Agricultural Food Chemistry **1971**, *19*, 273–275.
4. Teleky-Vamossy, G.; Petro-Turza, M. Evaluation of odour intensity versus concentration of natural garlic oil and some of its individual aroma compounds. Die nahrung **1986**, *30*, 775–782.
5. Cui, Z.W.; Xu, S.Y.; Sun, D.W. Dehydration of garlic slices by combined microwave-vacuum and air drying. Drying Technology **2003**, *21*, 1173–1184.
6. Lewicki, P.P.; Pawlak, G. Effect of drying on microstructure of plant tissue. Drying Technology **2003**, *21*, 657–683.
7. Senadeera, W.; Bhandari, B.R.; Young, G.; Wijesinghe, B. Influence of shapes of selected vegetable materials on drying kinetics during fluidized bed drying. Journal of Food Engineering **2003**, *58*, 277–283.
8. Pezzutti, A.; Crapiste, G.H. Sorptional equilibrium and drying characteristics of garlic. Journal of Food Engineering **1997**, *31*, 113–123.
9. Sharma, G.P.; Prasad, S. Drying of garlic (*Allium sativum*) cloves by microwave-hot air combination. Journal of Food Engineering **2001**, *50*, 99–105.
10. AOAC. *AOAC Official Methods of Analysis: Association of Official Analytical Chemists*. 15th Ed; Washington, DC. 1995.
11. Shankaranarayana, M.L.; Abraham, K.O.; Raghavan, B.; Natarajan, C.P. Determination of flavour strength in alliums (onion and garlic). Indian Food Packer **1981**, *35*, 3–8.
12. Rovedo, C.O.; Suarez, C.; Viollaz, P. Analysis of moisture profiles, mass Biot number and driving forces during drying of potato slabs. Journal of Food Engineering **1998**, *36*, 211–231.
13. Dufour, P.; Blanc, D.; Tiure, Y.; Laurent, P. Infrared drying process of an experimental water painting: Model predictive control. Drying Technology **2004**, *22*, 269–284.
14. Hernández, J.A.; Pavón, G.; García, M.A. Analytical solution of mass transfer equation considering shrinkage for modelling food-drying kinetics. Journal of Food Engineering **2000**, *45*, 1–10.
15. Báez-González, J.G.; Pérez-Alonso, C.; Beristain, C.I.; Vernon-Carter, E.J.; Vizcarra-Mendoza, M.G. Effective moisture diffusivity in biopolymer drops by regular regime theory. Food Hydrocolloids **2004**, *18*, 325–333.
16. Belhamri, A. Characterization of the first falling rate period during drying of a porous material. Drying Technology **2003**, *21*, 1235–1252.
17. Lozano, J.E.; Rotstein, E.; Urbicain, M.J. Shrinkage, porosity and bulk density of foodstuffs at changing moisture contents. Journal of Food Science **1983**, *48*, 1497–1502, 1553.
18. Ratti, C. Shrinkage during drying of Food stuffs. Journal of Food Engineering **1994**, *23*, 91–105.
19. Willis, B.; Okos, M.; Campanella, O. Effects of glass transition on stress development during drying of a shrinking food system. In *Proceedings of the Sixth Conference of Food Engineering (CoFE'99)* Dallas, TX, 1999: 496–

Available online at www.sciencedirect.com
SCIENCE DIRECT
LWT 39 (2006) 770–778
LWT
www.elsevier.com/locate/lwt

Heating process of soybean using hot-air and superheated-steam fluidized-bed dryers

Somkiat Prachayawarakorn[a,*], Paveena Prachayawasin[a], Somchart Soponronnarit[b]

[a]Department of Chemical Engineering, King Mongkut's University of Technology Thonburi, Suksawat 48 Road, Bangkok 10140, Thailand
[b]School of Energy and Materials, King Mongkut's University of Technology Thonburi, Suksawat 48 Road, Bangkok 10140, Thailand

Received 7 December 2004; received in revised form 24 May 2005; accepted 24 May 2005

Abstract

The present work investigated drying characteristics and inactivation of urease in soybean dried by superheated-steam and hot-air fluidized beds. The value of effective diffusion coefficient, which was determined by a method of slopes, was increased with increased drying temperature and increased moisture content. Furthermore, it depended on the type of heating medium, with higher moisture diffusion for soybean dried by hot air. Inactivation of the urease enzyme in both media showed difference in rate, in which the enzymatic inactivation was faster for soybean dried in superheated steam than in hot air. For the individual heating medium, the modified first-order reaction was adequately fitted to experimental data. The rate of inactivation was found to increase as the temperature and moisture content were increased. The urease enzyme was inactivated, along with maintaining protein solubility and lysine content being in standard range, as soybean was treated at a temperature between 135 and 150 °C for the hot air and the treatment temperature could be reduced to be lower than 135 °C by using superheated steam.

Keywords: Antinutritional factor; Drying; Fluidized bed; Superheated steam

1. Introduction

Full fat soybean, referred as soybean prior to oil extraction, is used as a feedstuff because of its high oil and high-quality protein contents. However, the presence of biologically active compounds in raw full fat soybean, such as trypsin inhibitors, haemagglutinins, lectins and saponins, limits the utilization of their nutritive values (Hensen, Flores, Tanksley, & Knabe, 1987; Liener, 1994), resulting in the compromised health and performance of nonruminants and immature ruminants. To eliminate or reduce antinutritional factors, heat treatment is needed. Different technological processes have been developed but all are based upon heating for a certain amount of time. Heat treatment methods frequently used are for example cooking, microwave treatment and roasting treatments (Hensen et al., 1987; Raghavan & Harper, 1974; Stewart, Raghavan, Orsat, & Golden, 2003). The present research is concentrating on roasting treatments. Roasting methods involve the treatment of soybean with a temperature varying between 110 and 170 °C (Cheong, 1997). There are many types of roasting technique such as rotary drum dryer, salt-bed roasting and conventional grain dryer. Most of these methods provide nonuniform cooking of soybean with uneven temperature distributions.

To improve temperature uniformity, fluidization is an alternative approach. With this technique, the heating fluid is forced through a bed of particles, with a sufficiently high flow rate that the lift force is counterbalanced with the weight of particles. This accordingly induces particles to suspend and simultaneously rotate in fluid stream, so that each particle in the bed intimately contacts with almost the same fluid temperature. While soybean kernels are being suspended, drying and inactivation of trypsin inhibitors

*Corresponding author. Tel.: +662427 0221; fax: +662428 3534.
E-mail address: somkiat.pra@kmutt.ac.th (S. Prachayawarakorn).

0023-6438/$30.00
doi:10.1016/j.lwt.2005.05.013

can take place simultaneously in the bed. Control of the fluidized-bed roasting for eliminating antinutritional factors in soybean is difficult since different variables, i.e. temperature, moisture content and time influence each other and are therefore difficult to separate independently (Osella, Gordo, González, Tosi, & Ré, 1997; Soponronnarit, Swasdisevi, Wetchacama, & Wutiwiwatchai, 2001). Thus, it is necessary to understand the involved parameters and their relationships in order to be able to control the roasting process effectively.

Air is commonly used as a drying medium. With hot air, the energy is largely consumed. There is a strong incentive to make the process more efficient. Superheated steam as drying medium is easier to get high energy efficiency than the hot air due to the possibility of reuse of the latent heat of evaporation (Berghel & Renström, 2002; Fitzpatrick, 1998). Fixed bed, fluidized bed, flash and impinging steam driers have been applied to dehydrate a variety of products including paddy, shrimp, sugar beet pulp and potato (Prachayawarakorn, Soponronnarit, Wetchagama, & Jaisut, 2002; Taechapairoj, Prachayawarakorn, & Soponronnarit, 2004; Tang & Cenkowski, 2000; Topin & Tadrist, 1997). Some of the agricultural products dried by superheated steam show better quality than ones dried by hot air, for example, paddy and shrimp, with higher head rice quality and less shrinkage, respectively.

This study is aimed at studying the drying rate and inactivation of antinutritional factors while soybean is treated by hot air and superheated steam. In addition, protein solubility of treated samples was determined.

2. Materials and methods

Raw soybean, with an initial moisture content of 135 g/kg dry matter was purchased from local market. The dry soybean was rewetted by adding the required amount of water to get the initial moisture contents of 19.5% and 135 g/kg dry matter. After rewetting, samples were kept in cold room at a temperature range between 8 and 10 °C for a week to allow water to penetrate into kernels. Before processing, the soybean samples were taken out of cold storage and left under environmental condition until grain temperature reached ambient temperature. It was noted that the use of the rewetted soybean in this study might be limited to its application for real drying situation since the diffusivity obtained from the drying curve of the rewetted soybean and of the freshly harvested soybean was different.

2.1. Equipments

Fig. 1 schematically shows a system of superheated-steam fluidized-bed dryer. The system consists of four main components, i.e. a boiler, a drying chamber with a dimension of 15 cm diameter and 100 cm height, an electrical fan and heaters. The designed system can alternatively use either hot air or superheated steam. Before treating soybean with superheated steam, the hot air at the same temperature as the desired level of superheated steam was initially employed for warming up the components until their temperatures reached the desired level. Hot air was initially used to prevent possible condensation of steam in the system. The saturated steam, generated from a small boiler at 106 kPa absolute pressure, was then entered into the system by opening a valve V1 and at the same time, the air was exhausted to atmosphere at valve V8. The saturated vapour was reheated at unit No. 2 containing 13.5 kW electrical heaters to change its state to superheated vapour. The velocity required for fluidizing kernels in the bed was accelerated by the backward curve blade electrical fan, with a 2.2 kW motor connected to a frequency inverter to precisely adjust the flow rate.

The superficial velocity flowing through particle bed was approximately 3.2 m/s. Upon exiting the drying chamber, the fluid was conveyed to a reverse flow cyclone where the superheated steam was conditioned fully reused, whereas the hot air was partially exhausted to the atmosphere while a portion was mixed with fresh air and reheated.

Soybean, with an amount of 1 kg corresponding to a 10 cm bed height, was treated with hot air and superheated steam at temperatures of 120, 135 and 150 °C. A

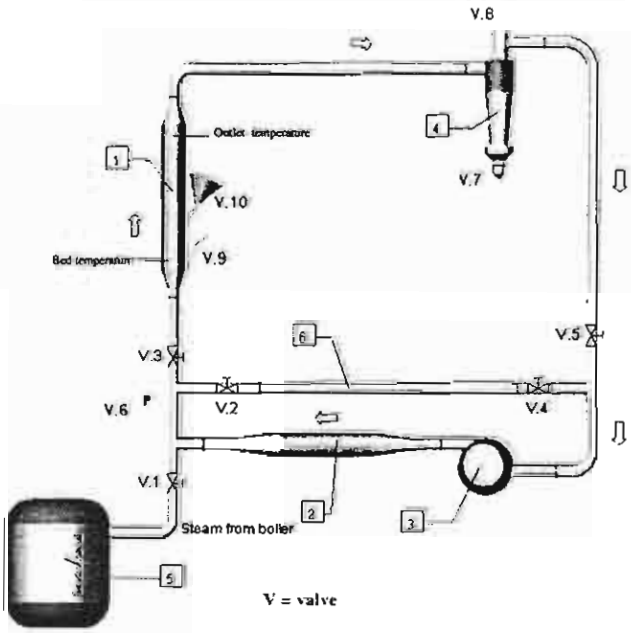

Fig. 1. Schematic diagram of superheated-steam fluidized-bed system: (1) fluidized-bed dryer, (2) heater unit, (3) fan, (4) cyclone, (5) boiler, (6) bypass line.

PID controller, with an accuracy of ±1 °C, was used to control the inlet temperature at desired level. The temperature at other two positions viz within bed and outlet of drying chamber was also monitored by inserting K-type thermocouples connected to a data logger (COMARK C8510), with an accuracy of reading ±1 °C. The temperature at positions in the system was measured every 30 s. Samples at the drying times of 2, 5, 7, 10 and 15 min were withdrawn from drying chamber at valve V9 to determine quantitatively the moisture content, urease activity, protein solubility and lysine content. After the sample was taken out of dryer at predetermined time, the new one was put into the dryer. The moisture content of soybean was determined by drying in an electrical oven at 103 °C for 72 h (ASA, 1990). An error in measuring moisture content by this method was less than 5%. Experiment for each drying condition was taken in replications and the average value was presented.

2.2. Urease activity measurement

Urease enzyme can be inactivated by heat treatment of soybean and its inactivation rate is similar to that of trypsin inhibitors (Baker & Mustakas, 1973; Osella et al., 1997). Hence, urease activity is practically used as a criterion for quality control of soybean meal. In this study, it was determined by Rasmussen's method (Rasmussen, 2002). The residual urease activity is expressed as the ratio of milliequivalents of ammonia produced from urea per gram of thermally treated soybean to that obtained from raw soybean. In uncooked soybean, ammonia was produced with an approximate value of 5 milliequivalents/g. The residual urease activity for adequately treated soybean is in the range of 10% and 20%. Below 10% indicates overheating.

2.3. Protein solubility measurement

Protein solubility is an important parameter of the feed meal industry which is used to characterize the quality of soybean after passing the heating process, in addition to determining trypsin inhibitors. Protein solubility was determined according to the AOCS method BA 10-63 (AOCS, 1979). This method involves the dispersion of proteins in 0.2% KOH solution. The protein solubility is defined as the ratio of nitrogen content in the supernatant after extraction with 0.2% KOH to total nitrogen content of the material. The total nitrogen content and the nitrogen content in the supernatant were determined by Kjeldahl method. The protein solubility required for feed meal should be in the range of 73–85% (ASA, 1990).

2.4. Lysine measurement

Lysine content in soybean was analysed by AccQ-Tag method (1993). The grounded soybean was hydrolysed by HCl solution at 110 °C for 22 h and was then derivatized with 6-aminoquinolyl-N-hydroxysuccinimidyl carbamate (AccQ-Flour reagent). The lysine content was determined by high-performance liquid chromatography.

2.5. Drying kinetics

Solid materials, when dried with superheated steam and hot air under the same inlet temperature, exhibit different phenomenological changes in rate of moisture removal. Difference in the moisture transport rate amongst both drying media is mostly explained by the temperature difference between the drying surface and drying medium (Schwartze & Bröcker, 2000; Sheikholeslami & Watkinson, 1992). This leads to different heat transfer rates, which may then influence the diffusivity as a parameter characterizing the internal structure and the nature of the solid.

In determining the effective diffusivity, it was assumed that soybean had a spherical shape and that Fick's equation for transient state, along with the initial and boundary conditions, can be solved analytically and expressed the solution as (Crank, 1975)

$$\frac{M(t)-M_{eq}}{M_{in}-M_{eq}}=\frac{6}{\pi^2}\sum_{n=1}^{\infty}\frac{1}{n^2}\exp\left(-\frac{n^2\pi^2D_{eff}t}{r^2}\right), \quad (1)$$

where D_{eff} is the effective diffusion coefficient (m^2/s), r is the particle radius (m), $M(t)$ is the moisture content of soybean at time t (decimal dry basis.), M_{in} is the initial moisture content, t is the drying time (s) and M_{eq} is the equilibrium moisture content. To obtain Eq. (1), it was assumed that gas-phase mass transfer resistance was negligible and the initial moisture content of soybean was uniform. At the present work, it was assumed that the equilibrium moisture content was nil since the kernel was contacted with a fluid at a temperature above 100 °C.

Several authors (Babalis & Belessiotis, 2004; Hebbar & Rastogi, 2001; Prachayawarakorn et al., 2002) used Eq. (1) to describe the diffusional flow of moisture inside the agricultural materials dried with various methods, i.e. infrared radiation, superheated steam and hot air. In their work, the effective diffusivity was determined by correlating the moisture data with Eq. (1) and then applying a nonlinear regression technique to estimate the diffusive parameter.

Because of nonlinearity of drying curves, a method of slopes was used to determine the effective diffusivity through which the moisture content of material was reduced under a given condition. Differentiation